The function of IL-17F in infection and inflammation

by

Chunsheng Zhou

BS, University of California, San Diego, 2015

Submitted to the Graduate Faculty of the

School of Medicine in partial fulfillment

of the requirements for the degree of

Doctor of Philosophy

University of Pittsburgh

2021

UNIVERSITY OF PITTSBURGH

SCHOOL OF MEDICINE

This dissertation was presented

by

Chunsheng Zhou

It was defended on

April 26, 2021

and approved by

Partha S. Biswas, Associate Professor, Department of Medicine

Lawrence P. Kane, Professor, Department of Immunology

Anthony J. St. Leger, Assistant Professor, Department of Ophthalmology

Charles S. Sfeir, Associate Professor, School of Dental Medicine

Dissertation Director: Sarah L. Gaffen, Gerald P. Rodnan Endowed Chair and Professor of Rheumatology and Clinical Immunology, Department of Medicine

The function of IL-17F in infection and inflammation

Chunsheng Zhou, PhD

University of Pittsburgh, 2021

The IL-17 family of cytokines is structurally distinct from other cytokine subclasses, and is composed of IL-17A, IL-17B, IL-17C, IL-17D, IL-17E (IL-25) and IL-17F. Among the IL-17 family, IL-17A and IL-17F share the most homology at the amino acid level. Both of these cytokines activate qualitatively similar downstream signals via binding with the IL-17RA:RC receptor complex but with different binding affinities. Consequently, similar disease susceptibility is observed in *Il17a*$^{-/-}$ and *Il17f*$^{-/-}$ mice in some animal models, for example autoimmune glomerulonephritis (AGN). However, IL-17A and IL-17F sometimes exhibit distinct biological activities in other settings, both infectious and autoimmune. This dichotomy is particularly illustrated in oropharyngeal candidiasis (OPC) and dextran sulfate sodium (DSS)-induced colitis. The mechanisms behind the surprisingly different *in vivo* functions of IL-17A and IL-17F remain largely underexplored. In order to further understand the function of IL-17F and potentially explore the mechanism by which IL-17A and IL-17F exhibit distinct roles *in vivo*, I took advantage of a naturally occurring human mutation that causes reduced binding affinity of IL-17F to the IL-17RA/RC receptor (IL-17F.S65L). In this dissertation, I describe the development of an IL-17F.S65L mouse strain (*Il17f*$^{S65L/S65L}$), which I used to decipher the function of IL-17F in the settings of OPC, DSS colitis, and AGN. In Chapter 3, I show that *Il17f*$^{S65L/S65L}$ mice have increased susceptibility to OPC, which is similar to *Il17a*$^{-/-}$ but not *Il17f*$^{-/-}$ mice. In Chapter 4, I present data showing that *Il17f*$^{S65L/S65L}$ mice and *Il17a*$^{-/-}$ mice also have a similarly increased susceptibility to DSS colitis that contrasts with *Il17f*$^{-/-}$ mice. Surprisingly, however, the murine IL-17F.S65L

mutation does not impact the development of AGN, despite the fact that *Il17a*$^{-/-}$ and *Il17f*$^{-/-}$ mice were both fully resistant to kidney damage in this disease model. For each model system, I present the outcomes and our current understanding of the underlying mechanisms. Overall, this dissertation research has helped to delineate the different *in vivo* activities of IL-17A and IL-17F and could potentially be beneficial for the development of IL-17F targeted therapy.

Table of Contents

List of Tables

List of Figures

List of Abbreviations

α-MEM – Minimum Essential Medium α

AGN – Autoimmune glomerulonephritis

AIDS – Acquired immunodeficiency syndrome

AIRE – Autoimmune regulator

AP-1 – Activator protein 1

APC – Antigen-presenting cell

APECED – Autoimmune polyendocrinopathy candidiasis ectodermal dystrophy

AMP – Antimicrobial peptide

ANCA – Antineutrophil cytoplasmic antibodies

ASF/SF2 – Alternative splicing factor 1 (ASF1), pre-mRNA-splicing factor SF2 (SF2)

BEL – Basal epithelial layer

BUN – Blood urea nitrogen

CARD9 – Caspase Recruitment Domain Family Member 9

CBAD – C/EBPβ activation domain

CCL – C-C motif ligand

CD – Crohn's disease

C/EBP – CCAAT-enhancer-binding proteins

CFU – Colony-forming unit

CIK – Connection to IκB kinase and Stress-activated protein kinases

CKD – chronic kidney damage

CMCD – Chronic mucocutaneous candidiasis Disease

CRISPR – Clustered Regularly Interspaced Short Palindromic Repeats

CTLA-8 – Cytotoxic T-lymphocyte–associated antigen

CXCL – C-X-C motif ligand

C. XIVa – Clostridium cluster XIVa

DMEM – Gibco Dulbecco's Modified Eagle Medium

DSS – Dextran sulfate sodium

DTT – Dithiothreitol

EAE – Experimental autoimmune encephalomyelitis

E. coli – *Escherichia coli*

EDTA – Ethylenediaminetetraacetic acid

EGF – Epidermal growth factor

ELISA – Enzyme-linked immunosorbent assay

ERK – Extracellular-signal-regulated kinase

FBS – Fetal bovine serum

FGF2 – Fibroblast Growth Factor 2

FITC – Fluorescein isothiocyanate

FN III – Fibronectin type III

GBM – Glomerular basement membrane

G-CSF – Granulocyte colony-stimulating factor

GM-CSF – Granulocyte-macrophage colony-stimulating factor

GSA – Gene Specific Analysis

GWAS – Genome-wide association study

HBSS – Hanks' Balanced Salt Solution

HIV – Human immunodeficiency virus

HDR – Homology directed repair

HuR – Human antigen R

IACCUC – Institutional animal care and use committee

IBD – Inflammatory bowel disease

IFN – Interferon

IL – Interleukin

IgA – Immunoglobulin A

ILC – Innate lymphoid cells

IKK – inhibitor of NF-κB kinase

K4 – Keratin 4

K5 – Keratin 5

K13 – Keratin 13

K14 – Keratin 14

K19 – Keratin 19

LT – Lymphotoxin

MAPK – Mitogen-activated protein kinase

MCPIP – MCP-induced protein

MMP – Matrix metalloproteinase

mRNA – Messenger ribonucleic acid

MRSA – Methicillin-resistant *staphylococcus aureus*

MYD88 – Myeloid differentiation primary response 88

NIAID – National institute of allergy and infectious diseases

NIH – National Institutes of health

NIK – NF-κB-inducing kinase

NF-κB – Nuclear factor kappa-light-chain-enhancer of activated B cells

NGF – Nerve growth factor

Ni-NTA- Nickel charged nitrilotriacetic acid

NK – Natural killer cells

OD – Optical density

OPC – Oropharyngeal candidiasis

PAM – Protospacer adjacent motif

PAMP – Pathogen associated molecular patterns

PBS – Phosphate-buffered saline

PCR – Polymerase chain reaction

PEN-STREP – Penicillin-Streptomycin

RBP – RNA binding protein

RORγT – RAR-related orphan receptor gamma

S. aureus – *Staphylococcus aureus*

SD – Standard Deviation

SDS-PAGE – Sodium dodecyl sulfate - Polyacrylamide gel electrophoresis

SEFIR – Similar expression of fibroblast growth factor and IL-17R

SEFEX – SEFIR-Extension

SEL – Suprabasal epithelial layer

SEM – Standard error of the mean

sgRNA – Single guide RNA

SPF – Specific pathogen free

STAT3 – Signal transducer and activator of transcription 3

TAK – β-activated kinase

TCR – T-cell receptor

Teff – T effector cells

TGFβ – Transforming growth factor beta

Th17 – T helper 17

TILL – TIR-like loop

TIR – Toll-like receptor/Interleukin (IL)-1 receptor

TLR – Toll like receptor

TNBS – Trinitrobenzenesulfonic acid

TNFα – Tumor necrosis factor alpha

TRAF – TNF Receptor Associated Factor

Treg – T regulatory cells

TRIF – TIR-domain-containing adapter-inducing interferon-β

UC – Ulcerative colitis

UCSC – University of California Santa Cruz

UTR – Untranslated region

WT – Wild type

YPD – Yeast extract peptone dextrose

Acknowledgements

The journey of Ph.D. training is a memorable life experience but also full of challenges. I would like to appreciate all the people who help me to conquer these challenges and provide a great deal of support for completing doctoral studies. First of all, I would like to give my sincere gratitude to my mentor, Dr. Sarah Gaffen for all her time and efforts to lead me through my training over the years. She is such a great mentor that does not only teach me how to become a good scientist but also cares my mental health and personal safety. All of these show her great love to her students.

I am deeply grateful to my thesis committee members, Drs Biswas, Kane, St. Leger, and Sfeir. This work would not be possible to accomplished without their invaluable advice and continuous support. I would particularly thank to all the past and present members of Gaffen lab, Yang, Rami, Felix, Tiffany, Bianca, Katie, Akash, Giraldina, Jamie, Agustin for all the scientific advice and great time we spend together. It's my pleasure to work with all of you and build up friendships throughout the years. I would give my special thanks to Katie for proofreading this dissertation. I would also like to thank Drs. Biswas, McGeachy and their lab members for great collaboration. I am grateful to Drs. Hand and Kaplan for providing their precious mice and facilities.

I would like to thank Dr. Haidong Dong in Mayo clinic and Dr. Li Li in BD Biosciences for leading to the field of immunology. I am deeply grateful to my lovely mother, Juhong, and my dear uncle, Quanhong, for their everlasting support, both mentally and physically. I would like to give my deepest appreciation and love to my wife Evelyn. Thank you for your love and comfort, which make me complete and strong to face all the challenges throughout my Ph.D. training. It is

my great honor to be with you throughout this journey. I am eternally grateful to the Mighty God. It is your will to bring me into Pittsburgh and the journey of the Ph.D. studies. Thank you for being with me and give me your strength and wisdom for my accomplishment. All glory be to God.

1.0 Introduction

1.1 Cytokines in the immune response

The immune system is a complex network through which the human body defends against infections. Impressively, the immune system is able to specifically recognize and eliminate pathogenic invaders yet keep responses benign to self or nonharmful components. Thus, the immune system is required to be tightly regulated, and communication among immune cells is critical to maintain appropriate regulation in the system.

Cytokines are signaling mediators that immune cells use for communication. They comprise proteins that are secreted by hematopoietic cells and many other types of cells in response to external stimuli. Cytokines regulate their target cells by binding to cognate cell surface receptors, which results in effector functions such as hematopoiesis, differentiation, migration, proliferation, survival, and apoptosis. The studies of cytokines started as early as the 1950s [1], but the term "cytokine" was first proposed by Stanley Cohen in 1974 [2]. Today, almost 200 cytokines or genes coding for cytokine-like activities have been described [3]. Cytokines are usually classified according to the type of receptors that they bind on target cells. Cytokine families include those that signal through (i) type I and type II hematopoietic cytokines, such as the IL-2, IL-6, IL-10, and type I, II and III IFN families; (ii) immunoglobulin (Ig) receptors, including the IL-1 family; (iii) TNF receptor family receptors; and (iv) chemokine G-protein coupled receptors. Additional cytokine families are characterized by their unique structures and functions, such as (i) the IL-17 family; (ii) growth factors and glycoprotein hormones with immunological functions, including insulin, TGF superfamily, and EGF family; and (iii) morphogen factors with immunological

function, including the Notch and Wnt systems [4]. The IL-17 family cytokines share unique structure features that distinguish them from the above-mentioned cytokine subclasses. In this dissertation, I will focus on the biological functions of IL-17A and IL-17F, two members of the IL-17 family of cytokines.

1.2 Interleukin (IL)-17 family cytokines and their receptors

IL-17A, originally named CTLA-8, is the founding member of the IL-17 family. By comparing sequence homology with IL-17A, five additional members were identified and named IL-17B, IL-17C, IL-17D, IL-17E (also known as IL-25), and IL-17F [5-11]. Among these cytokines, IL-17A and IL-17F share the most homology at the amino acid sequence level (56%) [6]. Protein structural analysis further elucidated the similarity between IL-17A and IL-17F in terms of tertiary structures. Superimposing the backbone C_α atoms of IL-17A to those of IL-17F revealed a comparable conformational arrangement (Figure 1.1) [12]. Studies of crystallographic structures of IL-17A and IL-17F showed that these two cytokines adopt a cysteine knot fold, which is commonly found in neurotropin proteins such as nerve growth factor (NGF) but not in other cytokine families [6, 13]. The cysteine knot fold is characterized by two pairs of anti-parallel β-strands bundled through two disulfide bonds and an extra pair of serine residues [12]. The β-strands, disulfide bridges and serine residues are conserved across all the six members of the IL-17 family. Thus, the cysteine knot fold is a distinctive structural feature in the IL-17 family of cytokines.

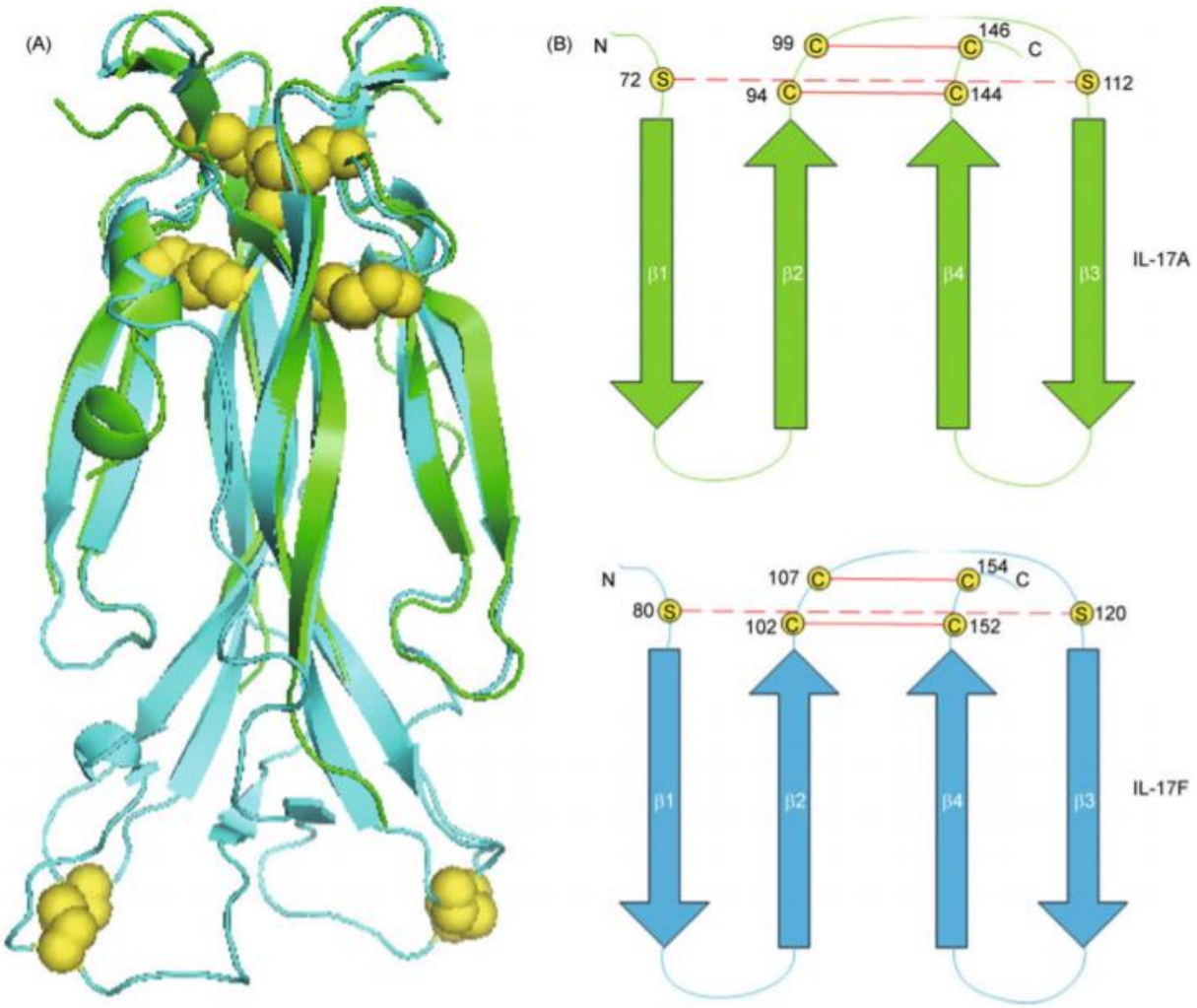

Figure 1.1: Structures of IL-17A and IL-17F

Figure is adopted from [12]. (A) Structures of IL-17A and IL-17F are superimposed as indicated. 145 C_α atoms were involved in the superimposition. Disulfide binds in IL-17F are indicated as yellow spheres. Figures were generated by the program PyMOL. (B) Topological diagram of IL-17A and IL-17F with the cysteine knot fold features. Conserved cysteines and serines are indicated by yellow circles. The two presented disulfide bonds are showed by red lines, and the third missing disulfide bond is indicated by a red dashed line.

It is not surprising that, given the unique structure of IL-17 family ligands, these cytokines signal through a receptor family that is also distinct from other known cytokine receptors. The IL-17R family contains 5 members, IL-17RA-RE [14, 15]. All of these members share a common intracellular motif known as a SEFIR (similar expression of fibroblast growth factor and IL-17R) and two extracellular fibronectin III-like (FnIII) domains, referred to as D1and D2) [16]. The intracellular SEFIR domain is structurally similar to the TIR domain found in the TLR/IL-1R family. This domain is critical for activating downstream signals and will be further discussed below [17]. FnIII domains are responsible for cytokine binding [12, 18]. A crystallographic structure of IL-17F in complex with IL-17RA revealed that a small loop of edge strands from the FnIII domains was inserted into a groove formed at the dimeric interface of IL-17F. This interaction therefore created a buried contact area containing multiple hydrogen bonds as well as salt bridges, which stabilized binding between the cytokine and its receptor. Crystallographic analysis of IL-17A in complex with IL-17RA revealed that IL-17A adopts a similar receptor-ligand interaction to IL-17F [19]. However, direct binding assays showed relatively low binding affinities of IL-17RA alone to IL-17A or IL-17F [18, 20]. Considering the low concentrations at which cytokines achieve their biological activities, it became clear that an extra component was needed to facilitate the interaction between the IL-17 cytokines and their receptors.

Indeed, the IL-17 cytokines were found to signal through heterodimeric receptor complexes. In the IL-17 family, most heterodimeric receptor complexes are composed of a common IL-17RA chain and a second chain that specifically binds to different members of the IL-17 family (Figure 1.2). IL-17A and IL-17F share IL-17RC as their second subunit [21]. Recent studies in 2019 suggested that IL-17A may also use IL-17RA:IL-17RD receptor complex for signaling and that IL-17F may have an ability to bind to an IL-17RC homodimers [22-24], though

neither of these studies has yet been replicated. Hence, our understanding of ligand-receptor binding activities of IL-17A and IL-17F is still developing. The members of IL-17 family and their respective receptor subunits are summarized in Figure 1.2 [15, 16].

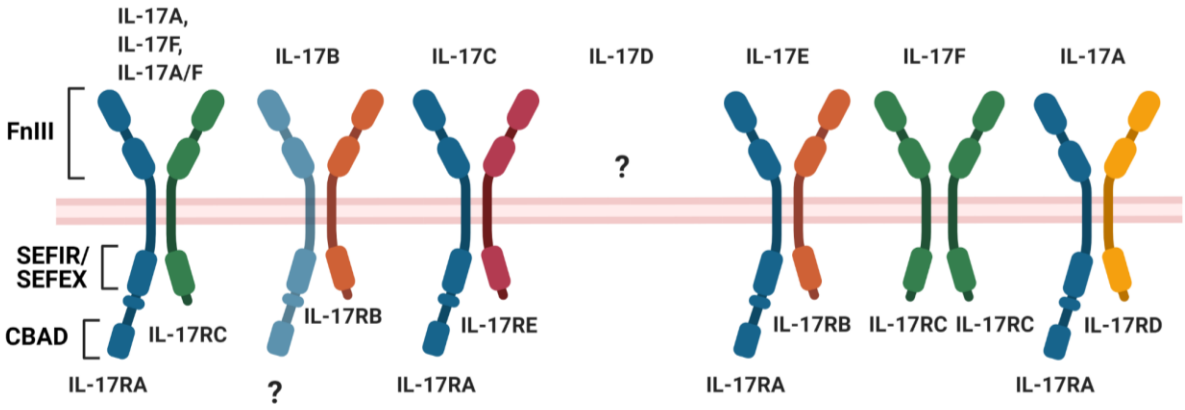

Figure 1.2: IL-17 Cytokine and Receptor Family

Members of IL-17 cytokines of family and their receptors are indicated. Each member of IL-17 receptor family is indicated with different colors. Many IL-17 family cytokines interact with a heterodimeric receptor composed of IL-17RA and a second chain belonging to the IL-17 receptor family, with an exception of IL-17F that has been recently showed to interact with IL-17RC homodimeric complex. IL-17 receptors share the SEFIR domain as a common cytoplasmic motif. Unique SEFEX and CBAD domains can also be found in cytoplasmic tail of IL-17RA.

1.3 IL-17A and IL-17F signal transduction

The highly conserved structure of IL-17A and IL-17F and their common receptor complexes causes them to trigger qualitatively similar signaling pathways. IL-17A promotes non-hematopoietic cells to express a characteristic gene signature, including a variety of cytokines (IL-

6, GM-CSF, G-CSF), chemokines (CXCL1, CXCL2, CXCL8, CCL2, CCL7, CCL20), matrix metalloproteinases (MMP1, 2, 3, 9, 13), transcriptional and posttranscriptional regulators (C/EBPs, IκBξ, Regnase-1, Arid5a), and antimicrobial peptides (β-defensins, S100A proteins, lipocalin 2) [25-28]. IL-17F induces a similar, yet not entirely overlapping, gene profile [28-32]. Lack of either IL-17RA or IL-17RC leads to a complete loss of responsiveness upon the activation of IL-17A or IL-17F [21].

Dimerization of the cytokines is required for the binding of IL-17A or IL-17F to the IL-17RA:RC receptor complex. IL-17A and IL-17F can be produced as homodimers but also exist as an IL-17A/F heterodimer [33]. All of these dimers (IL-17A:A, F:F, A:F) can bind and signal through the IL-17RA:RC receptor complex but with different binding affinities and signaling strengths, with AA>AF>FF [34, 35].

Not surprisingly, the intracellular domains of IL-17RA and IL-17RC are critical for IL-17 signal transduction [36-38]. As noted above, the SEFIR is a conserved intracellular domain found in all members of the IL-17R family including IL-17RA and IL-17RC [17]. Although the structure of the SEFIR is similar to that of a TIR domain, IL-17RA signaling does not require canonical TIR adaptors such as MYD88 and TRIF [38]. Rather, Act1, also known as connection to IκB kinase and Stress-activated protein kinases (CIKS), is the essential adaptor for SEFIR domain in all known IL-17-dependent pathways [25, 39]. Act1 also contains a SEFIR motif, which mediates homotypic interactions with the SEFIR domains in IL-17RA and IL-17RC [40]. Upon the binding of IL-17RA to its ligand, a conformational change occurs in the N-terminal region of the IL-17A dimer. Specifically, β-strands 1 and 2 of IL-17A (figure 1.1) bend toward IL-17RA, and the loops connecting β-strands 1-2 and 3-4 move away from the FnIII domain of the receptor. The conformational change leads to steric clashes that prevent the binding of another IL-17RA to the

IL-17A dimer and favor the selective interaction with IL-17RC to form the heterodimeric signaling complex. The IL-17RA/RC receptor complex provides a platform for the homotypic interactions with Act1. Act1 is thus recruited to the signaling complex for the downstream signaling [16, 18, 19, 41].

However, the conserved SEFIR domain alone is not sufficient to drive IL-17 signal transduction. Detailed mutagenesis studies of IL-17RA showed that deletion of ~100 residues after the SEFIR domain in IL-17RA significantly dampens IL-17 signaling activity [28, 38]. This extension of the SEFIR in IL-17RA was first termed TILL (TIR-like loop) because of its similarity to the BB-loop in TIR domains, and later renamed "SEFIR-Extension" (SEFEX) (shown in Figure 1.2). The SEFEX and the SEFIR together make a composite domain that is important for activation of TNF Receptor Associated Factor 6 (TRAF6), another critical component in IL-17 signaling pathway [28]. Surprisingly, the SEFEX is not conserved among IL-17 family receptors. However, deletion studies suggest that a short extension of the SEFIR motif in IL-17RC is similarly required for receptor functionality [36, 42]. Therefore, the SEFIR and SEFEX together comprise an essential composite domain needed for IL-17 signal transduction.

The IL-17 signaling pathway is initiated by an interaction between Act1 and TRAF6. Act1 is a lysine-63 (K63) E3 ubiquitin ligase that ubiquitinates TRAF6 upon IL-17 stimulation of the receptor [43, 44]. The ubiquitination of TRAF6 provides a scaffold for the recruitment of the transforming growth factor β-activated kinase (TAK)1 and the inhibitor of NF-κB kinase (IKK) complex, which further activates the canonical nuclear factor κB (NF-κB) transcription factor [45-47]. However, the non-canonical NF-κB pathway, characterized by NF-κB-inducing kinase (NIK), was not found to be activated by IL-17A or IL-17F [15]. IL-17 signaling also activates mitogen-activated protein kinase (MAPK) pathways, which include extracellular signal-regulated kinase

(ERK), p38 and JUN N-terminal kinase (JNK) [48-51]. All these pathways work together to transcriptionally activate the target genes downstream of IL-17A and IL-17F.

In addition, post-transcriptional gene regulation plays an important role in IL-17 signaling, which is mainly established by controlling mRNA stability. IL-17A and IL-17F only modestly activate transcription factors such as NF-κB and thus are weak inducers of inflammatory cytokines [51, 52]. However, IL-17A and IL-17F show a strong synergistic effect when stimulated together with other stimuli, including but not limited to TNFα, lymphotoxin (LT), IFNγ, or candidalysin (a fungal toxin found in *C. albicans*) [25, 52, 53]. One of the mechanisms by which IL-17 synergizes with other cytokines is to promote mRNA stabilization [54, 55]. Specifically, IκB kinase epsilon (IKKi) and TBK1-mediated phosphorylation of Act1 recruits TRAF2 and TRAF5 to the Act1:IL-17R complex. TRAF2 and TRAF5 can sequester the RNA-destabilizing factor ASF/SF2 away from the 3' UTR of at least some target mRNAs, which is best documented for *Cxcl1* [56]. Furthermore, TRAF2 and TRAF5 also recruit the RNA binding protein (RBP) human antigen R (HuR), which leads to the activation of HuR via Act1-dependent ubiquitination. Activated HuR then directly binds to the 3' UTR of client mRNA transcripts and sterically blocks the binding of ASF/SF2 [57]. Therefore, removal of ASF/SF2 and the activation of HuR together prevent the degradation of target mRNA.

Due to the proinflammatory role of IL-17-induced signals, negative regulation is critical to prevent development of severe inflammatory side effects. One inhibitory mechanism is mediated by the C/EBPβ activation domain (CBAD) located in the cytoplasmic tail of IL-17RA (shown in Figure 1.2). Deletion of this domain leads to exacerbated IL-17-mediated inflammation [28]. The CBAD domain is required for phosphorylation of C/EBPβ through ERK and glycogen synthase kinase 3 β(GSK-3β). Phosphorylated C/EBPβ binds to the promoters of IL-17 target genes as a

transcriptional repressor, which restricts expression of IL-17 induced genes, including *Il6* and *lcn2* [58]. Additionally, TRAF3 and A20 are two inhibitory factors that associate with the CBAD that negatively regulate the IL-17 signaling pathway. By binding to the CBAD domain in IL-17RA, TRAF3 blocks the recruitment of Act1 to the receptor complex [59]. A20 is a deubiquitinase that is induced by IL-17 signaling. A20 dampens the NF-κB and MAPK pathways by deubiquitinating the K63-linked ubiquitin chains on TRAF6 [60, 61]. Therefore, A20 acts as a negative feedback regulator of IL-17 receptor signaling via the CBAD region.

Similar to the post-transcriptional activation of IL-17 target genes, modulating mRNA stability is another mechanism to limit IL-17-induced gene expression. Regnase-1, also known as the endoribonuclease MCPIP1 (MCP-1-induced protein 1), negatively regulates IL-17 signaling by degrading mRNAs. IL-17 promotes Regnase-1 expression via NF-κB and also stabilizes Regnase-1transcripts (*Zc3h12a*) by activating the DEAD box protein DDX3X [62, 63]. Regnase-1 recognizes and degrades the IL-17-induced mRNA transcripts such as *Il6* and *Nfkbiz* by binding to specific stem-loop structures in their 3' UTR [62]. A 3' UTR-independent mechanism for Regnase-1 function has also been reported, through degradation of *Il17ra* and *Il17rc* mRNAs [62]. Notably, Regnase-1 is a deubiquitinase (DUB). Through its DUB activity, Regnase-1 removes ubiquitin moieties on TRAFs and further inhibits the NF-κB and JNK signaling pathways [64]. Additionally, numerous other mRNA binding proteins and microRNAs that promote mRNA decay or suppress translation exist, and are reviewed in detail elsewhere [25].

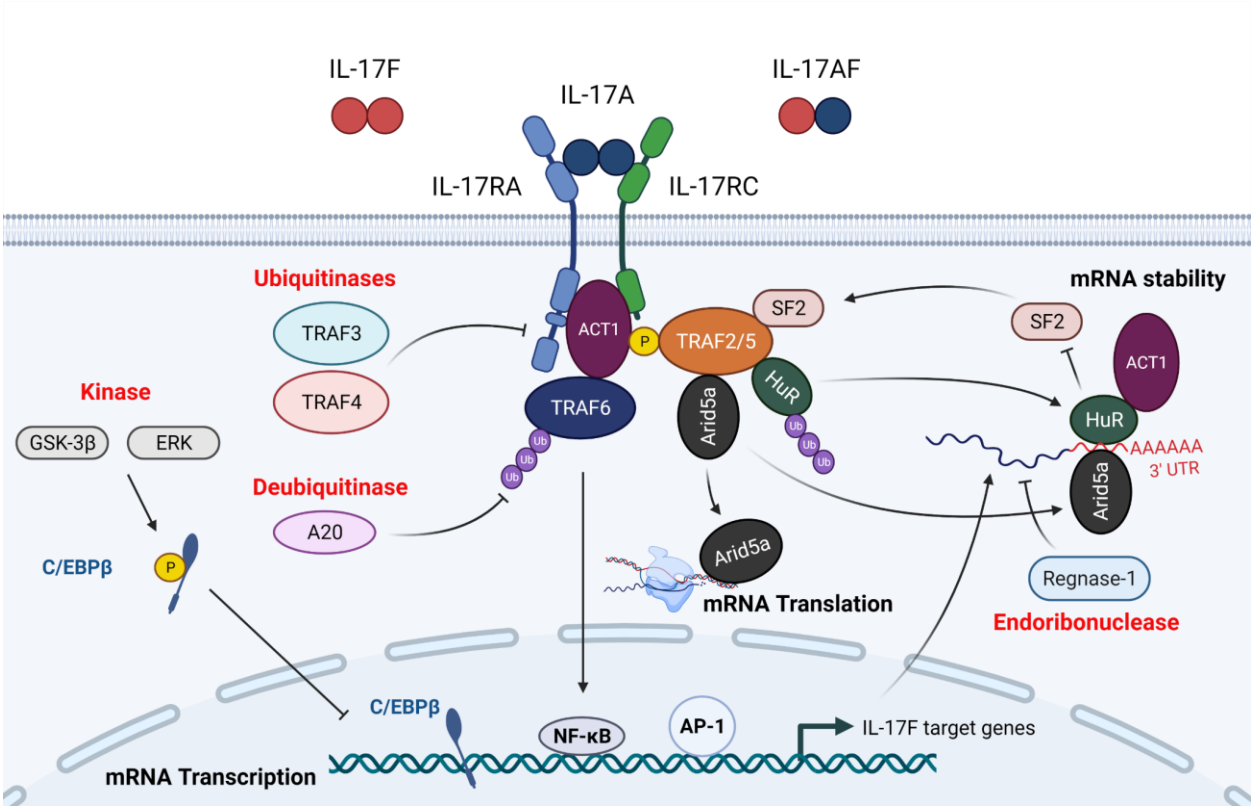

Figure 1.3 Interleukin (IL)-17RA/RC signaling pathways

IL-17 signaling starts with the interaction between IL-17A, IL-17F, or IL-17AF with the IL-17RA/RC receptor complex. Ligand binding to the receptor complex recruits the adapter Act1 through homotypic interactions via SEFIR domains. IL-17 signaling upregulates the expression of target genes through promoting mRNA transcription and mRNA stability. The mRNA transcription pathway is imitated by Act1, which induces K63-linked ubiquitylation of TRAF6, which consequently activates the MAPK, NF-κB, and C/EBPβ, pathways. These pathways trigger transcriptional activation of downstream target genes. For the mRNA stability pathway, phosphorylation of Act1 recruits TRAF2 and TRAF5, which sequesters the mRNA-destabilizing factor ASF/SF2 and recruits mRNA-stabilizing factor HuR. TRAF2 also recruits Arid5a upon IL-17 stimulation. Arid5a consequently promotes mRNA stability and enhances translation of multiple genes. IL-17 signaling pathways can be negative regulated by multiple classes of inhibitors, including ubiquitinases, deubiquitinases, endoribonucleases, kinases. Representative inhibitors of each class are indicated. Numerous other activators and inhibitors of IL-17 signaling pathway are reviewed in detail elsewhere.

1.4 Biological activities of IL-17A and IL-17F

The principle source of IL-17A and IL-17F is Th17 cells, a subtype of $CD4^+$ T helper (Th) cells characterized by expression of IL-17A and IL-17F [65, 66]. In addition to Th17 cells, many innate immune cells also secret IL-17A and IL-17F, such as γδ T cells, innate $TCR\alpha\beta^+$ cells, Type 3 innate lymphoid cells (ILC3), natural killer (NK) cells, and NKT cells [67-69]. Th17 cells and the innate IL-17A-secreting cells are collectively termed "Type 17" cells, and these populations all respond to IL-23 for optimal activation (reviewed in [67]).

Genetic deletions of IL-23 or IL-17A, or antibodies blocking their function, significantly ameliorate the development of autoimmune disease models such as experimental autoimmune encephalomyelitis (EAE), indicating a driving role of IL-17A and IL-23 in autoimmunity [66, 70-72]. Consistent with this, IL-17A is associated with human immune pathology. For example, IL-17A is increased in synovial fluid of many rheumatoid arthritis patients, IL-17A-secreting cells can be found in cerebrospinal fluid of multiple sclerosis patients [73-75], and IL-17A expression is detectable in biopsies from skin lesions of psoriasis patients [76]. Based on these and other findings, IL-17A-targeted therapies have been developed and show remarkable efficacy in psoriasis [77]. Currently, three neutralizing antibody agents that block the functions of IL-17A are clinically available (Table 1.1): secukinamab, ixekizumab, and brodalumab. Secukinamab and ixekizumab target IL-17A and to a lesser extent IL-17A/F [78, 79]. Brodalumab blocks IL-17RA, thus inhibits IL-17A, AF and F but may also inhibit signaling from other members of the IL-17 family [80]. Recently, bimekizumab, a monoclonal antibody that selectively inhibits IL-17A and IL-17F, was developed (Table 1.1). A phase 3 clinical trial of bimekizumab showed promising results in patients with moderate to severe plaque psoriasis [81]. Notably, systemically delivered

IL-17-directed therapies have side effects such as recurrent *C. albicans* infection and inflammatory bowel disease (IBD), indicating the protective role of IL-17A in those diseases [82-84].

Because of the clinical significance of IL-17A and IL-17F, various animal models have been used to determine the *in vivo* functions of IL-17A and IL-17F. Due to the qualitatively similar signaling pathways and cellular sources shared by IL-17A and IL-17F, there is much overlap in their *in vivo* biological activities. However, several reports demonstrated a different, even somewhat opposing, roles of IL-17A and IL-17F *in vivo*. Notably, determining the physiological function of the IL-17AF heterodimer is challenging, thus its specific role *in vivo* is mostly unknown. The similar yet distinct biological activities of IL-17A and IL-17F are summarized in Table 1.2. To delineate the differences between IL-17A and IL-17F in relevant biological settings three model systems have been used for the studies in this dissertation, including oropharyngeal candidiasis (OPC), DSS-colitis, and autoimmune glomerulonephritis (AGN). Each animal model will be discussed in detail below.

Table 1.4.1 IL-17 target therapies in psoriasis

Generic name	**Target**	**Reference**
Secukinamab	IL-17A (IL-17A/F)	[79]
Ixekizumab	IL-17A (IL-17A/F)	[78]
Brodalumab	IL-17RA	[80]
Bimekizumab	IL-17A and IL-17F	[81]

Table 1.4.2 The biological activities of IL-17A and IL-17F in infectious and inflammatory diseases

	IL-17A	**IL-17AF**	**IL-17F**	**Reference**
C. rodentium infections	Protective	Not determined	Protective	[85]
S. aureus mucocutaneous infection	Protective	Not determined	Protective	[85]
Lung inflammation	Pathogenic	Not determined	Pathogenic	[86]
Mucocutaneous candidiasis	Protective	Not determined	Mildly protective	[87]
Experimental autoimmune encephalomyelitis (EAE)	Pathogenic	Not determined	Not required	[86]
Autoimmune glomerulonephritis (AGN)	Pathogenic	Not determined	Pathogenic	[88]
Dextran sulfate sodium (DSS)-induced colitis	Protective	Not determined	Pathogenic	[86, 89]

1.4.1 The role of IL-17 signaling in oropharyngeal candidiasis (OPC)

1.4.1.1 Function of IL-17A; evidence from clinical studies

Fungal infections are a serious threat to human health, yet do not receive as much attention as other pathogens [90]. Approximately 1.7 billion people suffer from superficial fungal infections worldwide [91]. Although superficial infections are generally easy to cure, fungi are often life-threatening upon invasive infection. The number of deaths caused by the top 10 invasive fungal pathogens exceeds even than that of tuberculosis and malaria [90].

Candida albicans is one of the most common disease-causing fungi. *C. albicans* is a commensal microbe that can be found on mucosal surface of most humans. *C. albicans* usually stays benign under healthy conditions but can cause pathogenic infections in settings of immunodeficiency, antibiotic use, and extremes of age, among other conditions. $CD4^+$ T cells play an important role in the immunity against *C. albicans*, as 95% of HIV^+ patients suffer from recurrent *C. albicans* oral infections during progression to AIDS.

There is much evidence that human Th17 cells are responsible for preventing mucosal infections of *C. albicans*, demonstrated by clinical data from various cohorts of chronic mucocutaneous candidiasis disease (CMCD) [92-95]. For example, patients with IL-17RA, IL-17RC, and Act1 mutations are susceptible to recurrent mucocutaneous candidiasis [96-99]. Similarly, CMCD is associated with *STAT3* and *RORC* mutations that are associated with reduced Th17 frequencies [100-102]. Additionally, OPC is a safety concern for IL-17A blockade therapy for autoimmune disease, though the incidence is actually quite low. Approximately 2-3% of patients who receive anti-IL-17A neutralizing antibodies exhibit recurrent *C. albicans* oral infection [83, 84, 103].

1.4.1.2 Lessons from an "experiment of nature" IL-17F deficiency in CMCD patients

An unusual cohort of rare CMCD patients that harbor a dominant negative mutation of IL-17F provided fascinating insights into the function of IL-17F, and were the first direct hint that there is a protective function of IL-17F and/or IL-17AF in anti-fungal immunity against *C. albicans*. Genetic analysis of CMCD patients revealed a heterozygous serine-to-leucine mutation in the *IL17F* gene at position 65 (IL-17F.S65L) after the leader sequence [99]. Serine 65 in IL-17F plays a role in facilitating the binding of IL-17F to the IL-17RA receptor, as the polar side chain of serine can interact with K135 of IL-17RA in a water-mediated manner [19]. Replacement of the serine with a non-polar leucine residue dampens the binding of the IL-17F to IL-17RA by interfering with the interaction between S65 of IL-17F and K135 of IL-17RA. Thus, the mutation impairs the binding capacity of IL-17F to its receptor but does not interfere the dimerization of IL-17F, either with another IL-17F or with IL-17A. *In vitro* experiments showed that a mutant IL-17F homodimer (IL-17F.S65L/IL-17F or IL-17F.S65L/IL-17F.S65L) or IL-17A/F heterodimer (IL-17F.S65L/IL-17A) failed to activate IL-17 signaling in human fibroblasts, as measured by the expression of the target genes *IL6* and *CXCL1*. Notably, IL-17A homodimers were still functional in these patients yet were clearly insufficient to fully protect from candidiasis (although the incomplete penetration of the IL-17F.S65L mutation may indicate some protective role of the remaining IL-17A homodimers). Therefore, the IL-17F.S65L mutation in the CMCD patients implied a significant contribution of IL-17F and/or IL-17AF to the antifungal immune response in human.

1.4.1.3 Animal research predicts clinical outcomes - Understanding IL-17A and IL-17F by murine OPC

Studies in mice by the Gaffen lab predated most of the above human analyses, and first demonstrated a role for IL-17 signaling in OPC [104]. Mice lacking IL-17RA, IL-17RC or the signaling adaptor Act1 are all highly susceptible to systemic, oral, and dermal candidiasis [36, 105-108]. *Il17a*$^{-/-}$ mice or mice treated with IL-17A neutralizing antibodies also show a modestly elevated susceptibility after oral challenge of *C. albicans*, though the fungal burden is significantly less than *Il17ra*$^{-/-}$ and *Act1*$^{-/-}$ mice [87]. In contrast, *Il17f*$^{-/-}$ mice are fully resistant to OPC. However, mice with IL-17A and IL-17F double deficiency show a higher susceptibility to OPC than IL-17A single deficient mice, indicating that IL-17F does participate in immunity to *C. albicans* in the setting of oral infection [87, 109]. Unfortunately, due to a lack of reagents that selectively and efficiently block IL-17A/F, the *in vivo* function of the IL-17A/F heterodimer cannot be determined in the murine OPC model.

1.4.1.4 *C. albicans* recognition and the induction requirement of type 17 immunity

A morphological transition from yeast to hyphae is a key driver for *C. albicans* to induce both virulence and the host immune response. Under effective immunosurveillance, *C. albicans* mainly exists in its yeast form and does not trigger detectable signs of disease. Conversely, in an immunodeficient condition, *C. albicans* yeast transition to a hyphal form that induces tissue damage and activates antifungal immunity. Mutations in the fungus that block the yeast to hyphae transition (such as *efg1*$^{\Delta/\Delta}$ *cph1*$^{\Delta/\Delta}$ double knockout or *eed1*$^{\Delta/\Delta}$) render *C. albicans* avirulent in mouse models of systemic and oral candidiasis [110, 111].

For an immune response to be initiated, the immune system first recognizes pathogen associated molecular patterns (PAMPs) on infecting microbes (figure 1.4). In *C. albicans,* the cell

wall component β-(1,3)-glucan is a major PAMP. To escape immunosurveillance, *C. albicans* shield their β-(1,3)-glucan in the inner cell wall with an outer layer of a glycosylated mannoproteins (mannan). *In vivo* studies demonstrated that β-glucan is masked at the early stage of infection, but becomes exposed and accessible to pathogen recognition receptors (PRRs) during the progression of an infection. The unmasking process might be caused by an impaired integrity of the mannan layer during the host-pathogen interaction, which might be mediated by innate immune cells induced damage. [112, 113].

Dectin-1 is the main receptor that recognizes β-(1,3)-glucan during an antifungal immune response. Dectin-1 on antigen presenting cells (APC) directs the development of adaptive immunity by promoting the production of IL-1β, IL-6 and IL-23 via a Syk/CARD9-mediated pathway. The production of these cytokines skews the polarization of Th17 cells [114-116]. In addition, other PRRs such as TLR2, NLRP3, and NLRP10 are also reported to initiate the immune response by recognizing the PAMPs during *C. albicans* infection [117-122]. Notably, mice lacking expression of *Dectin1* or *Card9* are resistant to OPC, indicating an alternative signaling pathway for initiating anti-fungal immunity.

Another mechanism to initiate anti-fungal immunity is achieved through fungal virulence factors, and of particular relevance to this dissertation is Candidalysin (Figure 1.4). Candidalysin is an amphipathic pore-forming peptide derived from the hyphal-specific *ECE1* gene [123]. However, Candidalysin is not needed for hyphal formation, and its activities are separable from those of β-glucan and other hyphal cell wall components. Upon *C. albicans* oral infection, Candidalysin induces oral epithelial cell damage and promotes the release of IL-1α, IL-1β and IL-36. IL-1α and IL-1β activate TCRαβ^{+} cells to promote IL-17A expression. The activation of TCRαβ^{+} cells is mediated by both cell-intrinsic and extrinsic mechanisms, as transferring IL-1R-

deficient T cells into WT mice or WT T cells into *Il1r*$^{-/-}$ mice showed a deficient TCRαβ^{+} cell proliferation during OPC [124]. Despite this, mice with IL-1R signaling deficiency are only mildly susceptible to OPC, indicating that other players are involved in antifungal immunity against *C. albicans* oral infection. Our lab also reported that IL-36, another IL-1 family cytokine, activated a protective pathway that is distinct from IL-1R-mediated type 17 immunity, as *Il36r*$^{-/-}$ mice showed increased fungal burdens during OPC, without altered expression of IL-17A or IL-17A-dependent target genes [125]. Taken together, these findings demonstrate that Candidalysin is an essential initiator of type 17 immune responses upon *C. albicans* oral infection, through IL-1- and IL-36-family cytokines.

In addition, Candidalysin promotes the expression of c-Fos, an activating protein-1 (AP-1) transcription factor. Incubation with Candidalysin in cultured mucosal epithelial cells results in upregulation of c-Fos via a p38-MAPK-mediated pathway [123, 126]. c-Fos appears to be a key factor to induce antifungal immunity. *In vitro* experiments showed that loss of c-Fos in an oral epithelial cell line dampens the expression of inflammatory cytokines, including IL-1α, IL-6, and G-CSF [127]. *In vivo,* c-Fos is upregulated by *C. albicans* hyphae but not *C. albicans* yeast during OPC, suggesting that c-Fos might be a central molecular sensor of the switch between these states of the pathogen [128]. However, to date the functional role of c-Fos *in vivo* has not been explored in depth, as a complete c-Fos knockout mouse is embryonically lethal. However, based on our studies of Candidalysin, c-Fos is predicted to initiate an effective early response to *C. albicans* in the oral cavity.

In addition to Candidalysin, the activation of type 17 immune responses in the setting of OPC requires the commensal microbiome. Germ free mice show a decreased level of oral resident TCRαβ^{+} cells [129], which are an important cellular source of IL-17A during acute OPC. Indeed,

the commensal microbiome is important for anti-fungal immunity, as germ-free mice or mice treated with antibiotics showed an upregulated *C. albicans* gut colonization [130]. Moreover, gentamicin treatment leads to an impaired host resistance to *C. albicans* infection at the ocular surface [131]. Therefore, the commensal microbiome is essential for appropriate response of type 17 immunity against oral infections of *C. albicans*.

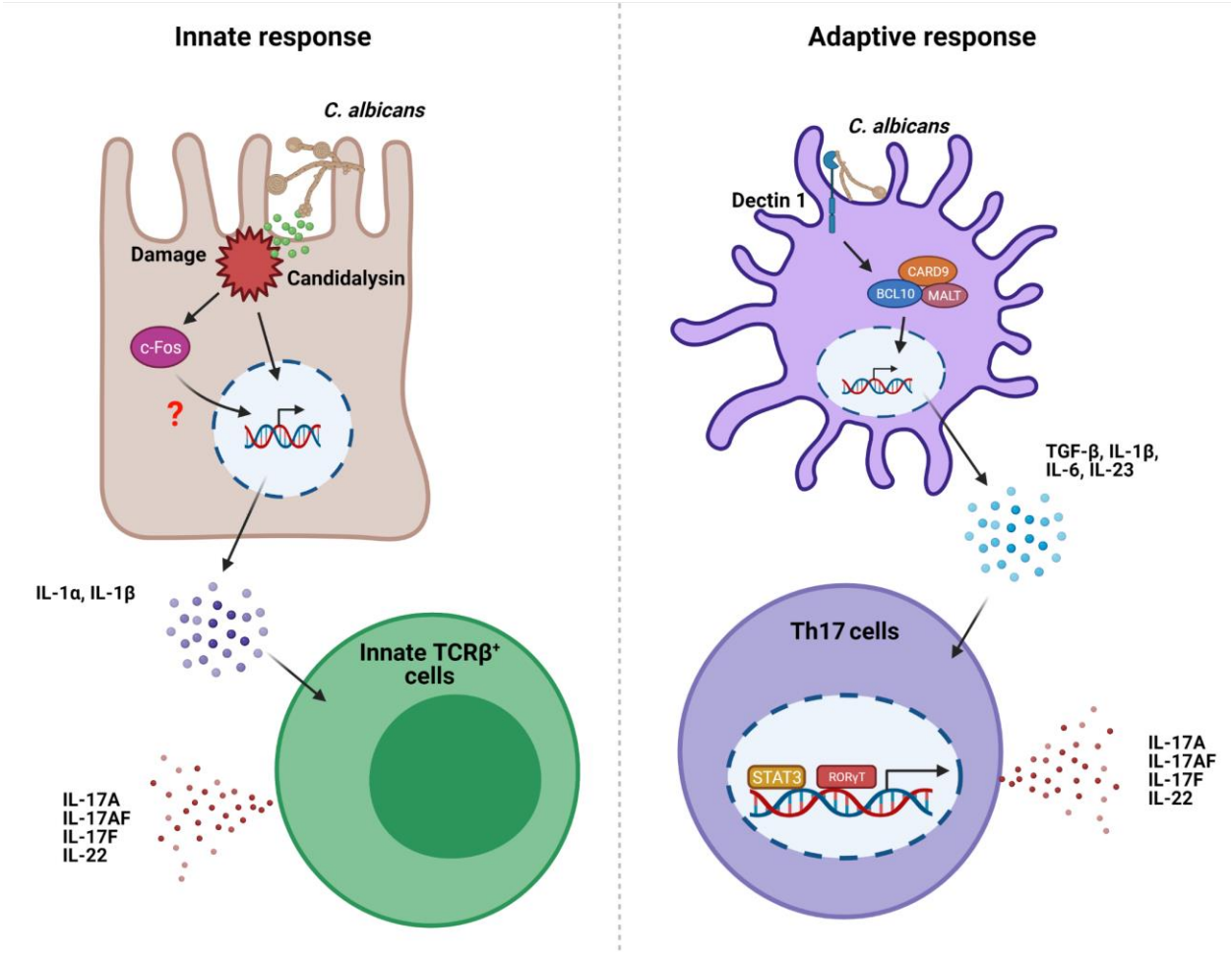

Figure 1.4 Activation of Type 17 immune response during OPC

Left: *C. albicans* hyphae secretes Candidalysin during invasion of oral epithelial cells. Candidalysin induces oral epithelial damage. This signal promotes the induction of IL-1α and IL-1β, which enhances type 17 immune response by activating innate TCRβ$^+$ cells. Candidalysin also promotes the expression of c-Fos, whose *in vivo* function is not well studied yet. Right: antigen presenting cells recognize *C. albicans* by Dectin 1. Consequently, the production of Th17 polarizing cytokines is activated via CARD9-BCL-10-MALT1 signaling pathways. These cytokines facilitate the Th17 cell differentiation and activation via transcriptional factor STAT3 and RORγT, which leads to the production of IL-17A, IL-17AF, IL-17F and IL-22.

1.4.1.5 Oral epithelium: One target site of IL-17 signaling

The oral epithelium is the first physical barrier to *C. albicans* infection in the mucosa. Disruption of the epithelial barrier promotes fungal susceptibility upon *C. albicans* oral infection, which is demonstrated by autoimmune polyendocrinopathy-candidiasis-ectodermal dystrophy (APECED) disease. APECED is an inherited autoimmune disease caused by *AIRE* gene deficiencies. APECED patients suffer from only one major infection, CMCD, which was originally attributed to circulating autoantibodies against both IL-17A and IL-17F. However, a recent study showed that type 17 immunity is actually intact in both mice and humans with *AIRE* deficiency [132]. Instead, enhanced production of IFN-γ by type 1 immunity is observed within the oral mucosa of *Aire*$^{-/-}$ mice as well as APECED patients. The overexpression of IFN-γ leads to epithelial barrier disruption, which further promotes mucosal fungal susceptibility.

The oral epithelium is not only a passive physical barrier that limits microbial invasion, but also an active site of immunosurveillance. The oral epithelium is compartmentalized into multiple layers according to the expression of unique keratins that function to maintain epithelial integrity (Figure 1.5) [133]. The basal epithelial layer (BEL) is characterized by keratin 5 (K5) and keratin 14 (K14) expression. Epithelial stem cells are located in the BEL [134, 135], which makes basal epithelial cells highly proliferative. Therefore, BEL is responsible for maintaining epithelial integrity and wound repair by replenishing terminally differentiated superficial cells that are sloughed during the antifungal immune response [136-138]. Keratin 4 (K4) and keratin 13 (K13) are found in intermediate and superficial layers, collectively termed the suprabasal layer. During invasion, *C. albicans* induces epithelial cell damage in the suprabasal layer, which further induces the innate type 17 response as described above. In turn, IL-17A and IL-17F target the epithelial cells in the suprabasal layer to mediate protection to OPC. Conditional knockout of IL-17RA in the K13^{+} epithelial layer (the suprabasal cells) leads to a higher fungal burden and impaired antimicrobial peptides secretion, whose

fungal burden is only slightly less *Il17ra*$^{-/-}$ mice [139]. Therefore, beyond serving as a physical barrier, the oral epithelium is a key site for initiation of the innate type 17 response during OPC and it also responds to IL-17, by virtue of restricted IL-17RA expression.

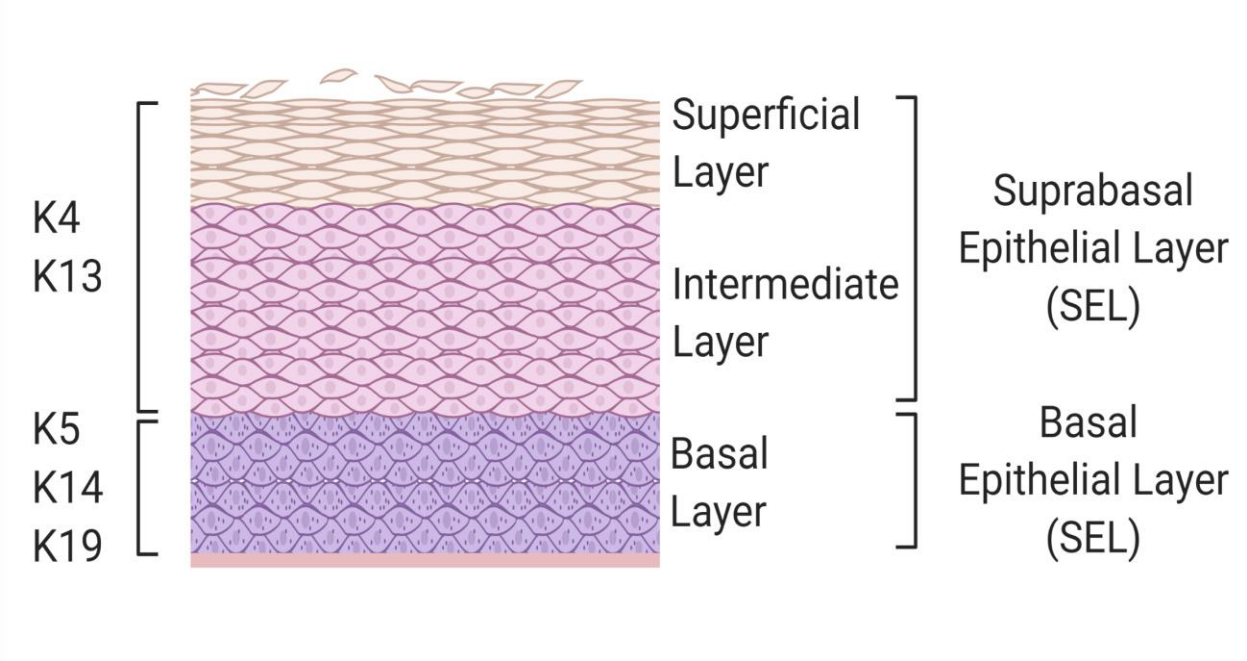

Figure 1.5 Structure of the oral mucosa

Keratinizing epithelium of the tongue is compartmentalized into the superficial layer, intermediate layer, and basal layer. Intermediate layer and superficial layers collectively are termed a suprabasal layer. Each layer expresses unique sets of keratins. The suprabasal layer is characterized by expression of K4 and K13. The expression of K5, K14, and K19 is observed in the basal epithelial layer.

1.4.1.6 Mechanism of IL-17-mediated fungal clearance

IL-17A promotes fungal clearance through expression of neutrophil-attracting chemokines (CXCL1, CXCL2, and CXCL5) and antimicrobial peptides (AMPs, namely β-defensins, lipocalin 2 and S100A8/9) [105, 139]. Neutrophils are critical for antifungal immunity [136, 140, 141]. Mice with neutrophil depletion or lacking CCR2 (a common chemokine receptor) are susceptible to oral

infection with *C. albicans* [141]. During OPC, neutrophil recruitment is partially dependent on IL-17 signaling, as *Il17ra*$^{-/-}$ mice show an impaired recruitment of neutrophils to the oral mucosa following *C. albicans* oral challenge [36, 105, 142]. Thus, neutrophils are one of the critical factors for IL-17-mediated antifungal immunity. Furthermore, IL-17A-induced antifungal immunity is mediated by antimicrobial peptides, which is illustrated by the impaired expression of β-defensin 1 and β-defensin 3 in *Il17ra*$^{-/-}$ mice and also by the increased susceptibility to OPC in *Defb1*$^{-/-}$ and *Defb3*$^{-/-}$ mice [139, 143].

1.4.2 The role of IL-17 signaling in autoimmunity

1.4.2.1 IL-17A and IL-17F in inflammatory bowel disease (IBD)

The gastrointestinal (GI) system provides an environment that is beneficial for the growth of extremely rich and diversified microbial flora [144]. The intestinal commensal flora benefits the host through metabolism of non-absorbed food components and tuning of the immune system. However, pathogenic microorganisms also take advantage of the GI tract for colonization and invasion. Therefore, the intestinal immune system mediates effective surveillance against pathogenic bacteria but also maintains tolerance to antigens from commensal bacteria. Perturbation of this tightly regulated environment can lead to chronic intestinal inflammation. IBD is a chronic inflammatory disorder in GI tract, which has two major classifications, ulcerative colitis (UC) and Crohn's disease (CD). IBD has a prevalence of 0.3% in industrialized countries, including North America, Oceania, and Europe [145]. IBD patients suffer from diarrhea, abdominal pain, and rectal bleeding. In addition, clinical studies have revealed a correlation between IBD and increased risk of intestinal cancer [146].

The intestinal epithelium is a physical barrier to bacterial invasion. Loss of barrier integrity leads to a 'leaky gut' and may initiate the pathogenesis of IBD. Increased intestinal permeability allows microbiome-derived molecules to cross the mucosa where some can induce uncontrollable inflammation. Impaired barrier integrity is a characteristic feature of most CD and UC patients [147]. Recently, genetic studies identified several mutations in tight junction related genes, such as *CDH1*, *LAMB1*, and *GNA12*, in cohorts of UC patients [147-149]. Loss of epithelium integrity leads to gut inflammation, including the upregulation of inflammatory cytokines.

IL-23 is a critical cytokine that mediates the immune response in IBD. GWAS analysis illustrated a strong association between UC and IL-23R, a connection that was among the first to link the Th17 pathway and human autoimmune disease [150]. Single nucleotide polymorphisms in IL-23R have been identified in several independent cohorts of UC patients [150]. Serum IL-23 is elevated in both UC and CD patients [151-154]. Animal studies further indicated an essential role of IL-23 in the pathogenesis of IBD, as IL-23-deficiency significantly alleviated inflammation scores in various models of experimental colitis [155-159]. Recently, neutralizing antibodies that block IL-23 demonstrated promising results in clinical trials of IBD [160].

IL-23 is known to upregulate Th17 cells but also acts on unconventional IL-17A-secreting cells such as γδT cells, NKT cells, and ILC3 [67, 161]. Notably, a population of IL-17A-producing ILCs was reported to mediate intestinal immune pathology through IL-23-dependent signaling pathway in CD40-induced colitis models [162]. In agreement with animal studies, an increased number of ILC3s was also found in CD patients. Consistent with the upregulation of IL-17A-producing cells during intestinal inflammation, overexpression of IL-17A has been detected in the lamina propria and serum from IBD patients [163]. These data indicated that IL-17A might contribute to the pathogenesis of IBD.

Surprisingly, in contrast to the clear pathogenic role of IL-23, IL-17A was found to be protective in IBD, which was unfortunately illustrated in clinical trials of IL-17A blockade therapies on CD patients. Two IL-17 blocking agents, secukinumab (targeting IL-17A) and brodalumab (targeting IL-17RA), were evaluated in CD [164, 165]. Both studies demonstrated worsening outcomes in patients belonging to the active treatment groups, and trials were halted as a result. Preclinical studies in different animal models of IBD showed variable and even somewhat contrasting results (Table 1.3).

In agreement with the results from human studies, the murine DSS colitis model indicated a protective role of IL-17A in IBD. Either deletion of the IL-17A gene or administration of neutralizing antibodies against IL-17A led to an increased severity of DSS-induced colitis in mice [86, 166-169]. Further research revealed that IL-17A protects mice from DSS colitis by maintaining intestinal integrity. Mice treated with anti-IL-17A antibodies showed an abnormal cellular localization of the tight junction protein occludin. Under physiological conditions, occludin is localized to the tight junction complex to regulate intestinal permeability. However, in mice treated with anti-IL-17A antibodies, occludin was instead found in the cytoplasm, leading to increased intestinal permeability [167]. In a separate report, IL-17A was found to synergize with fibroblast growth factor (FGF2) to promote the repair of damaged intestinal epithelium during DSS colitis [169]. These results from animal models are consistent with the emerging picture from clinical observations that IBD is a side effect of secukinumab treatment. Therefore, the balance of data in both mice and humans strongly indicate that IL-17A is protective in colitis.

Interestingly and surprisingly, IL-17F was reported to exhibit an opposing role in DSS colitis, unlike IL-17A. Specifically, Iwakura et al. showed that loss of IL-17F led to decreased, rather than increased, susceptibility to DSS colitis, which was ascribed to a specific class of gut

bacteria that could promote Treg induction [89]. Sequencing of 16S ribosomal RNA (rRNA) revealed a different fecal bacterial profile between *Il17f*$^{-/-}$ and WT mice. In particular, the frequency of one of the main groups of commensal bacteria, *Clostridium* cluster XIVa (*C.* XIVa), was significantly higher in *Il17f*$^{-/-}$ compared to WT mice. *C.* XIVa colonization was shown to activate intestinal epithelial cells to express TGFβ, which then promoted the differentiation of Treg [170]. An altered balance between Treg cells and T effector cells (Teff) in the GI tract was suggested to contribute to the development of IBD in this experimental setting [171]. Therefore, the upregulation of *C.* XIVa in *Il17f*$^{-/-}$ mice led to an increased number of colonic Tregs, which explained the reduced DSS colitis seen in *Il17f*$^{-/-}$ mice. This finding was concordant with the observation in IBD patients that Treg levels are decreased in peripheral blood but increased in the intestinal mucosa, consistent with a migration of Treg to the inflamed site [172-174]. Several studies in experimental colitis also demonstrate a potent anti-inflammatory action of Treg in IBD [175-177].

All these data suggested that IL-17F, unlike IL-17A, is pathogenic in the setting of DSS colitis. However, the mechanism of the different biological activities between IL-17A and IL-17F during DSS colitis is still not clear, and remains one of the very few examples where IL-17A and IL-17F appear to act in a discordant manner (Table 1.3).

Table 1.4.3 Functions of IL-17A in mouse models of IBD

Treatment	Colitis model	Effect on colitis	Reference
IL-17A KO	DSS	Disease worse	[86, 167, 169]
IL-17A antibody	DSS	Disease worse	[166, 168]
IL-17F KO	DSS	Disease alleviated	[86, 89]
IL-17A KO	T-cell transfer	Disease worse	[178, 179]
IL-17A antibody	T-cell transfer	Disease alleviated	[159, 180]
IL-17A +IL-17F antibody	T-cell transfer	Disease alleviated	[181]
IL-17F KO	T-cell transfer	Disease alleviated	[89]
IL-17RA KO	TNBS	Disease alleviated	[182]
IL-17 receptor fusion protein	TNBS	Disease alleviated	[182]
IL-17A antibody	H. Hepaticus	Disease alleviated	[183]

1.4.2.2 The role of IL-17 signaling in autoimmune glomerulonephritis (AGN)

Chronic kidney disease (CKD) is a serious health issue and also a social and economic burden. Approximately 10% of the western population is affected by CKD [184]. As the disease progresses, patients commonly suffer from end stage renal failure, which requires dialysis or transplantation. The kidney is a frequent target of systemic inflammatory and autoimmune disorders. Renal involvement is commonly found in many cases of systemic autoimmunity against ubiquitous antigens [185]. Less common immune responses specifically against renal antigens have also been identified. For example, anti-glomerular basement membrane (anti-GBM) nephritis is caused by a specific autoimmune response to this renal antigen [186, 187]. GBM rupture and inflammation in glomeruli induce a crescent structure that can be observed in renal biopsies [188].

Chronic autoimmune disease with the presence of crescents in more than 50% of glomeruli is defined as crescentic glomerulonephritis [189, 190].

IL-17A is emerging as a key activator of the renal autoimmune response. IL-17A protects the kidney from infectious pathogens such as *C. albicans*, uropathogenic *E. coli*, and methicillin-resistant *S. aureus* [107, 191-193]. However, IL-17 can be pathogenic if not properly regulated and thereby contribute to AGN. Lupus patients exhibit an upregulated serum level of IL-17, elevated circulating IL-17-producing cells, and increased IL-17 production from lymphocytes, compared to healthy volunteers [194, 195]. In addition, the serum level of IL-17A was increased in patients with IgA nephropathy, which was proposed to be pathogenic by inducing the production and glycosylation of IgA1 in B cells [196, 197]. Single cell RNAseq analysis from kidney biopsies of patients with ANCA-associated glomerulonephritis also revealed a highly enriched tissue resident memory T cells with a Th17 gene signature [198]. Therefore, observations in the clinic indicated a pathogenic role of IL-17A in AGN.

Murine models of experimental AGN have been used to evaluate the function of IL-17 signaling in autoimmune kidney disease (Table 1.4). *Il23p19*$^{-/-}$, *Il17a*$^{-/-}$, and *Il17ra*$^{-/-}$ mice in various models of AGN demonstrate a requirement of IL-17 signaling for kidney pathogenesis [199-201]. During AGN, IL-17A is mostly produced by kidney-infiltrating CD4^{+} and γδ^{+} T cells in response to kidney injury [201, 202]. Renal tubular epithelial cells (RTEC) are the main target cells of IL-17 signaling. Multiple IL-17A target genes, including *Il6*, *Cxcl1*, *Cxcl5*, *Ccl20*, and *Lcn2*, are involved in process of AGN development. Specifically, IL-6 stimulates tubular atrophy and accelerates fibrosis during AGN [203]. CXCL1 and CXCL5 are necessary for neutrophil infiltration, which is believed to contribute to kidney pathology [201]. CCL20 is an essential chemokine for Th17 cell recruitment, thus establishing a positive feedback loop for IL-17A

production [202]. Lipocalin 2 is a major biomarker for kidney damage and is also an active player in disease progression, as *Lcn2*$^{-/-}$ mice showed a dramatical reduction of renal lesions during AGN.

Although the role of IL-17A in AGN is starting to be relatively well understood, our knowledge of IL-17F in this disease is still limited. One study showed that *Il17f*$^{-/-}$ mice are resistant to kidney damage, indicating that IL-17F plays a similar role to IL-17A in AGN models [88]. In that study, the lower level of kidney damage in *Il17f*$^{-/-}$ mice was attributed to decreased expression of neutrophil-attracting chemokines. However, because the IL-17F target gene profile largely overlapped that of IL-17A, other factors such as *Lcn2* and *Il6* may also be involved in the IL-17F-mediated pathway during AGN. Therefore, further research is required to understand the *in vivo* function of IL-17F during AGN.

Table 1.4.4 Animal models of nephritis (adapted from [204])

Model	Etiology/Mechanism	Translation to human disease	Reference
MRL/*lpr* & NZB/W nephritis	Spontaneous, immune complex LN	Partial	[205-207]
Anti-GBM nephritis	Immune, necrosis	Partial	[208-211]
Anti-Thy 1 nephritis	Immune, crescents, mesangiolysis	Partial	[212-214]
Alport syndrome	Early crescentic proliferation, late sclerosis	Mice have same genetic defect as patients but early crescentic proliferation is not found in patients	[215-218]

1.5 Summary

IL-17A signaling is essential for immunity against some fungal and bacterial infections. Conversely, IL-17A is also a critical pathogenic factor in certain autoimmune diseases. Thirty years have been passed since the cloning of IL-17A. However, there are still many questions that need to be answered regarding IL-17 signaling, in particular the role of the closely-related cytokine IL-17F. IL-17A dimerizes with IL-17F to form IL-17A/F heterodimer. *In vitro* studies of IL-17A/F heterodimer indicated a similar gene induction profile of IL-17A/F compared with IL-17A and IL-17F[34, 35]. Although the *in vivo* formation of IL-17A/F heterodimers can be clearly observed, the physiological role of IL-17AF is still very unclear. IL-17A and IL-17F activate qualitatively

similar signaling, and exert similar biological activities in many animal models, including AGN. However, these closely related cytokines exhibit opposite roles in a setting of chemically induced colitis. Thus, the mechanisms of IL-17A and IL-17F *in vivo* function are still not well defined.

A mutation in IL-17F, IL-17F.S65L, was identified in a single-family cohort of CMCD patients. This "experiment of nature" might help us to further understand the functions of IL-17A and IL-17F. The S65 residue in human IL-17F is conserved among many species, including mice. Therefore, I created an IL-17F.S65L mutant mouse strain in order to probe the role of IL-17F in various diseases. In this dissertation, I use this mutant strain to further demonstrate the role of IL-17F and IL-17AF in varying systems where IL-17F and IL-17A have similar or differing impacts, including OPC (Chapter 3), DSS colitis (Chapter 4), and AGN (Chapter 4).

2.0 Methods and Materials

2.1 Materials

2.1.1 Mice

Il17f$^{Thy1.1}$ reporter mice were previously described [219]. *Il17ra*$^{-/-}$ mice were a gift from Amgen. *Act1*$^{-/-}$ mice were from U. Siebenlist, National Institutes of Health. *Il17a*$^{-/-}$ mice and *Il1f*$^{-/-}$ mice were from Y. Iwakura, Tokyo University of Science, and were described previously [85]. Wild-type (WT) mice were from The Jackson Laboratory, Taconic Farms, or generated from breeding colonies. All mice were on the C57BL/6 background. Age-matched mice (6–10 week) were used for experiments with both sexes in OPC model. Male mice were used in DSS colitis model and Female mice were used in AGN model. Experiments were performed in accordance with protocols approved by the University of Pittsburgh IACUC and NIAID and followed guidelines in the Guide for the Care and Use of Laboratory Animals of the NIH.

2.1.2 Cell and cytokines

ST2 cells (murine bone marrow stromal cell line) were cultured in α-MEM (Minimum Essential Medium α) supplemented with 1% L-glutamine, 1% Pen-Strep, and 10% FBS. CMT93 cells (murine colonic epithelial cell line) were cultured in DMEM (Gibco Dulbecco's Modified Eagle Medium) supplemented with 1% Pen-Strep, and 10% FBS. Ear derived fibroblast cell line

were cultured in DMEM supplemented with 1% Pen-Strep, 50μM β-mercaptoethanol, and 50% FBS.

2.1.3 Antibodies

Antibodies used are listed in Table 2.1

Table 2.1.1 List of antibodies

Antibody	Vendor	Purpose	Catalog#	Dilution
CD3	BioXCell	T cell activation	BE0001-1	
CD28	BioXCell	T cell activation	BE0328	
IL-17A	BioXCell	Cytokine blocking	BE0173	
c-Fos	Cell Signaling	Immunohistochemistry	2250S	1:100
CD4 BV605	Invitrogen	Flow cytometry	Q10092	1:500
CD45 Pacblue	Invitrogen	Flow cytometry	48-0451-82	1:100
CD45 AF700	Biolegend	Flow cytometry	103128	1:100
CD11b AF700	Biolegend	Flow cytometry	101212	1:100
Ly6G PE	BD biosciences	Flow cytometry	551461	1:100
Thy1.1 APC	Biolegend	Flow cytometry	202526	1:100
TCRβ PE	Biolegend	Flow cytometry	109207	1:100
TCRγδ Pacblue	Invitrogen	Flow cytometry	48-5711-82	1:100
Foxp3 APC	Invitrogen	Flow cytometry	17-5773-82	1:100

2.1.4 qRT-PCR primers

Primers for qPCR to determine the enteric bacterium level are listed in Table 2.2, and primers for qRT-PCR were purchased from Qiagen and are listed in Table 2.3

Table 2.1.2 List of bacterium qPCR primers

Bacteria name	Forward	Reverse
16S (8F&R357)	AGAGTTTGATCMTGGCTCAG	CTGCTGCCTYCCGTA
Clostridium XIVa	AAATGACGGTACCTGACTAA	CTTTGAGTTTCATTCTTGCGAA

Table 2.1.3 List of commercial qRT-PCR primers

Gene Symbol	Organism	Catalogue #
Cxcl1	Mouse	QT00098875
Cxcl2	Mouse	QT00115647
Defb3	Mouse	QT00265517
Gapdh	Mouse	QT01658692
Il6	Mouse	QT00098875
Il17a	Mouse	QT00103278
Il17f	Mouse	QT00144347
Il22	Mouse	QT00128324
Il33	Mouse	QT00135170
S100a9	Mouse	QT00105252

2.2 Methods

2.2.1 Generation of *Il17f*$^{S65L/S65L}$ knock-in mice

Il17f$^{S65L/S65L}$ mice were created by CRISPR/Cas9 by the Transgenic and Gene Targeting (TGT) and Innovative Technologies Development (ITD) Cores facility in Department of Immunology, University of Pittsburgh. Briefly, a S.py. Cas9 target sequence overlapping the Ser65 codon in the mature *Il17f* sequence (following signal peptide cleavage) was selected: GTTCCCCTCAGAGATCGCTG **AGG**. The protospacer adjacent motif (PAM) in bold was not included in the sgRNA. Cas9 mRNA and the sgRNA were produced as described [220, 221]. A 127-mer oligonucleotide (Ultramer, IDT) was used as template for homology-directed repair (HDR): *Il17f*-S65L-HDRv3: 5'-CATCCTGCTTTACTTTTTATTTTTTTCCTTCAGCATCACT-CGAGACCCCCACCGGTTCCCTCTAGAAATCGCTGAGGCCCAGTGCAGACACTCAGG CTGCATCAATGCCCAGGGTCAGGAAGACAGC-3'. The oligonucleotide contains a substitution to convert Serine 65 to Leucine, which contemporaneously breaks an HPY188I restriction site (underlined) to facilitate genotyping. The sequence also contains an additional silent substitution, bringing a total of 4 mismatches (red, above) between the sgRNA target sequence and the designed allele, thus limiting further re-editing of the mutant allele by Cas9. C57BL/6J embryos were microinjected with the sgRNA (50 ng/µl), the HDR oligonucleotide (0.5 µM) and Cas9 mRNA (100 ng/µl). Embryos that developed to the 2-cell stage were transferred into pseudopregnant female surrogates. Five homozygous founders were identified by PCR amplification of the target region (Forward: 3'-ATGGGAGAAACCCCGTTTTA-5'; reverse: 3'-TCCAACCTGAAGGAATTAGAACA-5') followed by restriction digestion of the PCR product with HYP188I. The correct sequence was validated by Sanger sequencing of the PCR products

following TOPO cloning. Potential off-target sequences of the target sequence were identified using the CRISPOR website [220]. There were only 2 potential off-target sequence with fewer than 4 mismatches in the mouse genome (Table 2.4). There were no mutations introduced at those sites, as determined by PCR and Sanger sequencing. The line was backcrossed twice to C57BL/6J mice prior to colony expansion.

Table 2.2.1 Off-target screening of *Il17f*^{S65L} mutant mice

[a]Two off-target sites with up to 3 bp mismatches were predicted in creation of Il17fS65L/S65L mice, located on chromosomes 3 and 5. Precise locations and sequences are shown.

[b]PCR primers used to amplify and sequence these regions are indicated. See Materials and Methods section for details.

N/A, not applicable.

	Off Target 1[a]	*Off Target 2*[a]
Score	0.958618437118	0.455082125604
Chromosome	3	5
Start	131,315,589	141,241,627
End	131,315,611	141,241,649
Strand	-	+
Target Pattern	GTTCCCCTCAGAGATCGCTGAGG	GTTCCCCTCAGAGATCGCTGAGG
Mismatch	3	3
Sequence	GTTCTGTTCAGAGATCGCTGTGG	GCTCCCCTCACAGAGCGCTGCGG
Mismatch Location	5, 6, 7	2, 11, 15
Target Number	1	1
Target Strand	+	+
Mmismatchln2	1	1
Region	Intergenic	Exonic
GeneUCSCID	N/A	Uc009ail.2
GeneSymbol	N/A	*Sdk1*
Primer-forward[b]	AGCTCCAATAAGGCCACACC	CACCTGGTGTCGTCCCAC
Primer-reverse[b]	CACGAGGACTAGACAGCGAC	CTCCGATGAGCAGCGAGC

2.2.2 Model of OPC

C. albicans (WT or indicated mutant strains) were inoculated in 10 ml yeast extract peptone dextrose (YPD) and incubated for 14-16 hours at 30 ℃ with continuous agitation. The *C. albicans* suspension was prepared for a final cell density of 2×10^7 cells/ml, which is determined by a 1.2 OD value (wavelength = 600nm) via BioTek Plate Reader. During the *C. albicans* oral challenge, mice were anesthetized by 15 mg/ml ketamine and 1.5 mg/ml xylazine with a dose of 6.7x weight of the mouse + 20 ul via intraperitoneal injection (i.p.). The fully anesthetized mice were sublingually inoculated by 2.5 mg cotton balls that saturated with the previously prepared *C. albicans* suspension for 75 minutes. Sham mice were similarly inoculated with the same type of cotton balls saturated with PBS. Before and after the oral challenge, the mice were also treated with 1ml of 0.9% saline by subcutaneous injection. 200 ug/ml anti–IL-17A or isotype control antibodies (BioXCell) were administered i.p. on days -1, 1, and 3 relatives to *C. albicans* infection. The mice weights were monitored daily. The mice were harvested at day 1, day 2, and day 5 for different experiment purpose. On day 1, One longitudinal half of the tongue were harvested, flash frozen in liquid nitrogen and stored at -80ºC for RNA extraction. The other half of the harvested tongue were fixed in 10% formalin for paraffin embedded sections preparation. On day 2, the harvested tongues were longitudinally cut by half. The half of the harvested tongues were flash frozen in liquid nitrogen and stored at -80ºC for RNA extraction. The other half of the tongues were processed for flow cytometry. On day 5, the longitudinal half of the tongue were homogenized by gentleMACS system (C-tubes, program E, Miltenyi Biotec). 100ul of the tongue homogenates were plated on YPD agar plates containing ampicillin. The plates were incubated at 30 ℃ for 48 hours, and the colonies on plates were enumerated to estimate the colony forming units per gram (CFU/g) of tongue.

2.2.3 Leukocytes isolation and enrichment from tongue tissues

The harvested tongues were chopped into small piece and digested with 500 ul of DNase1 (1mg/ml, Roche), and Collagenase IV (0.7mg/ml) in HBSS at 37°C for 30 minutes. The single cell suspensions were filtered by 70 μm cell strainer and separated by Percoll gradient centrifugation with 40% percoll diluted in PBS.

2.2.4 Flow cytometry

The single cell suspensions were stained with 1:500 GhostDye Violet 510 (TONBO Biosciences, CA) in PBS to exclude dead cells. The indicated fluorescent tagged antibodies (table 2.1) targeted on surface markers were diluted in FACS buffer with a dilution factor 1:100. The surface maker was stained with diluted antibodies on ice for 20 minutes or overnight. If the intracellular staining is required, the cells were permeabilized by Foxp3/Transcription factor staining buffer set (Invitrogen) for 45 minutes at 4 ℃. The intracellular antibodies were 1:100 diluted in permeabilization buffer, and stained the cells for 30 minutes at 4 ℃. Data were acquired on an LSR Fortessa and analyzed with FlowJo (Tree Star).

2.2.5 RNA extraction, Quantitative PCR and RNAseq

For frozen tissues, the harvested tissue was homogenized in 500μl of Qiazol lysis buffer (Qiagen) by a GentleMACS Dissociator (M-tubes, program RNA-02, Miltenyi Biotec). The homogenate was thoroughly mixed with chloroform, and the mixture was centrifuged for 20 minutes. The upper aqueous layer was collected for further RNA isolation following manufacturer's protocol of

the RNeasy Mini Kit (Qiagen). For cultured cell samples, cells were homogenized in 350 ul of RLT buffer by vortex. The cell homogenates were used for RNA extraction by RNeasy Mini Kit (Qiagen) following manufacturer's protocol. Total RNA concentration was determined by Nanodrop and normalized to 200 ng/ml. 500 ng or 1000 ng of RNA was used for reverse transcription into cDNA. cDNA synthesis was performed via Superscript III First-Strand synthesis system (Invitrogen) by following the manufacturer's protocol. Relative quantification of mRNA expression was determined by real-time PCR with Perfecta SYBR Green FastMix ROX (Quanta BioSciences) normalized to *Gapdh* on a 7300 Real-Time PCR System (Applied Biosystems). All primers were commercially purchased from QuantiTect Primer Assays (Qiagen) and are listed in Table 2.3. For RNASeq, cDNA libraries preparation and RNAseq was performed by the Health Sciences Sequencing Core at the University of Pittsburgh. The RNAseq results were analyzed by Partekflow software. Specifically, the trimmed Sequencing reads were aligned to the UCSC mouse reference genome (mm10, GRCm38.75) using STAR. The aligned reads were quantified to annotation model, and the differential gene expression was determined by GSA analysis.

2.2.6 IL-17RA deficient cell line development

Ears were harvested from *Il17ra*$^{-/-}$ mice and disinfected with 70% ethanol. The harvested ears were chopped into small piece and digested with 950 ul of collagenase 1 in DMEM at 37°C for 3 hours with continuous agitation. The single cell suspensions were filtered by 70 μm cell strainer and seeded into 6-wells-plate with DMEM containing 50% FBS. The FBS concentration in medium is decreased to 30 % after 3 days and further decreased to 20% at day 6 post seeding. The primary cells were immortalized by transfection of 2μg SV40 Large T Ag expression plasmid with Fugene HD (Promega) when the cell number reached to 6×10^4 cells/well.

2.2.7 IL-17F and IL-17F.S65L activation

Murine ST2 cells, CMT93 cells, and ear derived fibroblasts were seeded into 6-wells-plate with a total number of 6×10^4 - 8×10^4 cells. The cells were cultured for overnight to reach a 60-80% confluence. IL-17F (Peprotech or Bon Opus) or IL-17F.S65L (Bon Opus) were used to activate the cells for 3 hours or 6 hours. Murine TNFα were added to make a final concentration as 2 ng/ml for synergy effect. The cells were harvested by trypsin treatment and stored in -80 ℃ for future RNA extraction

2.2.8 Th17 differentiation and ELISA

Total spleen was homogenized in 10 ml PBS using bottom of a 5 ml syringe. The cell suspension was passed through a 70 μm cell strainer, and the red cells were lysed by ACK lysis buffer (Gibco). $CD4^+$ T cells were isolated from the cell suspensions using $CD4^+$ T cells isolation kit (Miltenyi Biotech, cat# 130-104-454). 2×10^5 $CD4^+$ T cells were plated into flat bottom 96-wells-plate that is pre-coated with anti-CD3 and anti-CD28 antibody (5 μg/ml each) at 4 ℃ overnight. Naïve $CD4^+$ T cells were differentiated into Th17 cells by complete RPMI medium containing Th17 cocktails (IL-1β 50ng/ml, IL-6 50ng/ml, IL-23 50ng/ml, TGFβ 5ng/ml). Th0 control were treated only with complete RPMI medium. After 4 days, supernatant was collected, and the concentration of IL-17A was determined by murine IL-17A ELISA kit (eBioscience). ELISA were performed following manufacturer's protocol. Samples were analyzed in triplicate for each experiment.

2.2.9 Histology and Immunohistochemistry

Paraffin section of formalin fixed tongue tissues were processed by Histology Core facility of the University of Toledo Medical Center. Paraffin embedded sections were stained as described in the Cell Signaling immunofluorescence protocol (https://www.cellsignal.com/learn-and-support/protocols/protocol-ihc-paraffin). Briefly, the paraffin section was deparaffinized by incubating with xylene and rehydrated by incubating with 100% ethanol followed by another incubation with 95% ethanol. The antigen was unmasked by steaming the section in 10 mM sodium citrate buffer (pH 6.0). 5% normal goat serum in TBST was used to block the section for 1 hour at room temperature. Samples were stained overnight with primary antibodies, c-Fos (clonal: 9F6, Cell Signaling 2250S), and subsequently incubated with secondary antibodies for 30 minutes at room temperature. The staining was developed by incubating with ABC reagent (Vectastain ABC Kit, Vector Laboratories) for 30 minutes followed by another incubation with DAB Reagent (Vector Labs). Images were obtained on an EVOS FL microscope (Life Technologies).

2.2.10 Model of DSS colitis and FITC-Dextran Administration

2% or 2.5% of DSS (MP bio) were dissolved into drinking water and gave to mice for 7 days. Mice weight and disease activity index score were monitored daily. The disease activity index score was the combined score of weight loss, stool consistency, and bleeding, which can be defined as follow: Weight loss: 0 (no loss), 1 (1-5%), 2 (5-10%), 3 (10-20%), and 4 (>20%); Stool consistency: 0 (normal), 2 (loose stool), and 4 (diarrhea); Bleeding: 0 (no blood), 2 (visual pellet bleeding), and 4 (gross bleeding, blood around anus). At the time point of choice, the mice were sacrificed, colon length was measured, and the colon tissues were harvested for flow cytometry or

stored in -80°C for qPCR. Oral gavage of FITC dextran was used to determine the gut epithelial integrity during DSS colitis. Briefly, at day 7 of DSS treatment, mice were off-fed for 4 hours, and FITC dextran (Sigma-Aldrich, catalog number: FD4) was administered to each mouse (40mg/100gram body weight, 200 microliter volume) via oral gavage with a needle attached to a 1 ml syringe. After 4 hours, mice were anesthetized and the blood was collected via cardiac puncture into an EDTA-coated tube. Plasma was separated by centrifuging the blood containing EDTA-coated tube at 5000 rpm for 20 min. The concentration of FITC in plasma was measured by BioTek Plate Reader with an excitation of 485 nm (20 nm band width) and an emission wavelength of 528 nm (20 nm band width).

2.2.11 Colonic lamina propria cell isolation

The colon tissue was "butterfly" opened and cut into 0.5-1cm pieces. Epithelial cells were stripped by stirring the colon tissue with RPMI buffer complement with 3% FBS, 5mM EDTA (Invitrogen), and 1mM DTT (Invitrogen) for 20 minutes at 37°C. The tissue sample was shaken in RPMI containing 2mM EDTA to further wash out the epithelial cells. Colonic tissue was then incubated in a digestion cocktail containing complete RPMI with 0.5mg/ml DNase and 20μg/ml liberase (Roche) at 37°C for 25 minutes. Digested tissue was processed through a 70μm cell strainer and a 40μm cell strainer. The single cell suspension is continued for flow cytometry.

2.2.12 Fecal bacterium isolation and enteric *C.* XIVa determination

Fecal samples were collected before the DSS treatment. Stools were homogenized by a 1000 μl peptide tip, and the DNA of fecal bacterium was isolated by following manufacturer's

protocol of the QIAamp Fast DNA Stool Mini Kit (Qiagen). Relative quantification of *Clostridium* XIVa DNA was determined by real-time PCR with Perfecta SYBR Green FastMix ROX (Quanta BioSciences) normalized to the amount of total bacteria (16S) on a 7300 Real-Time PCR System (Applied Biosystems).

2.2.13 Model of anti-GBM nephritis

Rabbit IgG (0.1 mg/ml) and complete Freund's adjuvant were emulsified at 1:1 ratio. Mice were immunized with the mixture of rabbit IgG + CFA by i.p. injection on day -3. On day 0, Serum containing anti-glomerular basement membrane antibodies was i.v. injected to *Il17f*$^{S65L/S65L}$ mice, *Il17a*$^{-/-}$ mice, *Il17f*$^{-/-}$ mice, as well as WT mice. On day 14 post i.v. injection, mice were euthanized and blood were harvested via cardiac puncture. Blood was incubated at 4°C overnight in a tilted position, and serum was collected in the next day. Blood urea nitrogen (BUN) was determined by Blood Urea Nitrogen Enzymatic Kit (Bioo scientific, cat# 5602-01) following manufacturer's protocol.

3.0 An Il-17F.S65L knockin mouse reveals similarities and differences in IL-17F function in oral candidiasis: A new tool to understand IL-17F

This is the author's version of the work. Sections of this chapter have been adapted from the original work published in *Journal of Immunology* and is posted here with permission from the journal.

Chunsheng Zhou[1], Leticia Monin[1], Rachael Gordon[2], Felix E.Y. Aggor[1], Rami Bechara[1], Tara N. Edwards[3], Daniel H. Kaplan[3], Sebastien Gingras[2], Sarah L. Gaffen[1*]

[1] Division of Rheumatology and Clinical Immunology, University of Pittsburgh, Pittsburgh PA

[2] Department of Immunology, University of Pittsburgh, Pittsburgh PA

[3] Department of Dermatology, University of Pittsburgh, Pittsburgh PA

[*] Correspondence: Division of Rheumatology and Clinical Immunology, BST S702, 200 Lothrop St., Pittsburgh PA 15261, USA. Phone: 412-383-8903. Email: sarah.gaffen@pitt.edu

3.1 Background

IL-17A and IL-17F exert similar yet distinct activities during OPC. *Il17a*$^{-/-}$ mice or mice treated with IL-17A-neutralizing antibodies exhibit elevated susceptibility to OPC compared to immunocompetent control mice [87], whereas *Il17f*$^{-/-}$ mice or WT mice treated with IL-17F neutralizing antibodies are fully resistant to *C. albicans* infection. However, there is evidence that IL-17F does participate in immunity to OPC, as dual blockade of IL-17A and IL-17F increases susceptibility to OPC over blockade of IL-17A alone [87, 109].

The physiological role of IL-17AF is still unclear. Although IL-17AF can be reliably detected (e.g., by sandwich ELISA), there are no commercial antibodies that block this isoform selectively and efficiently, and hence determining its specific role *in vivo* is challenging. Hints regarding IL-17F and IL-17AF function came from an unusual cohort of CMCD patients discovered by Puel *et al.* that carry a heterozygous serine-to-leucine mutation in the *Il17f* gene at position 65 (IL-17F.S65L) [99]. This mutated residue lies within the region of interaction between IL-17F and the IL-17 receptor. *In vitro*, this mutation impaired IL-17F binding to the receptor, but had no apparent impact on the ability of IL-17F to dimerize with IL-17F or IL-17A. Cultured human fibroblasts treated with an IL-17F homodimer containing this mutation (IL-17F.S65L/IL-17F or IL-17.S65L/IL-17F.S65L) or a mutant IL-17AF heterodimer (IL-17A/IL-17F.S65L) showed strongly impaired signaling *in vitro* [99]. Accordingly, the S65L substitution in human IL-17F appeared to be both a loss of function and a dominant negative mutation, causing functional blockade of both IL-17F and IL-17AF. Importantly, IL-17A homodimers were still found in these patients, yet were unable to fully protect against candidiasis. These data thus implied that IL-17F and/or IL-17AF are significant contributors to the antifungal immune response in humans.

As described in this chapter, I created an IL-17F.S65L mouse strain using CRISPR/Cas9 technology to exploit this "experiment of nature," [99] in order to better understand the functions of IL-17F and IL-17AF in immune responses. We found that *Il17f*$^{S65L/S65L}$ mice exhibited similar susceptibility to OPC as *Il17a*$^{-/-}$ mice, which contrasted with the known resistance of *Il17f*$^{-/-}$ mice to OPC [87]. Thus, S65K appears to be more than simply a loss-of-function mutation. The increased susceptibility of these mice to fungal infection was linked to impaired expression of CXC chemokines and concomitantly reduced neutrophil recruitment to the oral mucosa. but surprisingly not to expression of key antimicrobial peptides known to control OPC, such as β-defensin-3. Similar to IL-17A, IL-17F is expressed by γδ-T cells, innate TCRαβ^{+} cells, and possibly also by ILC3s. Previous research indicated that type 17 immunity is orchestrated by Candidalysin during acute OPC, and may be influenced by the commensal microbiome [124, 129]. Here, I found that the commensal flora is essential for antifungal immunity for *C. albicans* oral infection. In contrast, c-Fos, an important mediator of the Candidalysin-induced signaling pathway, surprisingly appears not to be required for fungal clearance during OPC.

3.2 Results

3.2.1 Murine IL-17F S65L is a loss-of-function mutation

The S65L residue in IL-17F which is mutated in humans with CMCD is conserved among many species, including mice [99]. The human IL-17F.S65L cytokine has no apparent signaling capacity *in vitro* [99]. To determine whether the mouse orthologue of IL-17F.S65L functions similarly to its human counterpart, a His-tagged murine IL-17F.S65L and a corresponding WT IL-

17F control, were expressed in Expi293 cells and purified from conditioned media on nickel-charged affinity resin (Ni-NTA) (Figure 3.1A). Recombinant IL-17F.S65L and IL-17F migrated according to their predicted dimeric sizes on a non-reducing SDS-PAGE gel (Figure 3.1B). The multiple bands observed in the reduced (R) and non-reduced (NR) gels are consistent with the expectation that these recombinant cytokines exist in multiple glycosylated and non-glycosylated forms (Figure 3.1B, Figure 3.2).

To evaluate the signaling capability of murine IL-17F.S65L, murine ST2 stromal cells were treated with increasing concentrations of IL-17F.S65L or WT IL-17F for 3 hours. Two IL-17F-inducible genes, *Il6* and *Cxcl1*, were assessed by qPCR as endpoints of signaling. As expected, a wild type version of IL-17F induced *Il6* and *Cxcl1* expression in a dose-dependent manner (Figure 3.1C). In contrast, IL-17F.S65L at most dosages (6.25-50 ng/ml) did not detectably upregulate *Il6* or *Cxcl1*. Expression of these genes was slightly enhanced by IL-17F.S65L at a supraphysiological dose (100 ng/ml), but nonetheless showed significantly reduced activity compared to non-mutated IL-17F (Figure 3.1C). Because IL-17F synergizes with other cytokines to induce gene expression [28, 32], we evaluated IL-17F.S65L responsiveness to a suboptimal dose of TNFα (2 ng/ml). Control IL-17F synergized with TNFα to induce *Il6* and *Cxcl1*, but IL-17F.S65L did not synergistically enhance expression of these genes (Figure 3.1D). Thus, analogous to the IL-17F.S65L mutation found in CMCD patients, a mouse IL-17F.S65L homodimer appears to be a loss-of-function mutation.

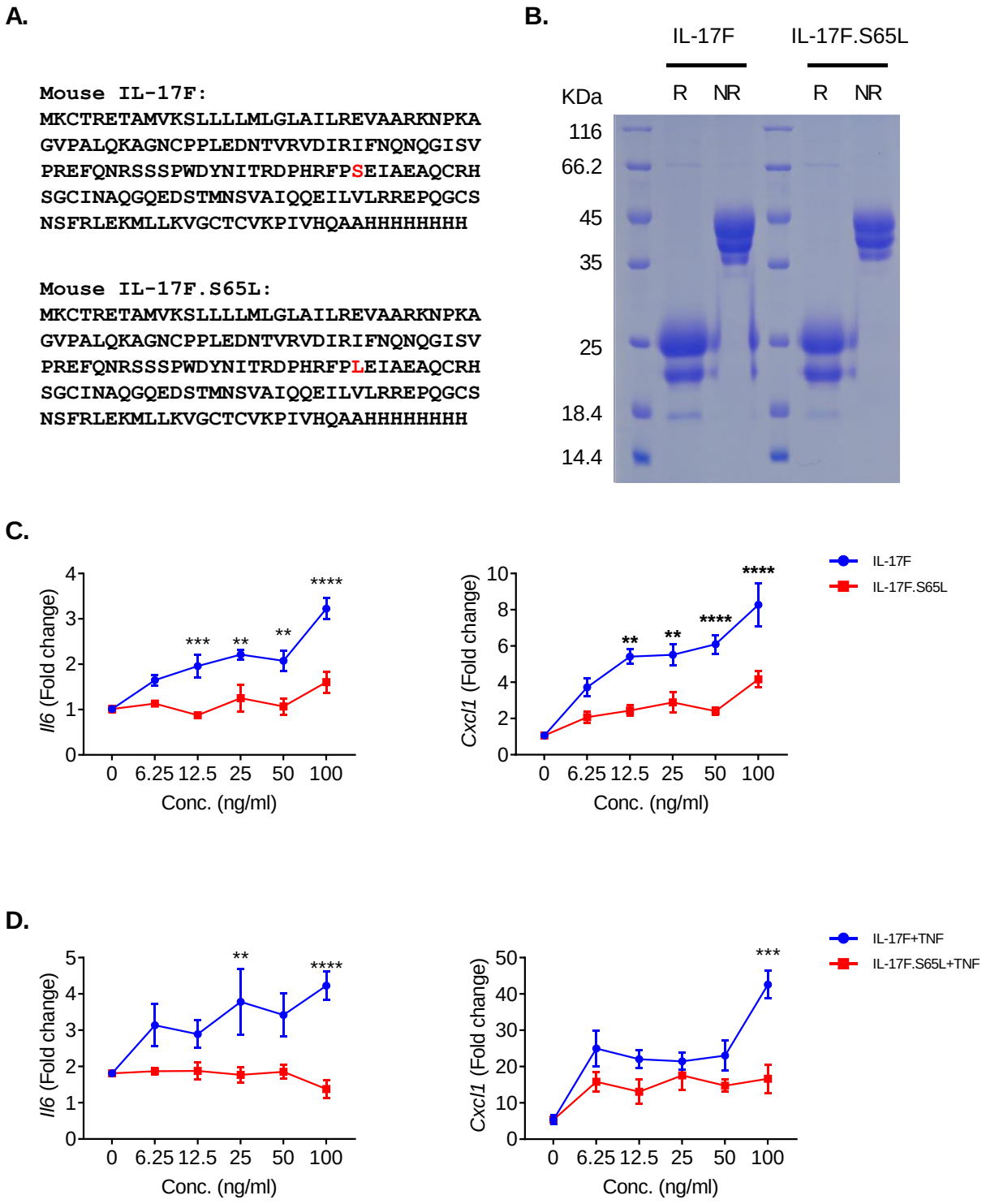

Figure 3.1 Murine IL-17F.S65L is a loss-of-function mutation

(A) Amino acid sequences of recombinant His-tagged WT IL-17F and the IL-17F.S65L mutant used in this study. The Ser65 residue is shown in red. (B) IL-17F and IL-17F.S65L were transfected into Expi293 cells. Culture medium

was collected on day 5 post transfection purified by Ni-NTA. The eluted fraction was analyzed by SDS-PAGE in reducing (R) condition and non-reducing (NR) conditions. Size markers are indicated at left. (C, D) ST2 stromal cells were treated with the IL-17F (blue) and IL-17F.S65L (red) at increasing doses in the absence (C) or presence (D) of TNFα (2 ng/ml) for 3 h. *Il6* or *Cxcl1* mRNA was assessed by qPCR. Data is graphed as fold-change relative to untreated conditions ± SEM from 2 independent experiments, analyzed by ANOVA. **P < 0.01, *** < 0.001, **** < 0.0001.

```
Name:  Sequence         Length:  169
MKCTRETAMVKSLLLLMLGLAILREVAARKNPKAGVPALQKAGNCPPLEDNTVRVDIRIFNQNQGISVPREFQNRSSPW      80
DYNITRDPHRFPSEIAEAQCRHSGCINAQGQEDSTMNSVAIQQEILVLRREPQGCSNSFRLEKMLLKVGCTCVKPIVHQA     160
AHHHHHHHH
.....................................................................N......      80
..N.....................................................................      160
.........                                                                     240

(Threshold=0.5)
---------------------------------------------------------------------
SeqName      Position  Potential   Jury    N-Glyc
                                 agreement result
---------------------------------------------------------------------
Sequence      74 NRSS   0.5910     (8/9)   +
Sequence      83 NITR   0.6987     (9/9)   ++
---------------------------------------------------------------------
```

Figure 3.2. Glycosylation site prediction in murine IL-17F

The IL-17F amino acid sequence (see Figure 3.1) 1 was analyzed for predicted N-glycosylation sites (NetNGlyc 1.0 server). Asn-X-Ser/Thr sequences are shown in blue, and Asn residues predicted to be N-glycosylated are shown in red. + potential > 0.5, ++ potential > 0.5 and jury agreement (9/9) or potential > 0.75.

3.2.2 *Il17f*$^{S65L/S65L}$ mice are modestly susceptible to OPC

To determine the function of the murine IL-17F.S65L mutation *in vivo*, we created an IL-17F.S65L mutant mouse strain by CRISPR/Cas9 technology. Sixteen founders were generated, 5 of which had a homozygous nucleotide replacement (Figure 3.3A, Figure 3.4). None of the founder lines were found to have mutations in either of the two predicted off-target sites, ascertained by

PCR of genomic DNA and sequencing (Table 2.4). Similar to *Il17a*$^{-/-}$ and *Il17f*$^{-/-}$ mice [85], there were no obvious abnormalities in the health of these mice when maintained in specific pathogen free (SPF) conditions, and they bred normally with Mendelian numbers of offspring.

In the family of patients where the S65L substitution was identified, 5/7 of the affected individuals experienced CMCD as heterozygotes (no homozygotes were described [99]), and thus we hypothesized that mice that are either homozygous or heterozygous for the IL17F.S65L mutation would be susceptible to mucosal candidiasis. Accordingly, mice were subjected to OPC by a 75-minute sublingual exposure to *C. albicans* (strain CAF2-1) by standard methods [222, 223]. In this model, WT mice typically clear *C. albicans* from the oral mucosa within 3 days and show no overt signs of illness, such as prolonged weight loss [105, 139]. We previously demonstrated that mice lacking IL-17RA or Act1 maintain a high fungal burden in the oral cavity after infection, which we typically measure at day 5 post infection (p.i.) [105, 106], Mice lacking IL-17A *(Il17a*$^{-/-}$ or given anti-IL-17A antibodies) have detectable fungal burdens, though consistently lower than *Il17ra*$^{-/-}$ or *Act1*$^{-/-}$ mice [87]. In contrast, mice lacking IL-17F *(Il17f*$^{-/-}$ or given anti-IL-17F antibodies) are fully resistant to OPC, at least within the detection limits of this system [87]. Here, we observed that *Il17f*$^{S65L/S65L}$ mice had significantly higher oral fungal burden compared to WT controls at 5 days p.i., at levels similar to those in *Il17a*$^{-/-}$ mice (Figure 3.3B). However, the *Il17f*$^{+/S65L}$ heterozygous mice did not have elevated fungal loads compared to the WT mice. Approximately 40% of the *Il17f*$^{S65L/S65L}$ and *Il17a*$^{-/-}$ mice still had a detectable fungal load at this time point, whereas almost all the WT and the *Il17f*$^{S65L/+}$ heterozygous mice fully cleared the infection (Figure 3.3C). *Il17f*$^{S65L/S65L}$ mice also lost slightly more weight than the WT mice, which was most evident at day 2 p.i. (Figure 3.3D, E). However, oral fungal burdens in *Il17f*$^{S65L/S65L}$ mice were not measurably different at day 2 (Figure 3.3F). Collectively, these results

indicate that IL-17F.S65L mutation contributes detectably, albeit modestly, to susceptibility to OPC in the mouse model, but only when the mutation is present on both alleles.

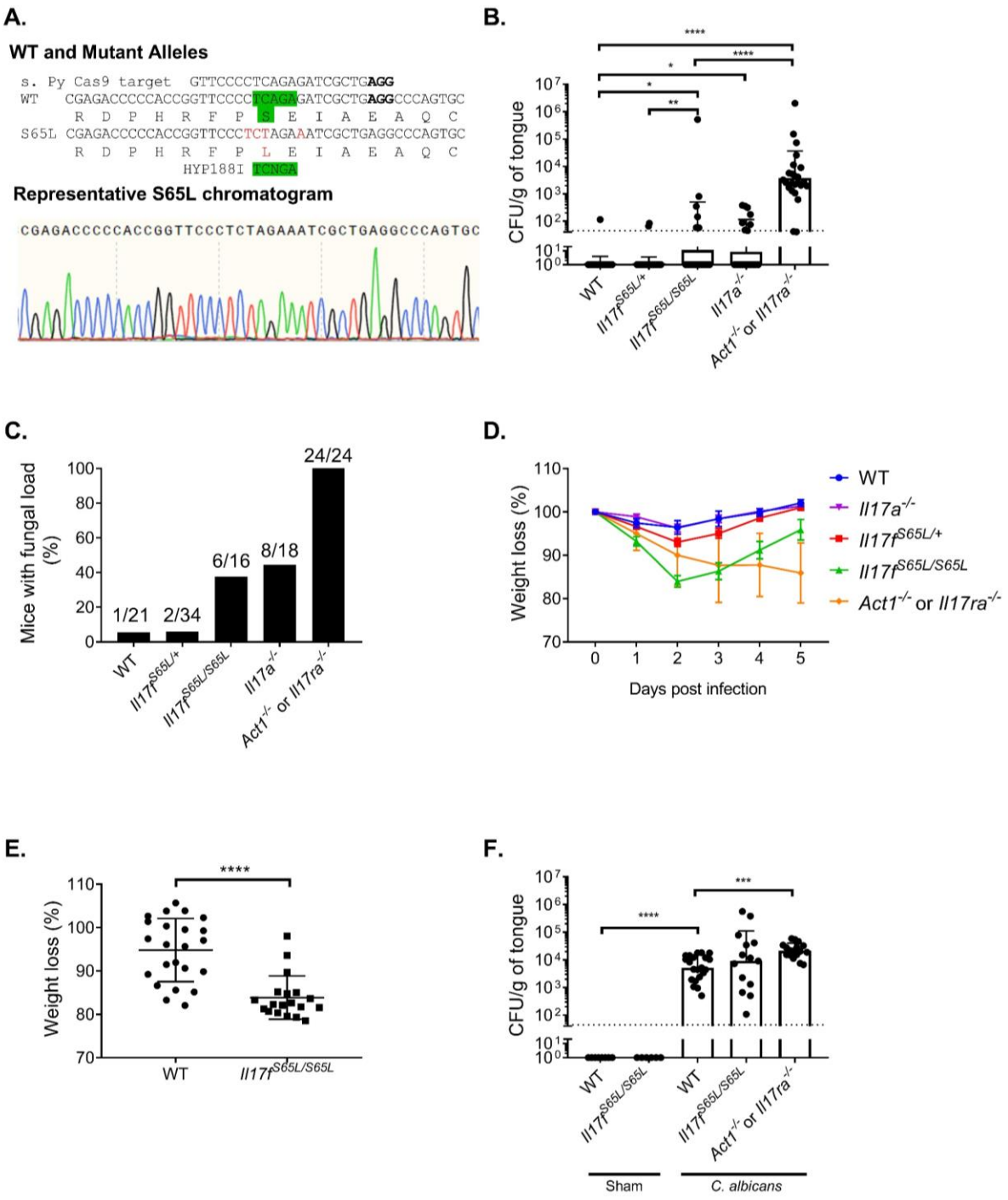

Figure 3.3 *Il17f*$^{S65L/S65L}$ mice are modestly susceptible to OPC

(A) Top: Schematic diagram of murine IL-17F.S65L substitution created by CRISPR/Cas9 including breaking of a new IHPY188I restriction site. Bottom: Representative chromatogram of genomic DNA sequencing from a representative founder mouse. (B) The indicated mice were infected sublingually with *C. albicans* or PBS (Sham).

Fungal burdens were assessed by CFU enumeration on YPD/Amp on day 5 p.i. Graphs show geometric mean + SD. Dashed line indicates limit of detection (~30 CFU/g). Data were compiled from five 5 experiments. Each symbol represents one mouse. (C) Data from panel B is represented as percentage of mice with detectable fungal load in the tongue. Values above indicate number of mice with fungal burden/total. (D) Weight in the animals from panel B was assessed daily and percentage loss relative to day 0 is shown for each time point. (E) Weight loss of *Il17f*$^{S65L/S65L}$ and WT mice at day 2 p.i. from panel B. Graph shows mean ± SD. (F) Fungal burdens were assessed on day 2 p.i.. Data are compiled from 3 independent experiments. Data were analyzed by ANONVA or Student's t-test, with Mann-Whitney analysis for fungal load analysis. *P < 0.05, ** < 0.01, *** < 0.001, **** < 0.0001.

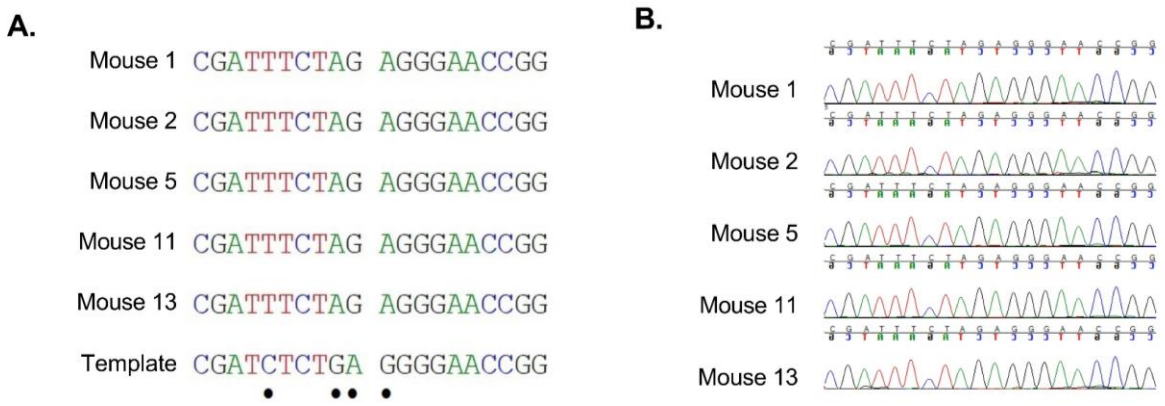

Figure 3.4 Genomic DNA sequencing of IL-17F.S65L mutation

Founder mice were created by CRISPR/Cas9. Genomic DNA of founders was extracted from tail tissue and subjected to sequencing. (A) DNA sequence of mice with an *Il17f*$^{S65L/S65L}$ homozygous mutation. Black dot indicates nucleotide replacement. (B) Chromatogram of the DNA sequence data showed in panel A.

3.2.3 *Il17f*$^{S65L/S65L}$ mice show mildly impaired neutrophil recruitment during OPC

To understand the immunological mechanisms by which the IL-17F.S65L mutation promotes susceptibility to OPC, we evaluated factors known to be critical for antifungal immunity that are mediated by IL-17R signaling [36, 105, 139]. Neutrophils are vital for fungal clearance in

OPC [140, 141, 224]. We have observed that *Il17ra*$^{-/-}$ mice show impaired recruitment of neutrophils to the oral mucosa following OPC induction [36, 105, 142]. IL-17F upregulates expression of neutrophil-attracting chemokines such as CXCL1 and CXCL2 [86, 88, 225], and both human and murine IL-17F.S65L showed impaired induction of these chemokines *in vitro* (Figure 3.1, [99]). Consistent with this, *Cxcl1* gene expression in the tongue was downregulated in *Il17f*$^{S65L/S65L}$ mice during *C. albicans* oral infection, though not completely impaired. However, expression of *Cxcl2* was similar between *Il17f*$^{S65L/S65L}$ mice and WT controls (Fig. 3.5A). Flow cytometry analysis revealed that early neutrophil recruitment to the tongue measured at day 2 p.i. was partially decreased in infected *Il17f*$^{S65L/S65L}$ mice, compared to WT (45% versus 57%) (Fig. 3.5B). There was also a trend towards reduced total numbers of neutrophils, though there was high variability in the number of cells recovered from the tongue (a common problem often encountered when isolating cells from this tissue [124, 226]). Thus, although not yet proven directly, impaired neutrophil recruitment in *Il17f*$^{S65L/S65L}$ mice may help explain OPC susceptibility in these mice.

Antimicrobial peptides (AMPs) such as β-defensins and calprotectin (S100A8/S100A9) have antifungal activity towards *C. albicans* [143, 227-230]. IL-17RA knockout mice show impaired AMP expression following *C. albicans* oral challenge [105, 139]. Surprisingly, the induction of *Defb3* and *S100a9* in the oral mucosa of *Il17f*$^{S65L/S65L}$ mice was equivalent to that in the WT upon oral *C. albicans* infection (Figure 3.5C). Therefore, the increased susceptibility to OPC in *Il17f*$^{S65L/S65L}$ mice is apparently not due to insufficient AMP expression. Moreover, these data suggest that IL-17F and/or IL-17AF signaling may be more critical for the neutrophil response than the induction of AMPs.

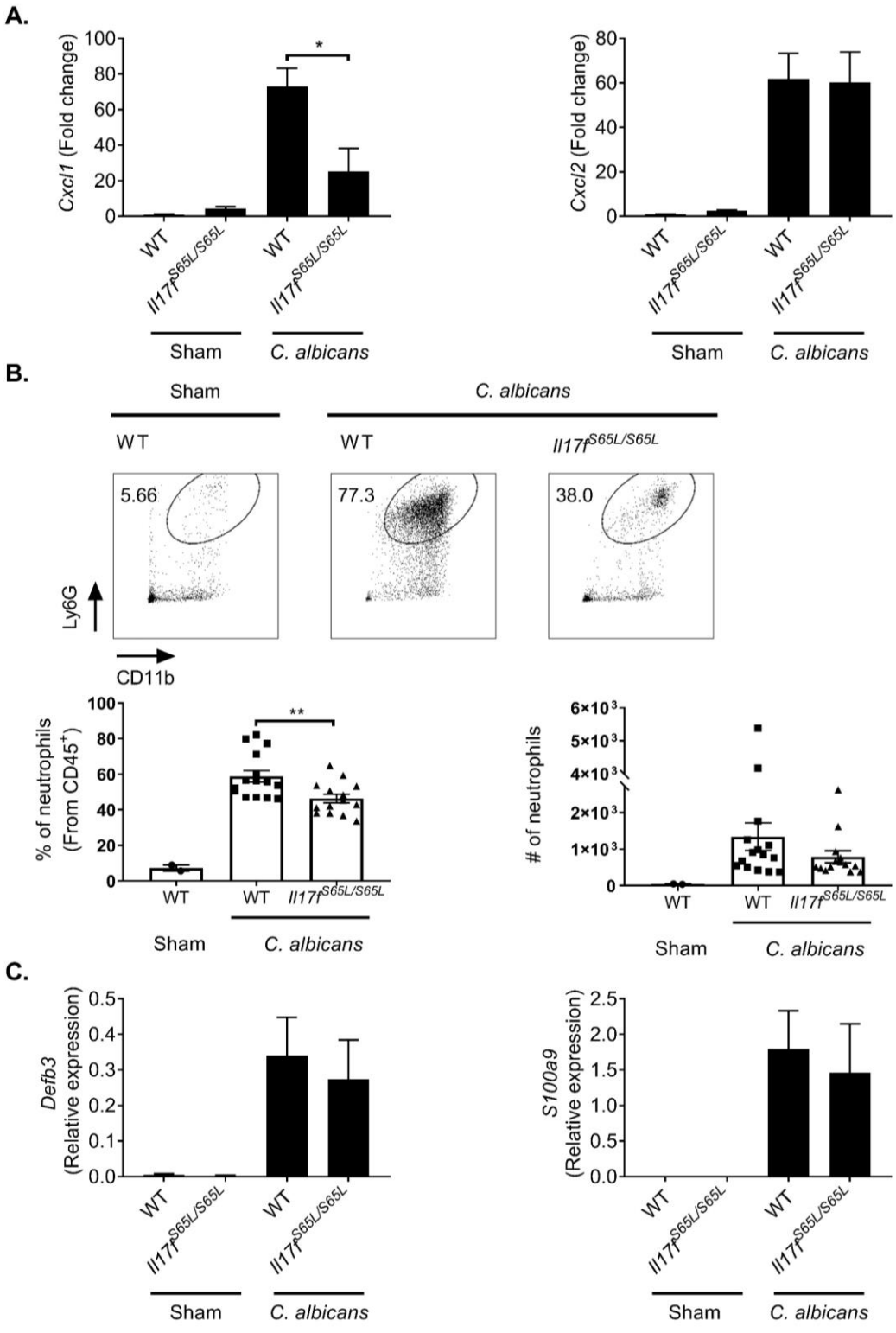

Figure 3.5 IL-17F.S65L mice exhibit impaired neutrophil recruitment during OPC

The indicated mice were infected sublingually with *C. albicans* or PBS (Sham). (A) Tongues were harvested at day 2 p.i.. Total mRNA from tongue homogenates was assessed by qPCR, normalized to *Gapdh*. Fold change compared to Sham is indicated. *Graphs* show mean + SEM. Data were merged from 2 independent experiments. (B) Single cell suspensions from tongues harvested at day 2 p.i. were analyzed by flow cytometry. Cells were gated on the $CD45^+$ live cell population and stained for CD11b and Ly6G. Left: representative FACS plots. Right: compiled results from 3 independent experiments. Graph shows mean ± SEM. (C) Total mRNA from tongue homogenates was assessed for *Defb3* (encoding β defensin 3) and *S100a9* by qPCR, normalized to *Gapdh*. Relative expression data are graphed as mean ± SEM merged from 4 independent experiments. Data were analyzed by ANOVA. *P < 0.05, **P< 0.01.

3.2.4 Increased OPC in *Il17f*$^{S65L/S65L}$ mice is not due to impaired IL-17A

IL-17A promotes antifungal activity in response to OPC [87, 231]. To determine if IL-17A expression was impacted in *Il17f*$^{S65L/S65L}$ mice, we assessed *Il17a* mRNA from tongue at day 2 p.i, a time point at which IL-17A normally peaks [142]. Interestingly, *Il17f*$^{S65L/S65L}$ mice showed elevated levels of both *Il17a* as well as *Il17f* compared to controls (Figure. 3.6A), suggesting that the higher fungal susceptibility in *Il17f*$^{S65L/S65L}$ mice is not likely due to impaired *Il17a* expression; rather, the mildness of disease susceptibility in these mice may be due to compensatory increases in IL-17A levels. To determine whether increased *Il17a* expression is directly caused by the IL-17F.S65L mutation in T cells, we subjected splenic $CD4^+$ T cells to *in vitro* differentiation for 3 days under Th17 conditions (IL-6, IL-23, TGFβ). IL-17A concentrations in culture supernatants were measured by ELISA. As shown, there was no significant difference in the amount of IL-17A produced by T cells obtained from *Il17f*$^{S65L/S65L}$, *Il17f*$^{-/-}$ or WT mice (Figure 3.6B). Thus, IL-17F.S65L does not directly cause an increase in IL-17A production in T cells.

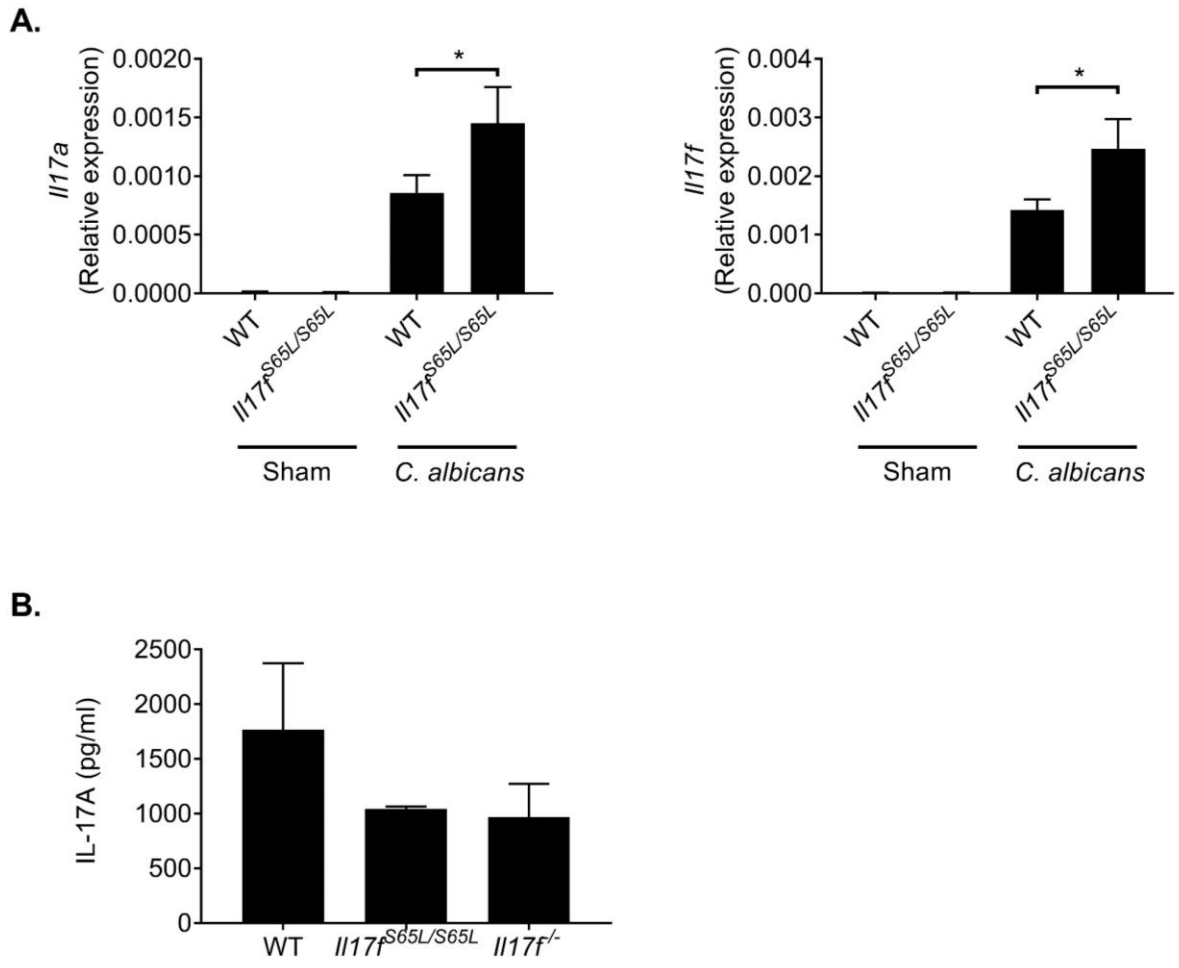

Figure 3.6 The IL-17F.S65L mutation does not influence IL-17A production from T cells

The indicated mice were infected sublingually with *C. albicans* or PBS (Sham). (A) At 2 days p.i., total mRNA was isolated from tongue and *Il17a* and *Il17f* measured by qPCR and normalized to *Gapdh*. Data show mean ± SEM from 4 independent experiments. (B) Naïve $CD4^+$ T cells from indicated mice were isolated from spleen and activated with anti-CD3 and anti-CD28 antibodies (5 ug/ml) under Th17 conditions (IL-1β, IL-6, IL-23 at 50 ng/ml and TGFβ at 5 ng/ml) for 4 days. IL-17A in supernatants was measured by ELISA. Data were analyzed by ANOVA. *$P < 0.05$.

To determine if the elevated IL-17A seen production in the tongue could compensate for IL-17F signaling in *Il17f*$^{S65L/S65L}$ mice, we treated mice with neutralizing antibodies against IL-17A [231] following OPC induction. In WT mice, blockade of IL-17A resulted in increased fungal burdens and an increased percentage of mice with fungal loads, measured at day 5 p.i., as

previously demonstrated (Figure 3.7A, B) [87]. However, IL-17A blockade in *Il17f*$^{S65L/S65L}$ mice did not further increase the oral fungal load compared to *Il17f*$^{S65L/S65L}$ isotype control mice or WT mice treated with α-IL-17A antibodies (Figure 3.7A, B). Thus, in contrast to findings in *Il17f*$^{-/-}$ mice [87], IL-17A does not compensate for the IL-17F.S65L mutation during OPC.

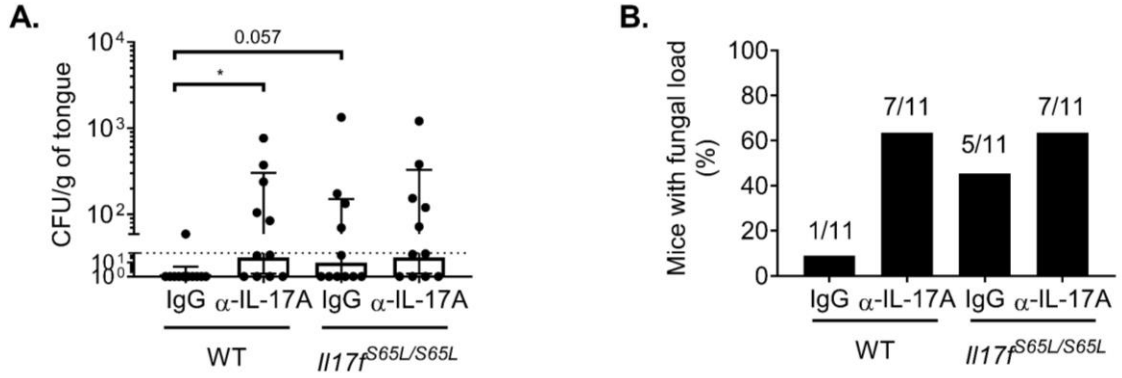

Figure 3.7 IL-17A does not compensate for IL-17F signaling in *Il17f*$^{S65L/S65L}$ mice during OPC

The indicated mice were infected sublingually with *C. albicans* or PBS (Sham). (A) Mice were injected i.p. with α-IL-17A neutralizing Abs or isotype control IgG (200ug) on days -1, 1, and 3 relative to the infection. CFU was determined on day 5 p.i.. Data were compiled from 2 independent experiments. (B) Data from panel A is represented as percentage of mice with detectable fungal loads. Values above indicate number of mice with fungal burden/total. *P < 0.05 by ANOVA and Mann-Whitney analysis.

3.2.5 IL-17F is produced dominantly by γδ T cells

Unlike humans, mice do not harbor *C. albicans* as a commensal microbe. Multiple studies have verified that the initial immune response to an oral *C. albicans* infection in mice is derived entirely from a rapid innate-like response [109, 124, 129, 232-234]. The predominant sources of IL-17A during acute OPC were previously shown to be unconventional, innate-like TCRαβ^{+} and

γδ-T cells [124, 129]. ILC3s were reported to produce IL-17A as well [109]. Using *Il17f*$^{Thy1.1}$ reporter mice [219], we observed increased levels of *Il17f*-expressing cells 2 days after *C. albicans* infection (Figure 3.8A), the time point at which *Il17f* mRNA expression peaks [87]. γδ-T cells constituted the majority of the Thy1.1^{+} population (64%), and TCRβ^{+} cells also comprised a significant portion of the Thy1.1^{+} cells (21%). A population of TCRγδ-negative TCRβ- negative cells (15.5%) that may be ILC3s was also observed (Figure 3.8B).

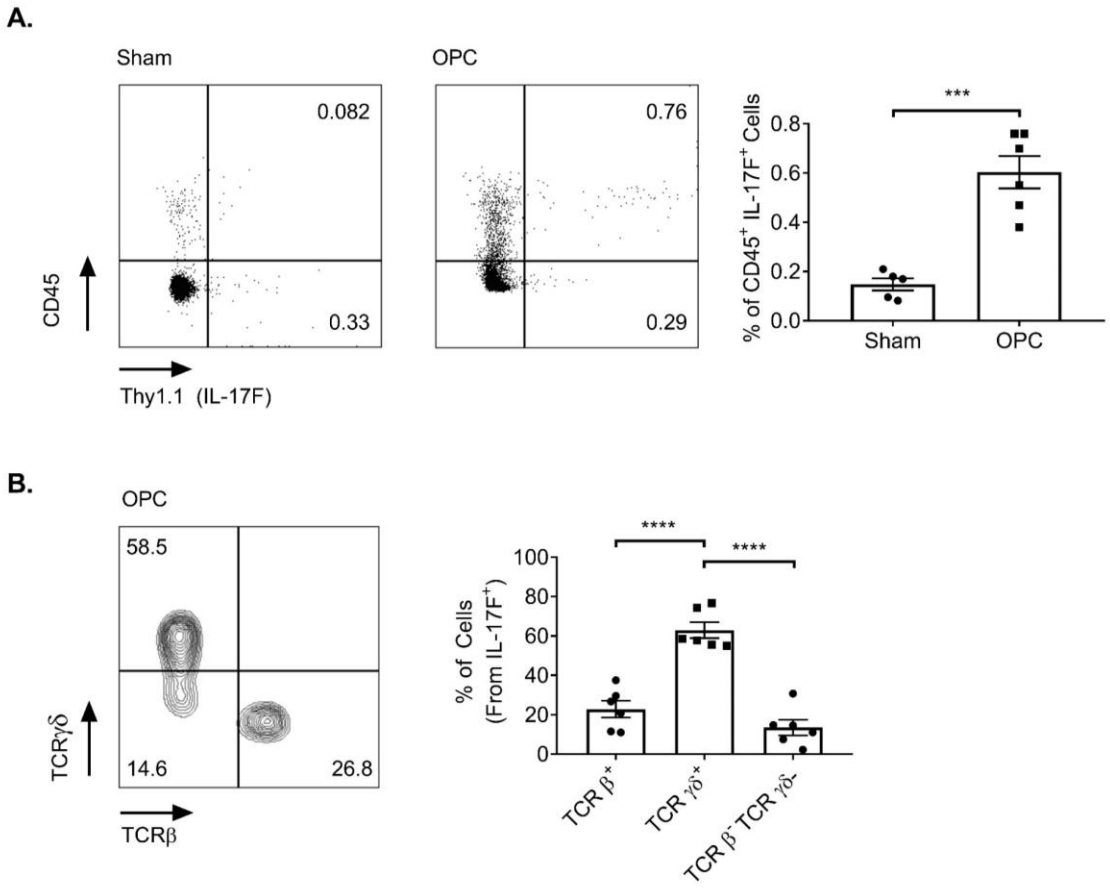

Figure 3.8 IL-17F is dominantly produced by oral γδ-T cells during OPC

Il17f$^{Thy1.1}$ reporter mice were subjected to OPC. At day 2 p.i., single cell suspensions from tongue were analyzed by flow cytometry. (A) Cells were stained for Thy1.1 (a reporter for IL-17F) and CD45 in the live lymphocyte gate. Left: representative FACS plots. Right: compiled results from 2 independent experiments. (B) Single cell suspensions from panel A were stained for TCRβ and TCRγδ in the CD45$^+$ Thy1.1$^+$ gate. Left: representative FACS plots. Right: compiled results from 2 independent experiments. Data were analyzed by ANOVA or Student's t-test. ***P < 0.001, **** < 0.0001.

3.2.6 The intestinal microbiome is required for fungal clearance during OPC

Microflora are known to regulate host immune responses. In the oral cavity, the commensal microbiome is required for the development or recruitment of innate-like TCRαβ$^+$ cells, because

innate-like TCRαβ^{+} cells are not detectable in germ-free mice [129]. Given the fact that innate-like TCRαβ^{+} cells are one of the major cellular sources of IL-17A and IL-17F during OPC (Figure 3.8B, [124, 129], I hypothesized that commensal flora are essential for IL-17-mediated antifungal immunity against *C. albicans* oral infection. To interrogate the contribution of the microbiome during OPC, germ-free mice were subjected to OPC for 5 days. In support of my hypothesis, germ-free mice demonstrated a significantly higher fungal burden compared to the WT specific pathogen free (SPF) mice (Figure 3.9). Notably, the fungal burden of germ-free mice at day 5 post infection was comparable to *Act1*$^{-/-}$ mice under SPF conditions, possibly indicating a loss of IL-17 signaling in germ free mice upon *C. albicans* oral infection (Figure 3.9).

Colonization of a single commensal microbe, segmented filamentous bacterium (SFB), in the small intestine induces Th17 cells in the lamina propria [235]. Therefore, I predicted that reconstituting SFB in germ-free mice would induce an oral type 17 immune response and thus promote fungal clearance during OPC. Accordingly, fecal pellets collected from SFB monocolonized mice were homogenized in PBS and introduced into germ-free mice by oral gavage. The mice treated with SFB were then challenged by *C. albicans* oral infection 14 days later. As expected, mice with SFB reconstitution were showed a reduced fungal burden compared to the PBS control under germ free conditions (Figure 3.9). Therefore, a single commensal microbe, SFB, is sufficient to promote fungal clearance during OPC.

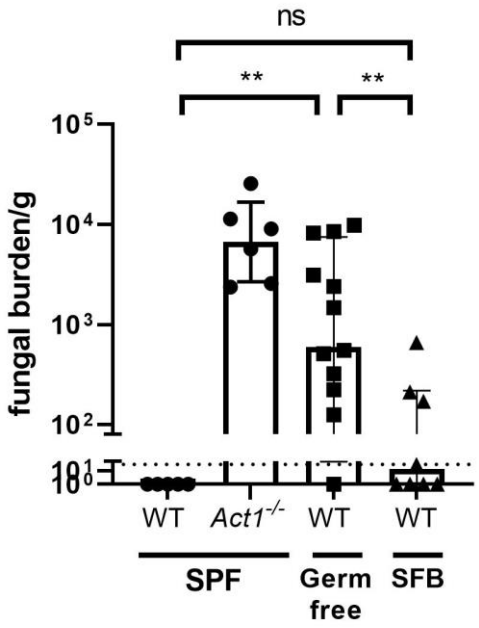

Figure 3.9 Commensal microbiome is essential for antifungal immunity during OPC

The indicated mice were subjected to OPC under germ-free or SPF conditions. The indicated mice with a age of 6 weeks were treated with SFB or PBS via oral gavage on -14 day relative to infection. Fungal burdens were assessed by CFU enumeration on YPD/Amp on day 5 post infection. Graphs show geometric mean ± SD. Dashed line indicates limit of detection (~30 CFU/g). **P < 0.01 by Mann-Whitney analysis.

3.2.7 c-Fos is not required for protection against *C. albicans* oral infection

During the early stages of a *C. albicans* oral infection, activation of innate type 17 immunity is dependent on Candidalysin secretion by *C. albicans* hyphae. c-Fos is upregulated by Candidalysin in cultured mucosal epithelial cells, such as the buccal oral epithelial cell line TR146 as well as A431 vulvovaginal cells [123, 236]. In addition, c-Fos has been reported to mediate the immune response to Candidalysin or *C. albicans* hyphae *in vitro*, as c-Fos deficiency in TR146 cell lines led to decreased expression of proinflammatory cytokines (IL-1α, IL-1β, IL-6, G-CSF, and GM-CSF) after treatment with Candidalysin or *C. albicans* hyphae [124, 127]. Thus, I

hypothesized that c-Fos may be required for mounting this early innate type 17 response to OPC. First, we examined c-Fos expression within the oral mucosa by immunohistochemistry (IHC). As shown, c-Fos is expressed tonically in the BEL of the tongue (Figure 3.10A). After infection with *C. albicans*, expression is also seen in the suprabasal SEL, starting at 8 hours p.i. and sustained for at least 24 hours (Figure 3.10A). Expression was not seen after infection with the yeast-locked (nonvirulent) *Egf1Δ/Δ* strain of *C. albicans* (Figure 3.10B), suggesting that the yeast-hyphal transition is needed to induce c-Fos expression in the oral epithelium. Thus, c-Fos is induced rapidly in the oral epithelium following infection with *C. albicans* in a hyphal-dependent manner.

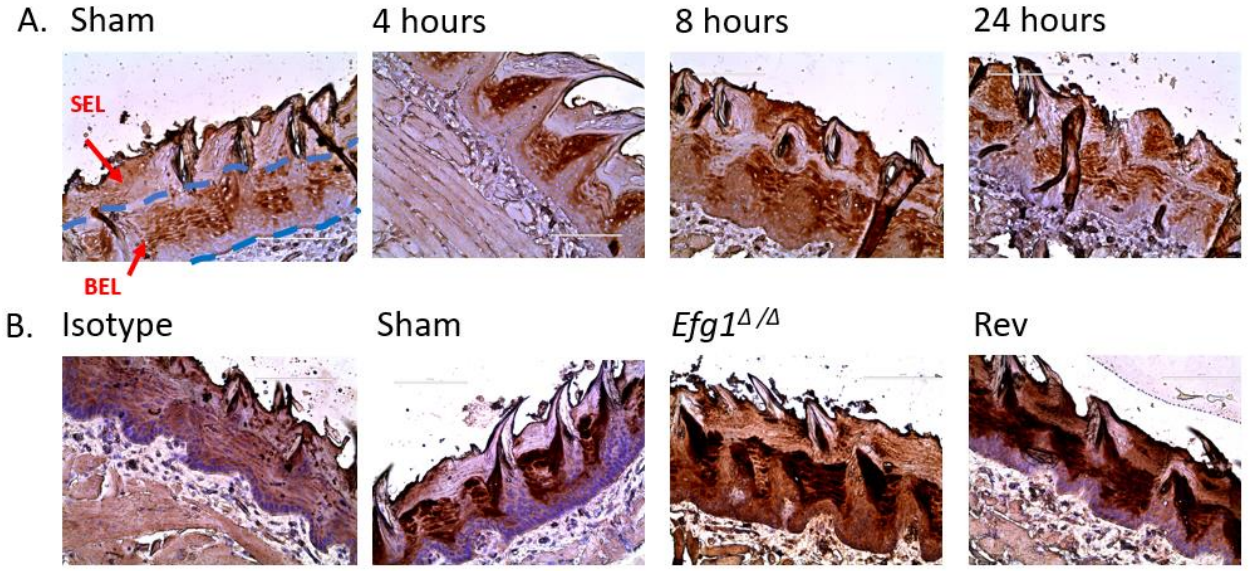

Figure 3.10 c-Fos expression at oral epithelium during OPC

(A) WT mice were subjected to OPC. Mice tongues were harvested at 4, 8, and 24 hours post infection, and c-Fos expression was analyzed by immunohistochemstiry (IHC). SEL and BEL are indicated by dashed lines and indicated by red arrows. (B) WT mice were orally challenged with *Efg1*$^{\Delta/\Delta}$ strain (yeast-locked) or revertant strain of *C. albicans* as indicated. c-Fos was stained by IHC at 24 hours post infection.

In order to elucidate the function of c-Fos in in the superficial oral epithelium during OPC, we crossed *fos*$^{fl/fl}$ mice to mice expressing the Cre recombinase under control of the murine keratin 13 (K13) promoter (*Cfos*^{K13}). This system (created by our lab) drives expression of Cre

recombinase in lingual, buccal, esophageal and vaginal epithelial cells, without expression in skin or intestinal epithelia [139, 142]. We confirmed that inducible expression of c-Fos in the SEL was absent in these mice at 24 hours p.i. (Fig 3.11A). *Cfos*^{K13} mice were infected sublingually with *C. albicans*, and weight loss and oral fungal burden were assessed at day 5. Sham (PBS)-infected WT mice and *Il17ra*$^{-/-}$ mice were used as negative and positive controls for infection clearance, respectively. As expected, WT mice fully cleared *C. albicans* by day 5 p.i., whereas *Il17ra*$^{-/-}$ mice maintained oral fungal burdens. To our surprise, the *Cfos*^{K13} mice were fully resistant to OPC, showing no weight loss or fungal clearance that was indistinguishable from WT mice (Figure 3.11B). As noted, resistance to OPC in mice requires a type 17 immune response, characterized by expression of a panel of innate immune cytokines. As shown, infected *Cfos*^{K13} mice showed normal induction of *Il17a*, *Il22*, *Il6* and AMPs such as S100A9 (Figure 3.11C).

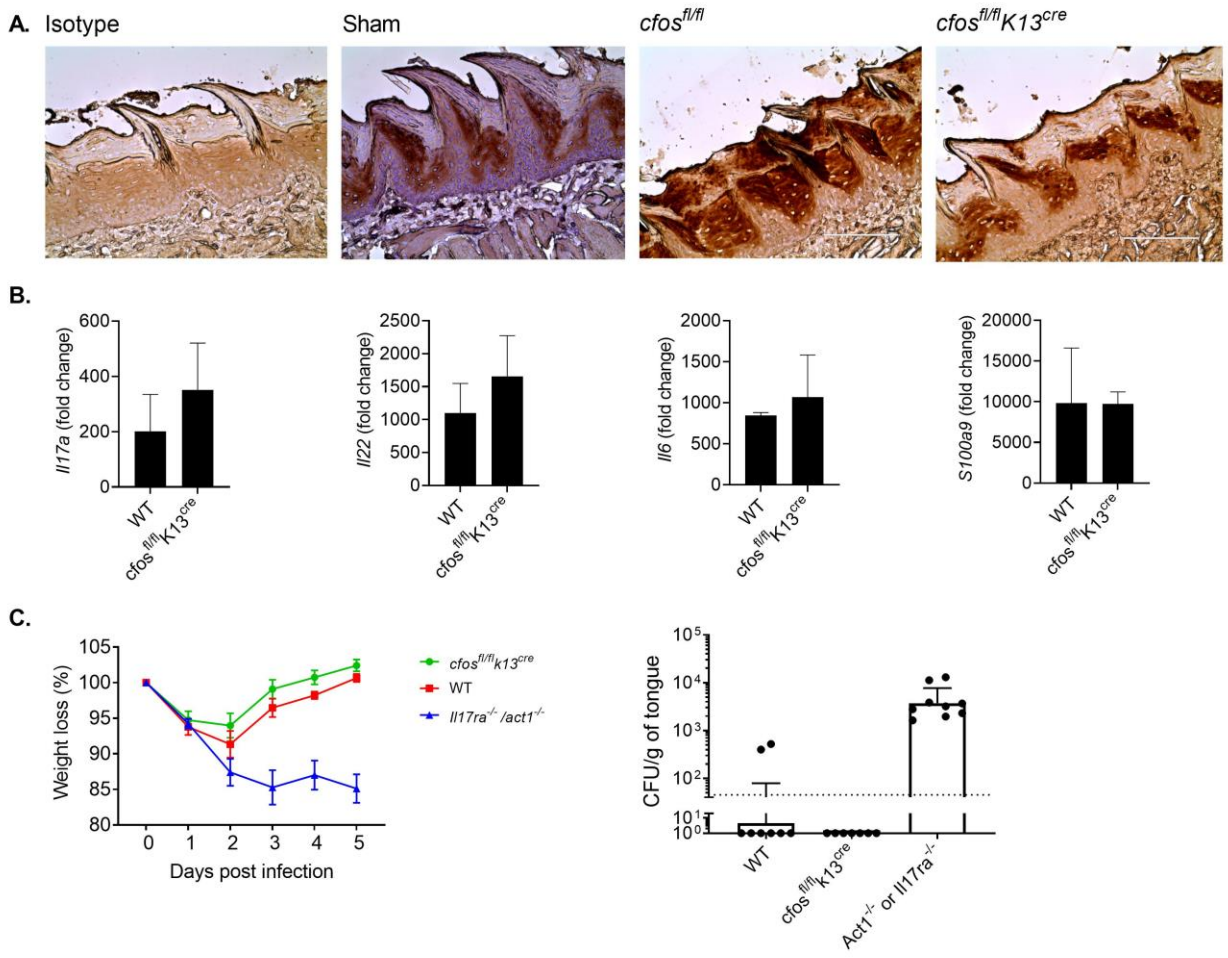

Figure 3.11 c-Fos is not required for antifungal immunity during OPC

The indicated mice were infected sublingually with *C. albicans* or PBS (Sham). (A) c-Fos expression was analyzed by IHC at 24 hours post infection. (B) Total mRNA was extracted from tongue homogenate at 24 hours post infection. mRNA expression of *Il17a*, *Il22*, *Il6*, and *s100a9* was assessed by qPCR and normalized to *Gapdh*. (C) Left: Mice weight was assessed daily and percentage loss relative to day 0 is shown for each time point. Right: Fungal burdens were assessed by CFU enumeration on YPD/Amp on day 5 p.i. Graphs show geometric mean ± SD. Dashed line indicates limit of detection (~30 CFU/g)

3.3 Discussion

C. albicans asymptomatically colonizes healthy individuals and typically only causes mucocutaneous infections in immunocompromised individuals [237, 238]. Deficits in IL-17 signaling or Th17 cell development are linked to superficial *C. albicans* infections [101, 239]. Although CMCD patients with null mutations in genes encoding IL-17RA, IL-17RC or ACT1 have all been described, no CMCD patients have been reported with a single IL-17A deficiency thus far [100]. Even anti-IL-17A biologics used to treat autoimmune disease cause only a modest increase in mucocutaneous *Candida* infections [103, 240].

In general, observations in mouse models of OPC have been accurate predictors of the immune correlates in oral candidiasis, especially with regards to the IL-17 axis [36, 105, 241, 242]. Mice treated with IL-17A neutralizing antibodies have lower fungal burdens compared to the *Il17ra*$^{-/-}$ mice during OPC [87, 231], which parallels the low percentage of patients who experience mild *C. albicans* mucocutaneous infections during secukinumab or ixekizumab treatment [78, 79, 103, 240]. Unlike humans [93, 243], laboratory mice do not harbor *C. albicans* as a commensal organism, and hence the acute OPC model system reflects events in the innate response [124, 125, 129, 232]. Nonetheless, mice generate potent and protective recall Th17 responses to *C. albicans* after a secondary encounter, similar to humans [232, 233, 244]. Humans with STAT3 mutations experience CMC [101], and although STAT3 is not required in CD4^{+} cells to protect from OPC, we recently found that STAT3 is essential in oral epithelium [129, 142]. Mice express different AMPs than humans do, especially in the saliva [245, 246]. Of relevance to *C. albicans* infections, the AMP β-defensin 3 is essential to prevent OPC in mice [139], though this protein has no direct orthologue in humans [247, 248].

Although humans with the IL-17F.S65L mutation were only described in a single kindred, the degree to which the phenotype of *Il17f*$^{S65L/S65L}$ knockin mouse is similar or different from humans is a matter of interpretation. While mice with a complete IL-17F deficiency do not recapitulate the CMC phenotype found in humans with the IL-17F.S65L mutation, mice with the analogous IL-17F mutation do exhibit OPC in the homozygous state, pointing to similarities among species. Puel *et al*. reported that 70% of the individuals carrying the IL-17F.S65L mutation (5/7) had a confirmed diagnosis of mild CMCD [99]. In contrast, almost all the *Il17f*$^{S65L/+}$ mice fully cleared *C. albicans* from the mouth and were statistically indistinguishable from WT controls. However, susceptibility was seen in mice carrying the mutation on both alleles, contrasting with the lack of susceptibility previously documented in *Il17f*$^{-/-}$ mice [87]. This observation could be interpreted to mean there is no dominant-negative activity of this mutation in mice. However, the CFU enumeration system used to quantify OPC likely underestimates the actual number of infectious fungi, since *Candida albicans* hyphae are not easily separable into single cells and hence each colony may represent more than a single organism [249]. The finding that fungal susceptibility in *Il17f*$^{S65L/S65L}$ mice more closely resembled that in *Il17a*$^{-/-}$ mice than that in *Il17f*$^{-/-}$ mice may imply there is some level of dominant-negative activity that the OPC model cannot sufficiently detect [87]. Additionally, there is one other report of a human IL-17F mutation, but unfortunately the nature of the mutation was not provided, so no functional inferences can be made [250].

Blocking IL-17A together with IL-17F increases susceptibility to OPC, compared to blockade of IL-17A alone [87, 109]. However, administration of IL-17A neutralizing antibodies (which also efficiently block IL-17AF [87]) in *Il17f*$^{S65L/S65L}$ mice did not further increase susceptibility to OPC, suggesting that residual IL-17A homodimers present in these mice do not

provide additional detectable protection. Clearly, there is more to learn about the role of IL-17F in antifungal immunity.

Taken together, the above results are consistent with a protective role for the heterodimer IL-17AF in OPC, which has been challenging to determine due to a paucity of reagents to study the heterodimer. Studies in human fibroblasts showed that the IL-17F.S65L mutation impaired signaling of both the IL-17F homodimer and the IL-17AF heterodimer [99]. The increased susceptibility to OPC in *Il17f*$^{S65L/S65L}$ mice could be due either to a contribution of IL-17F homodimer and/or the IL-17AF heterodimer. Nonetheless, neutralization of IL-17F did not cause an increase in fungal loads in WT mice [109], suggesting that a deficiency of the IL-17AF heterodimer rather than (or in addition to) IL-17F could be responsible for increased fungal loads in *Il17f*$^{S65L/S65L}$ mice. A protective role of IL-17AF could also explain why IL-17A blockade failed to further promote fungal infection in *Il17f*$^{S65L/S65L}$ mice. If IL-17AF is indeed the primary effector cytokine among the three IL-17RA/IL-17RC receptor ligands, the increased susceptibility to OPC caused by anti-IL-17A treatment could be due to blockade of IL-17AF rather than the IL-17A homodimer, as generally assumed [87]. Since *Il17f*$^{S65L/S65L}$ mice have a fully impaired IL-17AF signaling pathway, this could explain why anti-IL-17A antibody treatment did not lead to higher fungal burden than isotype control antibodies.

An unexpected observation made in these studies was that the IL-17F.S65L mutation affected CXCL1 mRNA expression and subsequent neutrophil recruitment in the setting of OPC, yet had no detectable impact on expression of the key antifungal AMPs, β-defensin 3 and S100A8/A9 (calprotectin). IL-17 is a potent regulator of the neutrophil axis, acting on target epithelial cells to induce chemokines that in turn recruit CXCR2-expressing neutrophils, among other myeloid cells [141]. It is unclear if this moderate suppression of neutrophils accounts for the

susceptibility phenotype in mice with the S65L mutation. In fact, not all studies of OPC have found that IL-17 regulates neutrophil infiltration during *C. albicans* infection [251]; the reason for the discrepancy among laboratories is unclear, but could possibly relate to effects of different local oral microbiota [252, 253].

Host-microbiota interactions play important roles in modulating the immune response, which is particularly prominent in antifungal immunity. Disruption of the oral microbiome by broad spectrum antibiotic therapy has been shown to increase proportions of *C. albicans* [254]. Similarly, mice treated with antibiotics show elevated fungal burdens during OPC [252]. Here, I further elucidated the role of the microbiome in mucosal *C. albicans* infections, showing that germ-free mice are highly susceptible to OPC at levels similar to mice with IL-17 deficiency.

Notably, SFB reconstitution in germ-free mice reversed the increased fungal burden during OPC. SFB is a commensal microbe commonly found in the gut of mice. Intestinal colonization of SFB has been shown to skew mucosal effector T cells to a Th17 dominated milieu [235]. Thus, the protective function of SFB during OPC might be mediated by upregulation of the type 17 immune response in oral mucosa. It should be noted that conventional, adaptive, Th17 cells are not activated during a first encounter with OPC, even in mice with a specific pathogen free (SPF) microbiome. Instead, innate TCR$\alpha\beta^+$ cells and $\gamma\delta$ T cells are major cellular sources of IL-17A and IL-17F during primary *C. albicans* oral infections [124, 129]. The colonization of innate TCR$\alpha\beta^+$ cells in the oral mucosa requires existence of commensal microbiota, as tongue tissue of germ-free mice showed a decrease in TCR$\alpha\beta^+$ cells [129]. Thus, the impaired fungal clearance in germ-free mice during OPC may be caused by a lack of oral mucosa-resident TCR$\alpha\beta^+$ cells, and reconstitution of SFB promotes fungal clearance by driving TCR$\alpha\beta^+$ cells to occupy a niche in the oral mucosa.

In agreement with this, intestinal colonization of SFB has been reported to induce inflammation in non-intestinal tissues. For instance, germ free mice that are normally resistant to EAE develop robust disease after monocolonization with SFB [255]. Presence of SFB in the gut can also protect mice from acute methicillin-resistant *Staphylococcus aureus* (MRSA) lung infection [256]. Therefore, intestinal colonization of SFB might similarly promote antifungal immunity against *C. albicans* in oral mucosa. However, I could not yet rule out the possibility that oral resident SFB could directly induce type 17 immune responses in the oral mucosa, an issue that will need to be explored further.

The activation of innate type 17 immunity against *C. albicans* is also attributed to Candidalysin, a virulence factor secreted by *C. albicans* hyphae. Candidalysin induces the immune response by stimulating oral epithelial cells to secrete IL-1α/β, which promotes proliferation of innate TCRαβ cells for IL-17 signaling [124]. c-Fos is a transcription factor that is upregulated upon candidalysin activation in an OEC line, TR146 [123]. TR146 cells lacking c-Fos showed an impaired immune response upon the *in vitro* challenge of *C. albicans* [127]. Thus, c-Fos appeared to be an important factor in Candidalysin-induced immunity against *C. albicans*. Based on this, I predicted that Candidalysin-induced c-Fos expression is critical for fungal clearance during OPC. Although I found that c-Fos is expressed in SEL in a *C. albicans* hyphae-dependent manner, loss of c-Fos in SEL surprisingly did not impact fungal clearance during OPC. Notably, Candidalysin not only activates the downstream c-Fos signaling pathway, but also damages OECs. Thus, damage-induced IL-1α/β expression might compensate for the loss of c-Fos in OECs during oral *C. albicans* infections. Furthermore, a single point mutation in Candidalysin, Ece1-III$_{62–93AA}$, is shown to activate c-Fos expression, but does not induce cell damage *in vitro*. The mutant peptide could still activate the non-damage associated cytokine G-CSF, but failed to induce expression of

IL-1α. This may indicate that a damage-dependent pathway, rather than c-Fos signaling, contributes to Candidalysin-mediated IL-1α/β secretion.

Although the IL-17RA/IL-17RC heterodimer is the canonical receptor complex thought to transduce signaling in response to IL-17A, IL-17F and IL-17AF [21, 42], several alternative configurations of the receptor have been recently proposed. IL-17RD was suggested by Chen Dong's group to act in keratinocytes in concert with IL-17RA to mediate IL-17A signaling, but not IL-17F signaling, to drive psoriasis-like skin inflammation [24]. Thus far, the binding capacity of IL-17AF to an IL-17RA/RD receptor complex has not been characterized. In the OPC model, *Il17rc*$^{-/-}$ mice phenocopy *Il17ra*$^{-/-}$ mice in terms of fungal loads and other aspects of disease [36], suggesting that IL-17RC is needed to mediate immunity. *Il17rc*$^{-/-}$ mice are also susceptible to dermal candidiasis [257]. Likewise, humans with *IL17RC* null mutations experience CMCD [98]. Hence, it is unlikely that an IL-17RC-independent receptor complex mediates host-defense during mucocutaneous candidiasis.

A recent structural analysis of the IL-17RC subunit unexpectedly revealed that IL-17F may have the ability to signal through an IL-17RC homodimeric receptor [258], though this would contrast with our prior molecular studies showing that a forced dimer of murine IL-17RC is not signaling-competent [28]. Interestingly, the binding site of S65 in IL-17F was shown to be located on IL-17RA [19]. A mutation on this residue is likely to impair the binding activity of IL-17F to IL-17RA rather than IL-17RC, so changes in binding affinity to IL-17RC homodimeric receptor would likely be less pronounced [23]. Putting this together, we speculate that the increased fungal burden in *Il17f*$^{S65L/S65L}$ mice is caused by reduced interactions of IL-17F with the IL-17RA/IL-17RC heterodimer, rather than with the IL-17RC homodimeric receptor (see detailed discussion of these receptors in Chapter 5.2).

In summary, results from this new IL-17F.S65L mutant mouse strain in the murine OPC model are generally, though not completely, in line with findings in CMCD patients with the IL-17F.S65L mutation. These data help reconcile the observations that, whereas a complete IL-17F deficiency does not promote candidiasis in mice, this naturally occurring IL-17F mutation in humans does. The potential utility of this new mouse strain goes beyond studies of candidiasis. Because these mice show a different phenotype from *Il17f*$^{-/-}$ mice with respect to OPC, they could be a valuable tool to interrogate the functions of IL-17F and the enigmatic IL-17AF heterodimer in other settings where these cytokines may participate, such as DSS colitis and AGN.

4.0 Divergent functions of IL-17-family cytokines in autoimmune disease: Lessons from a naturally occurring human mutation in IL-17F

4.1 Background

IL-17A and IL-17F exert similar yet distinct *in vivo* biological activities, which is illustrated by their roles in OPC (Chapter 3). In this chapter, I focus on using the IL-17F.S65L mice to define the *in vivo* functions of IL-17F in two autoimmune disease models, DSS colitis and AGN. Whereas IL-17A and IL-17F were reported to have opposite roles during DSS colitis [86, 89], *Il17a*$^{-/-}$ mice and *Il17f*$^{-/-}$ mice showed a similarly resistant phenotype in an AGN model [88].

In the DSS colitis model, IL-17A and IL-17F appear to have very different biological activities. Multiple groups have demonstrated that *Il17ra*$^{-/-}$, *Il17a*$^{-/-}$ and mice treated with IL-17A neutralizing antibodies all show exacerbated DSS colitis. This phenotype has been attributed to reduced intestinal repair [86, 166-168]. Consistently, in humans, IBD is a side effect of anti-IL-17A biologics for treatment of psoriasis [240]. In addition, clinical trials for IL-17A targeting therapies have been halted due to worsening outcomes in CD patients [164, 165]. Taken together, all these data suggest a protective role of IL-17A during DSS colitis.

In contrast, loss of IL-17F in the murine DSS colitis model led to an improved outcome, suggesting that IL-17F is pathogenic in this setting [86, 89]. The resistant phenotype of *Il17f*$^{-/-}$ mice during DSS colitis was attributed to regulation of enteric microbiota [89]. Specifically, *Clostridium* cluster XIVa was reported to be upregulated in *Il17f*$^{-/-}$ mice, leading to increased levels of intestinal resident Tregs, which are known to be responsible for controlling DSS- induced inflammation. Therefore, IL-17A and IL-17F function in an opposing manner during DSS colitis,

but the mechanism for this dichotomy is not well understood, and will be discussed here.

With respect to AGN, *Il23p19*$^{-/-}$, *Il17a*$^{-/-}$, and *Il17ra*$^{-/-}$ mice demonstrated a pathogenic role of IL-17A in various AGN models. Consistent with these findings, observations from clinical studies indicated that circulating IL-17A and the number of IL-17A-producing cells are upregulated in patients with chronic kidney disease, including IgA nephropathy, lupus nephritis, and ANCA-associated glomerulonephritis. These hint at a pathogenic function of IL-17A in human diseases. Multiple IL-17A target genes are involved in this process, which leads to direct kidney damage, tubular atrophy, fibrosis formation, and neutrophil recruitment during the development of AGN. The physiological function of IL-17F is not as well understood as IL-17A, in AGN models. There is one report indicating that *Il17f*$^{-/-}$ mice are resistant to anti-GBM nephritis, which is consistent with the phenotype of *Il17a*$^{-/-}$ mice in the same settings. Neutrophil-attracting chemokines, such as CXCL1 and CXCL5, were found to be decreased in *Il17f*$^{-/-}$ mice in the anti-GBM nephritis model, which might contribute to the protective phenotype of *Il17f*$^{-/-}$ mice. Therefore, different from DSS colitis model, data thus far indicate that IL-17A and IL17F exhibit similar biological activity in AGN. However, relatively little is known about this process, and drugs targeting IL-17/Th17 cells have not been used under these conditions.

IL-17F.S65L, a naturally-occurring mutation in IL-17F (see Chapter 3), may be a useful tool to understand the functional differences between IL-17A and IL-17F. The mouse IL-17F.S65L mutation appears to be mainly a loss-of-function mutation *in vitro*, as the IL-17F.S65L variant showed reduced activation of IL-17F target genes such as *Cxcl1* and *Il6* (Figure 3.1) [99]. However, the impact of the IL-17F.S65L mutation goes beyond a loss of IL-17F function *in vivo*. As described in Chapter 3, *Il17f*$^{S65L/S65L}$ mice demonstrated more *C. albicans* susceptibility more similar to *Il17a*$^{-/-}$ mice than to *Il17f*$^{-/-}$ mice. Thus, given the fact that a single point mutation in IL-

17F could cause an *Il17a*$^{-/-}$-like phenotype *in vivo*, we aimed to elucidate the phenotype of *Il17f*$^{S65L/S65L}$ mice in disease models in which IL-17A and IL-17F behave differently, in comparison to those where IL-17A and IL-17F share similar biological activities. Therefore, in this chapter, *Il17f*$^{S65L/S65L}$ mice were tested in DSS colitis and AGN. In agreement with the findings in the OPC setting, *Il17f*$^{S65L/S65L}$ mice showed a similar phenotype to *Il17a*$^{-/-}$ mice during DSS colitis. In contrast, the IL-17F.S65L mutation did not have any impact on the development of AGN. Details of these systems are discussed in detail in the following sections.

4.2 Results

4.2.1 IL-17A and IL-17F play opposing roles in DSS colitis

As noted, IL-17A was reported to be protective but IL-17F was pathogenic in DSS colitis [86, 89]. To determine the mechanistic basis for this difference between IL-17A and IL-17F, I used the above-described *Il17f*$^{S65L/S65L}$ mice in the DSS-induced model of colitis. Importantly, the enteric microbiota exert a major influence on outcomes of intestinal inflammation [259]. Thus, the phenotype of mice with DSS-induced intestinal epithelial damage can vary considerably across facilities. Before evaluating the phenotype of *Il17f*$^{S65L/S65L}$ mice in DSS colitis model, I confirmed the respective functions of IL-17A and IL-17F in DSS colitis in our hands. *Il17a*$^{-/-}$, *Il17f*$^{-/-}$, *or* WT controls (C57BL/6), were given 2% DSS in drinking water for 7 days. Weight was recorded daily, and colon length was measured upon sacrifice on day 10 post-treatment. Consistent with prior reports, mice lacking IL-17A (*Il17a*$^{-/-}$) or IL-17RA (*Il17ra*$^{-/-}$) lost significantly more weight than WT control mice, with most requiring sacrifice by day 8 for humane reasons (Figure 4.1A).

Commensurate with this, colon lengths of *Il17a*$^{-/-}$ mice were markedly shorter than WT mice (Figure 4.1B). Thus, as previously reported, IL-17A signaling through IL-17RA is protective in DSS colitis [86, 89, 166-168].

IL-17F also signals through IL-17RA, yet *Il17f*$^{-/-}$ mice did not lose as much weight as WT mice upon DSS treatment (Figure 4.1A), and *Il17f*$^{-/-}$ colons were significantly longer than WT colons at day 10 (Figure 4.1C). Therefore, and in agreement with previous reports, IL-17F is pathogenic in DSS and contrasts with IL-17A [86, 89].

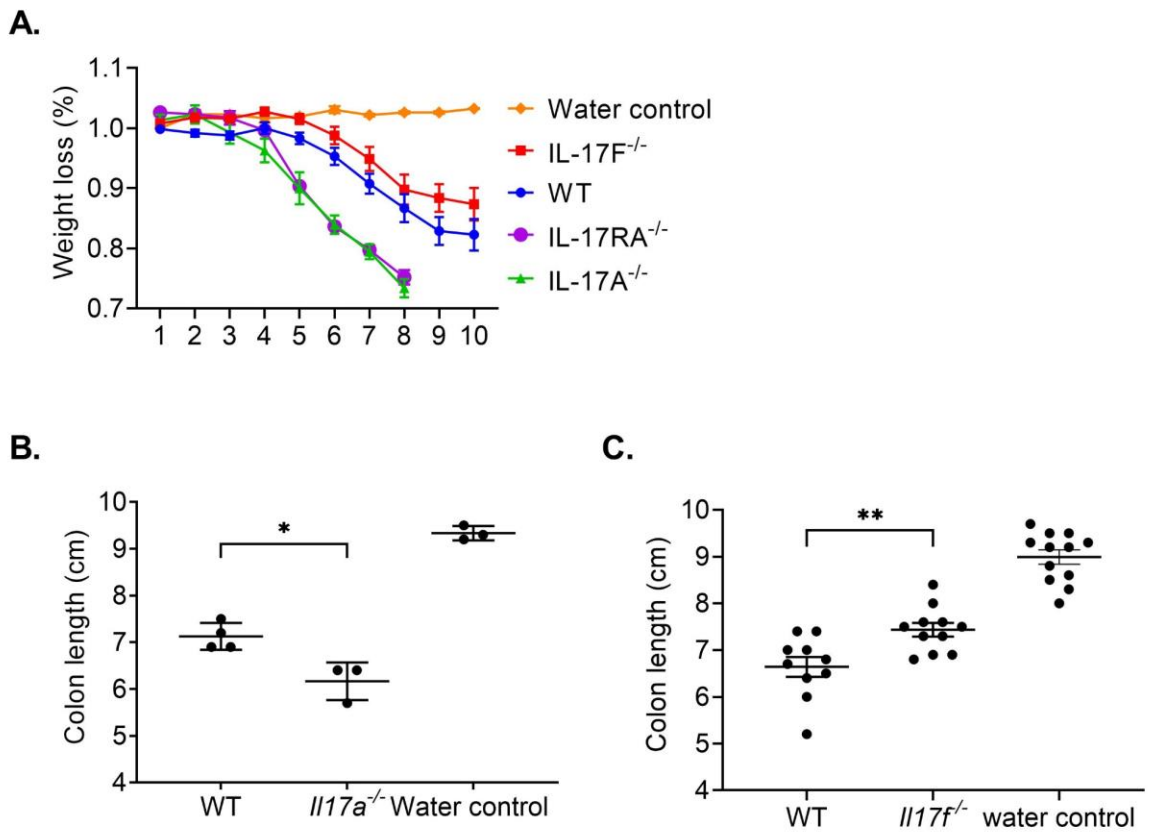

Figure 4.1 Inhibition of IL-17A and IL-17F showed opposite phenotypes in DSS-induced colitis.

The indicated mice were treated with 2% DSS-containing water for 7 days. The DSS-containing water was replaced with normal drinking water for another 3 days. (A) Body weight was monitored daily and the percentage relative to starting weight was shown for each time point. Mice with more than 25% weight loss were sacrificed for humane reason. Data were compiled from 5 experiments (B) Colon lengths of *Il17a*$^{-/-}$ mice were determined at day 8 post treatment. (C) Colon lengths of *Il17f*$^{-/-}$ mice were measured at day 10 post treatment. Data were compiled from 3 experiments. Each dot (B, C) represents an individual mouse. Graph shows mean ± SEM. Data were analyzed by student t test. *P < 0.05, **P < 0.01.

4.2.2 *Il17f*$^{S65L/S65L}$ mice showed an increased susceptibility in DSS colitis

Humans with an IL-17F.S65L mutation were identified on the basis of susceptibility to OPC, and the sequence surrounding this residue is highly conserved in mice [99]. IL-17F.S65L dimers (present in both mouse and human) are non-functional at physiological cytokine concentrations [99]. As shown in Chapter 3, *Il17f*$^{S65L/S65L}$ mice showed a susceptibility profile to OPC that was more similar to that of *Il17a*$^{-/-}$ mice than *Il17f*$^{-/-}$ mice, suggesting that the IL-17F.S65L mutation may in some way interfere with IL-17A function. Since DSS colitis is one of the few known conditions where IL-17A and IL-17F exhibit opposing phenotypes, we assessed the impact of this mutation in the context of intestinal inflammation. Accordingly, *Il17f*$^{S65L/S65L}$ mice were administered 2% DSS in drinking water, and scored for disease severity based on weight loss, stool consistency and rectal bleeding for 9 consecutive days. Upon sacrifice, colon length was measured. Strikingly, DSS treatment consistently caused *Il17f*$^{S65L/S65L}$ mice to lose more weight, exhibit higher disease scores, and have shorter colon lengths than WT mice (Figure 4.2A-C). Thus, as we observed during OPC, the *Il17f*$^{S65L/S65L}$ mice resembled IL-17A-deficient mice rather than IL-17F-deficient mice.

We next sought to understand the basis for susceptibility to DSS colitis in these settings. In *Il17a*$^{-/-}$ mice, susceptibility has been attributed in part to a loss of intestinal epithelium integrity, as discussed in details in Chapter 1.4.2.1 [167, 169]. To determine whether the *Il17f*$^{S65L/S65L}$ mice and *Il17a*$^{-/-}$ mice share a similar mechanism to promote colitis severity, *Il17f*$^{S65L/S65L}$ mice and WT control mice were orally treated with FITC-Dextran after 7 days of DSS treatment to measure gut epithelium integrity. Unexpectedly, *Il17f*$^{S65L/S65L}$ mice showed a similarly elevated FITC-Dextran concentrations compared to WT mice (Figure 4.2D). These data indicated that intestinal epithelium integrity is not attributable to increased DSS-induced inflammation in *Il17f*$^{S65L/S65L}$ mice, which

differs from findings in *Il17a*$^{-/-}$ mice.

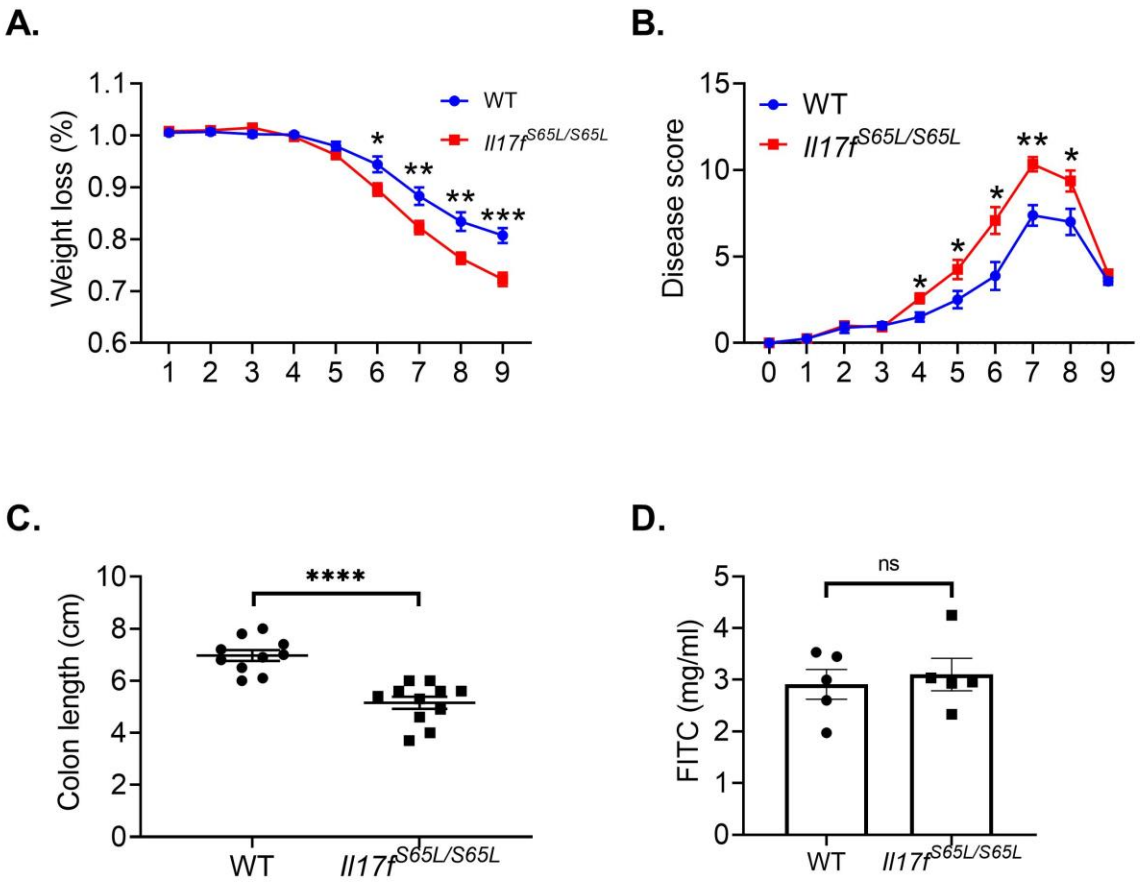

Figure 4.2 *Il17f*$^{S65L/S65L}$ mice are susceptible to DSS-induced colitis

The indicated mice were treated with 2% DSS-containing water for 7 days. The DSS-containing water was replaced with normal drinking water for another 2 days. (A) Body weight was monitored daily and the percentage relative to starting weight was shown for each time point. Mice with more than 25% weight loss were sacrificed for humane reason. (B) The disease scores were assessed daily and calculated based on weight loss, anal bleeding and stool consistency. (C) Colon lengths of *Il17a*$^{-/-}$ mice were measured at day 9 post DSS treatment. Each dot represents an individual mouse. Graph shows mean ± SEM. (A-C) Data were compiled from 3 individual experiments (D) Mice were oral gavaged with FITC-dextran at day 7 post DSS treatment. Mice were harvested 4 hours after oral gavage and plasma concentration of FITC-dextran was calculated. Each dot represents an individual mouse. Graph shows mean

± SEM. Data were compiled from 2 individual experiments. Data were analyzed by student t test. *P < 0.05, **P < 0.01, ***P < 0.001, ****P < 0.0001.

4.2.3 Decreased colonization of intestinal Clostridium cluster XIVa in *Il17f*$^{S65L/S65L}$ mice

IL-17F promotes pathogenesis in DSS colitis, and the damaging effect of IL-17F was reported to be caused by increased burden of *Clostridium* cluster XIVa in the colonic epithelium specific microbiota [89]. Therefore, I hypothesized that cohousing *Il17f*$^{S65L/S65L}$ mice with *Il17f*$^{-/-}$ mice would enhance the *C.* XIVa burden in *Il17f*$^{S65L/S65L}$ mice, and thus protect *Il17f*$^{S65L/S65L}$ mice against DSS-induced inflammation. To test this hypothesis, *Il17f*$^{S65L/S65L}$ mice were cohoused with *Il17f*$^{-/-}$ mice for two weeks, followed by another week of 2% DSS treatment. Surprisingly, cohousing *Il17f*$^{S65L/S65L}$ mice with *Il17f*$^{-/-}$ mice did not alter the susceptibility of DSS colitis in *Il17f*$^{S65L/S65L}$ mice (Figure 4.3B). Instead, the cohoused *Il17f*$^{-/-}$ mice showed greater weight loss, compared to their non-cohoused littermates (Figure 4.3A). Consistent with this, the colons of cohoused *Il17f*$^{-/-}$ mice were shorter than the non-cohoused controls (Figure 4.3B). To further explore this unexpected observation, I analyzed the *C.* XIVa burdens in stools collected prior to initiating DSS treatment. The fecal *C.* XIVa levels from *Il17f*$^{S65L/S65L}$ mice were lower than WT mice, which might contribute to the increased severity of DSS in *Il17f*$^{S65L/S65L}$ mice. However, in contrast to the previous report [89], the levels of *C.* XIVa in *Il17f*$^{-/-}$ mice and WT mice were comparable (Figure 4.3C). Notably, *C.* XIVa levels in the cohoused *Il17f*$^{-/-}$ mice were significantly lower than those in non-cohoused littermates but were comparable to levels of *C.* XIVa in *Il17f*$^{S65L/S65L}$ mice. Collectively, these data indicated that intestinal microbiota, likely via the *Clostridium* cluster XIVa, positively correlated with enhanced signs of intestinal inflammation in *Il17f*$^{S65L/S65L}$ mice.

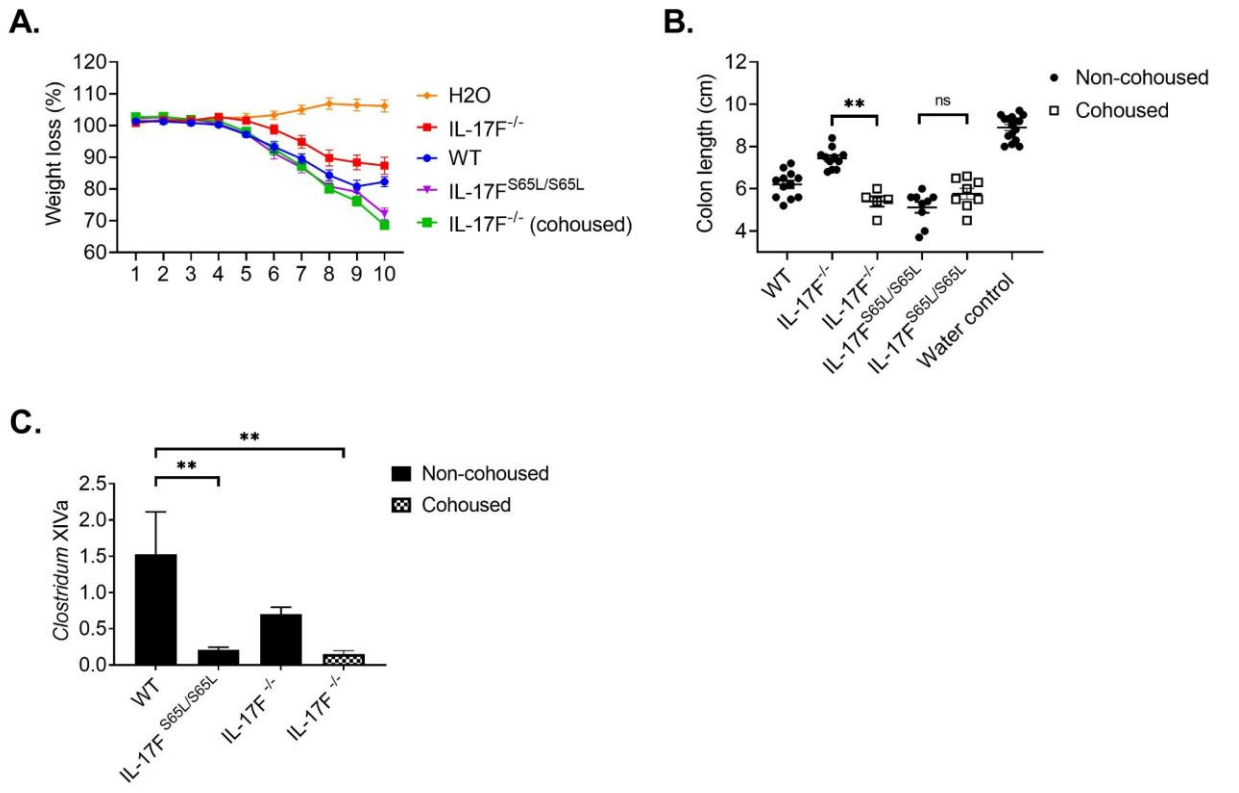

Figure 4.3 The commensl *C.* XIVa population is reduced in *Il17f*$^{S65L/S65L}$ mice

Il17f$^{S65L/S65L}$ mice and WT mice were cohoused for 2 weeks. The indicated mice were subjected for DSS treatment for 7 days. The DSS-containing water was replaced with normal drinking water for another 3 days. (A) Body weight was monitored daily and the percentage relative to starting weight was shown for each time point. Mice with more than 25% weight loss were sacrificed for humane reasons. (B) Colon lengths of the indicated mice were determined at day 10 post DSS treatment. Each symbol represents an individual mouse. Graph shows mean ± SEM. Data were analyzed with student t analysis. (A, B) Data were compiled from 3 individual experimets. (C) Feces from the indicated mice were collected before the DSS treatment. Fecal commensal bacteria were isolated and the level of *C.* XIVa was determined by qPCR analysis. Graph shows mean ± SEM. Data were compiled from 2 independent experiments and analyzed with Mann-Whitney analysis. **P < 0.01

4.2.4 IL-17F.S65L regulates colonic Treg cell levels

Colonic Tregs differentiation is dependent on signals derived from intestinal microbiota [260]. The *C.* XIVa cluster is a major constituent of the mouse gut microbiome and is known to promote Treg accumulation in the colon and thereby maintain gut homeostasis [170]. In particular, *Il17f*$^{-/-}$ mice were reported to have elevated levels of colonic Tregs compared to WT mice, with ablation of Tregs in *Il17f*$^{-/-}$ mice claimed to be responsible for reversing the impact of IL-17F deficiency [89]. To evaluate the function of IL-17F.S65L in regulating colonic Treg cells, we quantified colonic $CD4^+Foxp3^+$ cells in *Il17f*$^{S65L/S65L}$ mice at day 9 post-DSS treatment. As shown, the proportion of $CD4^+Foxp3^+$ Treg cells was decreased in DSS-treated *Il17f*$^{S65L/S65L}$ mice, compared to WT mice (Figure 4.3A, B). Thus, loss of colonic Treg cells correlated with exacerbated colitis in this setting. Consistent with the *C.* XIVa colonization results (Figure 4.3C), colonic Treg cell levels in *Il17f*$^{-/-}$ mice are comparable to those in WT mice (Figure 4.4A,C). Furthermore, co-housing with $Il17f^{S65L/S65L}$ mice led to a decreased numbers of enteric Treg cells in *Il17f*$^{-/-}$ mice (Figure 4.4B,C). Taken together, these data indicated that colonic Treg cells correlate with levels of *C.* XIVa. Therefore, the IL-17F.S65L mutation affects Treg cell frequencies in DSS colitis, which could be mediated by regulating intestinal *C.* XIVa.

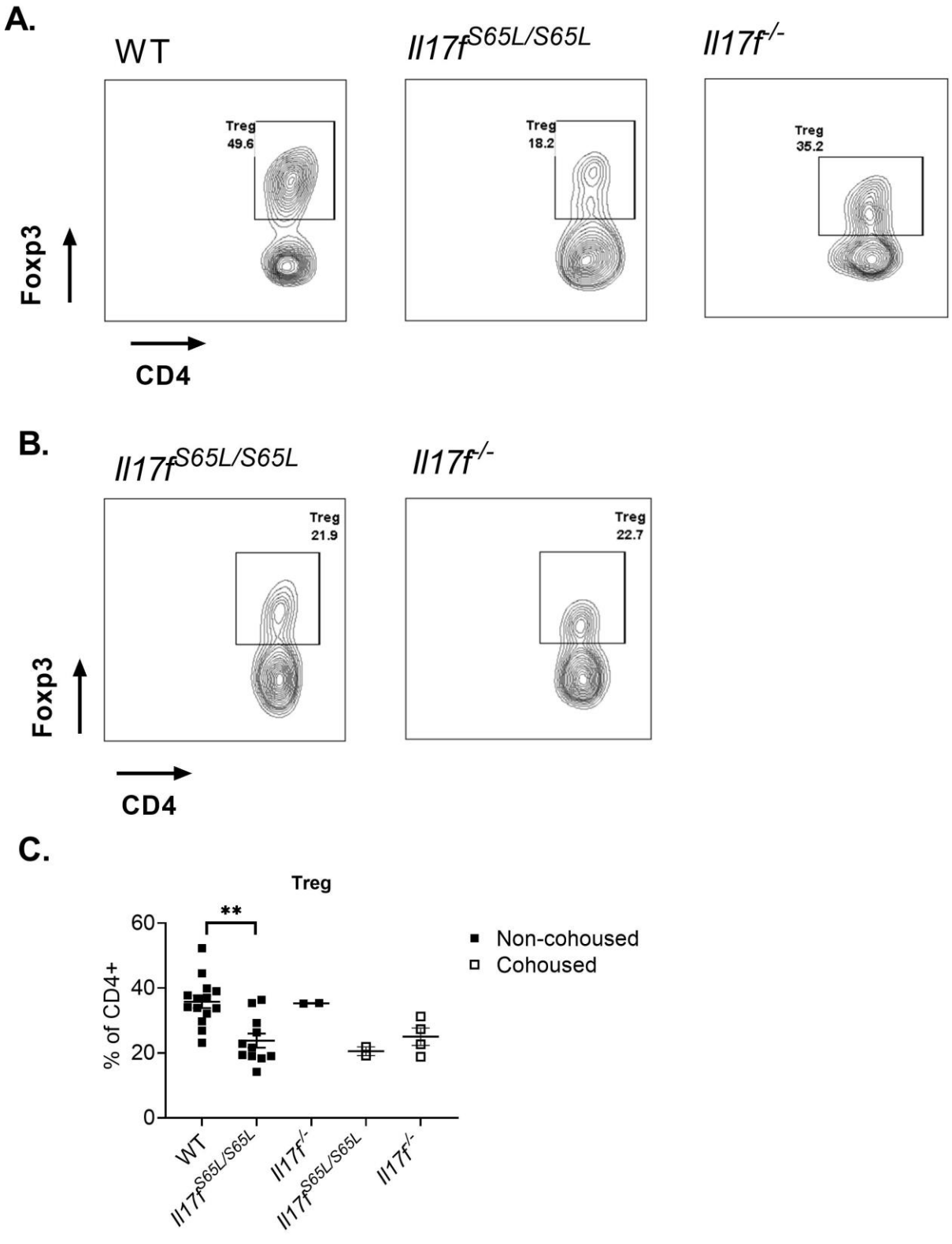

Figure 4.4 IL-17F.S65L mutation is associated with a reduced Foxp3^{+} Treg cell poplulation in colon

Il17f$^{S65L/S65L}$ and *Il17f*$^{-/-}$ mice were cohoused for 2 weeks to normalize the intestinal microbiome. The indicated mice were subjected for DSS treatment for 7 days followed by replacecment with normal drinking water for another 2 days. Single cell suspenstions were prepared from the colon tissues harveseted at day 9 post treatment, and cells were analyzed by flow cytometry. Cells were gated on the CD45$^+$ and CD4$^+$ live poplulation and stained for Foxp3. Representative FACS plots for (A) non-cohoused and (B) cohoused mice. (C) representative FACS plots for compiled results from 4 independent experiments showing percentages of Treg cells in the CD45$^+$ and CD4$^+$ live gate. Graph shows mean ± SEM. Data were analyzed by Student's t-test. ***P < 0.001

4.2.5 Defining signaling activities of IL-17A and IL-17F in DSS colitis

The above data showed that *Il17a*$^{-/-}$ and *Il17f*$^{S65L/S65L}$ mice are both susceptible to DSS colitis, whereas *Il17f*$^{-/-}$ mice develop less severe inflammation in this model. One hypothesis to explain this observation is that IL-17F signals through an alternative receptor that is distinct from IL-17RA/RC. As outlined in the Introduction section, recent studies indicated that IL-17F has the ability to bind to an IL-17RC/RC homodimeric receptor complex, though whether this dimer mediates downstream signals remains unproven [23]. Related to this, an IL-17F/IL-17RC axis was reported to promote expression of IL-33, based on results that IL-33 expression is upregulated in *Il17ra*$^{-/-}$ murine lung epithelial cells upon IL-17F but not IL-17A activation [22]. To examine a potential function of the IL-17F/IL-17RC axis in cultured cells, I created an IL-17RA-deficient fibroblast cell line from ear tissue of *Il17ra*$^{-/-}$ mice. As expected, after treatment with IL-17F, expression of *Il6* was upregulated in WT, but not *Il17ra*$^{-/-}$, fibroblasts (Figure 4.5A). Unlike a previous report [22], *Il33* was not detectably elevated by qPCR in response to IL-17F in either *Il17ra*$^{-/-}$ or control WT fibroblasts (Figure 4.5A). To determine if IL-17F was able to mediate *Il33* expression in other cell types, I stimulated murine colonic epithelial cells (CMT93) and a murine stromal fibroblast cell line (ST2) with IL-17F. As shown, *Il33* was not induced by IL-17F in any

of the tested cell lines (Figure 4.5B). These data indicated that IL-33 is likely not an IL-17F target gene, in contrast to published studies in this regard.

To determine if there were any other IL-17RA-independent genes induced by IL-17F, *Il17ra*$^{-/-}$ fibroblasts were treated with IL-17F for 8 hours and RNAseq analysis was performed. Gene-specific analysis (GSA; Partek flow) on RNAseq data revealed differential expression of genes in IL-17F-treated WT fibroblasts and the WT untreated controls. In total, 24 genes were found to be elevated by IL-17F in WT fibroblasts (Table 4.1). However, none of these 24 genes were evident in *Il17ra*$^{-/-}$ fibroblasts (Figure 4.5C, Table 4.2), which indicated that IL-17RA is required for IL-17F signaling, at least in fibroblasts. It is not surprising that the number of genes activated by IL-17F in WT fibroblasts is quite low, since IL-17F is known to be a weak activator for signal transduction [20, 86, 122, 152, 159, 228]. Notably, statistically significant differences were found in 22 genes between IL-17F activated and the sham control of *Il17ra*$^{-/-}$ fibroblasts. However, all of these genes are not upregulated by IL-17F activation in WT fibroblasts. In addition, the expression level of these genes in IL-17F activated *Il17ra*$^{-/-}$ fibroblasts is considerably low, with a LSmean <5 (Table 4.2.6). Thus, the statistical difference is likely attributed to technical variance without biological significance. Therefore, in contrast to published results [22], it appears that IL-17RC alone is not sufficient to mediate IL-17F signaling in fibroblasts.

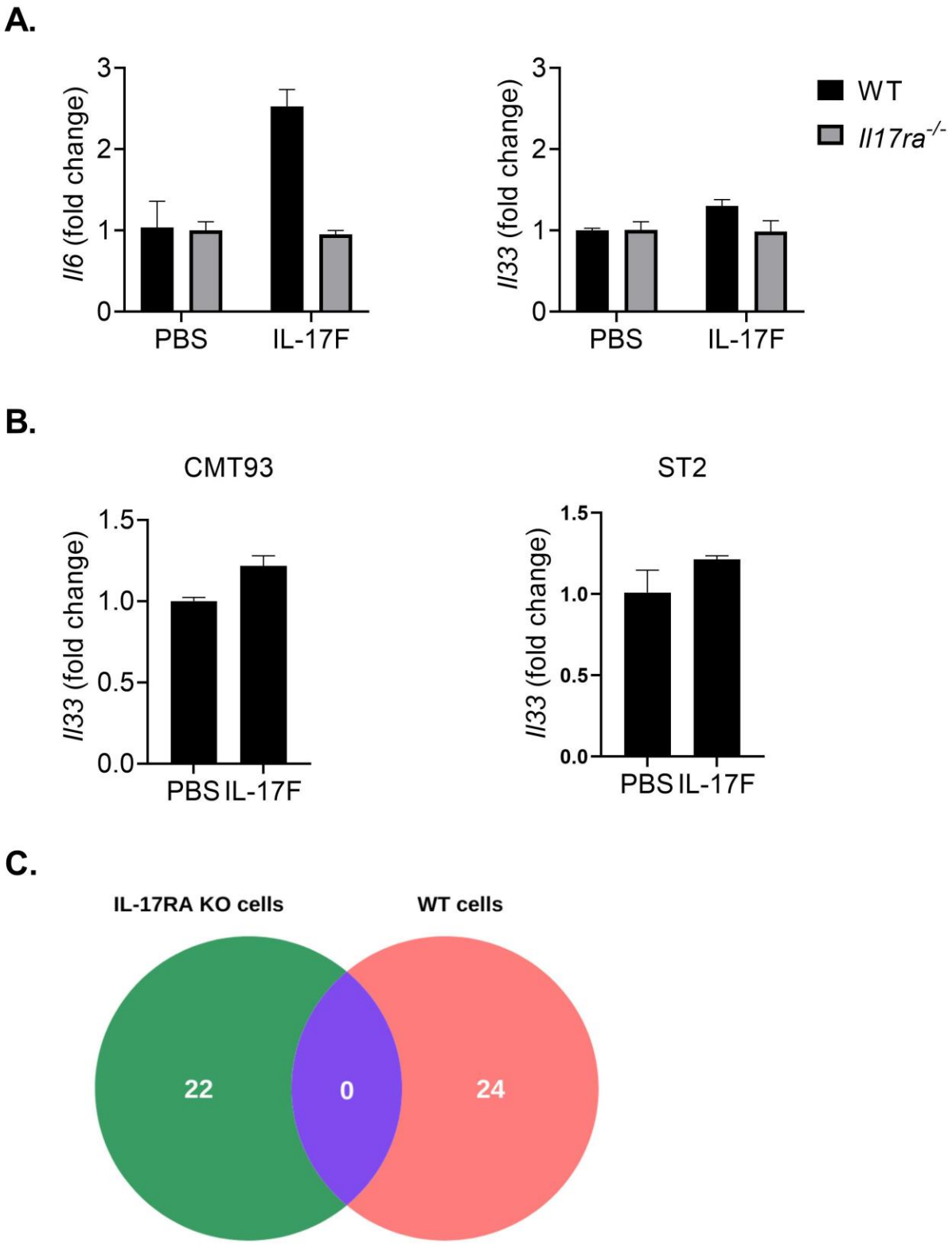

Figure 4.5 IL-17RA is required for IL-17F signaling

(A) Fibroblasts were isolated from ear tissues of *Il17ra*$^{-/-}$ or WT control mice and developed into cell lines [261]. *Il17ra*$^{-/-}$ cells and WT cells were activated with 200 ng/ml IL-17F for 6 hours. mRNA was extracted from the cells and indicated genes were analyzed by qPCR. Graph shows mean ± SEM. (B) The indicated cell lines were activated by 200ng/ml IL-17F for 6 hours. *Il33* expression was determined by qPCR. Graph shows mean ± SEM. (C) WT and IL-17RA deficient ear-derived fibroblast cell lines were treated with 200 ng/ml IL-17F for 8 hours. RNA-Seq was performed on mRNA extracted from WT and *Il17ra*$^{-/-}$ fibroblasts. Differential expression of genes in IL-17F-activated WT fibroblasts and WT sham control as well as IL-17F-activated *Il17ra*$^{-/-}$ fibroblasts and *Il17ra*$^{-/-}$ fibroblasts sham control were analyzed by GSA. Venn diagram shows differentially or overlapping upregulated genes upon IL-17F activation in *Il17ra*$^{-/-}$ fibroblasts and WT fibroblasts. Upregulated genes were defined as $P < 0.05$, fold change > 1.4, and total count > 5. 24 genes were upregulated by IL-17F in WT cells, and 22 genes were upregulated by IL-17F in *Il17ra*$^{-/-}$ fibroblasts. No overlapping genes were found by RNAseq analysis.

Table 4.2.1 Genes upregulated by IL-17F in WT fibroblasts

RNAseq analysis performed on WT fibroblasts upon IL-17F activation. Gene expression was compared between IL-17F treated cells and sham controls. The listed genes had $P < 0.05$, fold change > 1.4, and total count > 5.

Gene ID	P-value	Fold change	LSMean (IL-17F)	LSMean (Sham)
Cxcl5	1.90E-10	3.44	42.61	12.41
Lcn2	2.52E-10	3.73	14.26	3.82
Il6	7.72E-10	3.20	25.75	8.05
Ccl2	6.39E-09	1.74	91.58	52.53
Nfkbiz	2.09E-08	1.79	106.76	59.78
Ptx3	2.93E-08	1.46	219.86	150.87
U90926	3.53E-07	1.63	16.31	9.97
Cemip	6.21E-07	1.54	28.46	18.47
Ccl7	7.90E-07	1.60	14.36	8.98
Ntn1	8.72E-07	1.53	36.91	24.05
Zc3h12a	1.53E-06	1.55	20.47	13.20
Slc7a2	1.80E-06	1.50	28.88	19.21
Ccn5	2.09E-06	1.60	94.58	59.27
Cebpd	1.48E-05	1.62	31.08	19.15
Lif	2.11E-05	1.56	156.47	100.18
Slc16a2	2.52E-05	1.46	13.79	9.46
Ptgs2	3.64E-05	1.47	1285.61	872.82
Wdyhv1	4.12E-05	1.41	12.21	8.68
Ier3	5.30E-05	1.45	132.31	90.97
Atp2b4	1.47E-04	1.46	6.12	4.19
Cxcl1	9.48E-04	1.42	56.56	39.70
Egr1	1.77E-03	1.44	251.68	174.74
Ksr1	8.31E-03	1.40	4.97	3.55
Gm14308	2.39E-02	1.49	5.12	3.44

Table 4.2.2 Genes upregulated by IL-17F in *Il17ra*$^{-/-}$ fibroblasts

RNAseq analysis performed on *Il17ra*$^{-/-}$ fibroblasts upon IL-17F activation. Gene expression was compared between IL-17F treated cells and sham control. The listed genes had $P < 0.05$, fold change > 1.4, and total count > 5.

Gene ID	P-value	Fold change	LSMean (IL-17F)	LSMean (Sham)
Gm18180	1.75E-03	1.67	1.61	0.97
Gvin1	2.09E-03	3.18	2.78	0.87
Zfp882	2.80E-03	1.40	3.16	2.26
Gm13394	3.70E-03	1.50	4.05	2.69
Gm6245	4.07E-03	1.48	1.81	1.22
Cd72	4.47E-03	1.51	1.62	1.08
Itgb4	5.54E-03	1.41	1.80	1.27
Gm28635	5.60E-03	1.85	1.74	0.94
Gm49388	5.89E-03	1.96	1.55	0.79
Gm38357	7.35E-03	1.48	2.25	1.52
Hist1h2bq	9.76E-03	2.04	1.39	0.68
Fam83c	1.00E-02	1.45	1.24	0.85
Gm13493	1.33E-02	1.52	1.58	1.04
Gm18646	1.35E-02	1.45	1.52	1.05
Cpt1b	1.38E-02	1.48	1.07	0.72
Gm16421	1.51E-02	1.48	1.10	0.74
Zfp184	1.72E-02	1.43	1.68	1.17
Ccnb2-ps	1.87E-02	1.46	1.14	0.78
AY036118	2.02E-02	2.06	2.68	1.30
Gm29808	2.39E-02	1.47	1.04	0.71
Gm11353	2.77E-02	1.57	1.16	0.74
H19	2.99E-02	1.41	1.18	0.84

4.2.6 IL-17F.S65L does not affect the development of AGN

Although IL-17A and IL-17F playing contrasting biological roles in DSS colitis, *Il17a*$^{-/-}$ and *Il17f*$^{-/-}$ mice showed similar phenotypes in a murine model of AGN [88], with both strains resistant to kidney damage during development of AGN. We predicted that *Il17f*$^{S65L/S65L}$ mice would be resistant to AGN because (i) the IL-17F.S65L mutation appears to be a loss-of-function mutation in IL-17F *in vitro* (Figure 3.1), (ii) mice containing this mutation showed a phenotype similar to that of *Il17a*$^{-/-}$ mice in OPC and DSS colitis. To examine the function of the IL-17F.S65L mutation in a setting where both IL-17A and IL-17F have a similar phenotype, we opted to use AGN. To that end, *Il17f*$^{S65L/S65L}$ mice, as well as *Il17a*$^{-/-}$, *Il17f*$^{-/-}$, and WT control mice, were immunized with heterologous anti-GBM antibodies, which initiate autoimmune antibody-mediated inflammation against the basement membrane of kidney. Blood urea nitrogen (BUN) was measured at two weeks post-immunization to assess kidney damage. Consistent with previous reports [88], both *Il17a*$^{-/-}$ mice and *Il17f*$^{-/-}$ mice showed decreased BUN levels compared to the WT control mice (Figure 4.6), suggesting a pathogenic function of both IL-17A and IL-17F in AGN. However, surprisingly, *Il17f*$^{S65L/S65L}$ mice did not phenocopy the *Il17a*$^{-/-}$ or *Il17f*$^{-/-}$ mice in this model, as the BUN levels in *Il17f*$^{S65L/S65L}$ mice were comparable to those in WT mice (Figure 4.6). Thus, the IL-17F.S65L mutation does not prevent the development of AGN, which is surprisingly different from the findings in *Il17a*$^{-/-}$ and *Il17f*$^{-/-}$ mice.

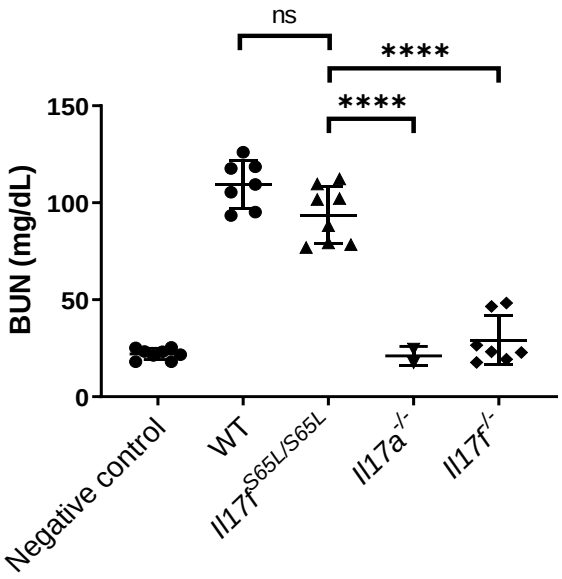

Figure 4.6 IL-17F.S65L mutation exhibits a distinct phenotype from loss of either IL-17A or IL-17F

The indicated mice were subjected to anti-GBM nephritis. Renal dysfunction at Day 14 was assessed by determination of the serum BUN level. Each dot represents an individual mouse. Graph shows mean ± SEM. Data were pooled from two independent experiments. Data were analyzed by ANOVA. ****P < 0.0001.

4.3 Discussion

Biologic drugs that target IL-17A were a major addition to the toolbox of drugs for autoimmunity. The initial studies of anti-IL-17A drugs showed that they are remarkably successful in treatment for psoriasis [77]. Currently, three monoclonal antibodies that block the IL-17A signaling pathway are available for psoriasis and psoriatic arthritis patients [78-80]. All of these treatments provide almost complete clearance of plaques in moderate-to-severe psoriasis. However, one of the side effects of such treatments is exacerbation of IBD, a major drug-safety concern [240]. Clinical trials to evaluate the efficacy of secukinumab in treatment of CD patients

had to be halted due to worsening IBD [164, 165]. This contrasts with the efficacy of ustekinumab, a neutralizing antibody that targets IL-12 and IL-23 [262] and more recently mirikizumab, which targets just IL-23 [263].

Subsequent mechanistic studies to explain the surprising impact on IBD indicated that IL-17A regulated intestinal epithelial permeability via an IL-23-independent pathway [167]. Notably, this finding might have been predicted based on early *in vivo* studies on murine DSS colitis which showed that mice treated with anti-IL-17A neutralizing antibodies, or genetically lacking IL-17A, IL-17RA or Act1 (a critical adaptor for IL-17 signaling pathway) all showed exacerbated disease during DSS colitis [41, 86, 166-169]. Thus, while the DSS colitis model is not a perfect reflection of the pathogenesis of human IBD, findings made from the DSS colitis model have been predictive with respect to involvement of the IL-17 pathway.

As noted above, DSS colitis is one of the few settings where blockade or deficiency of IL-17A and IL-17F exhibit opposing phenotypes [86, 89]. The clinical implications of this phenomenon are important, because pre-treatment with monoclonal antibodies against IL-17F mitigated the development of DSS-induced colitis, unlike anti IL-17A antibodies [89]. Therefore, blockade of IL-17F, but not IL-17A, may be beneficial for treatment of IBD. To explain this observation, Iwakura *et al.* suggested that the suppressed inflammation in *Il17f*$^{-/-}$ mice might be mediated by increased colonization of intestinal *C.* XIVa [89]. Here, I similarly found that *Il17f*$^{-/-}$ mice showed better outcomes during DSS colitis, yet the *C.* XIVa levels were comparable between *Il17f*$^{-/-}$ mice and WT mice, indicating a divergence of these phenomena. Thus, more mechanistic studies are clearly required to understand the basis of these observations and ultimately to translate these findings into the clinical setting.

The IL-17F.S65L mutation was discovered in kindred of patients with CMCD in Argentina, who unfortunately have been lost to follow-up [99]. The biological impact of the IL-17F.S65L mutation was illustrated by *in vitro* experiments, in which the IL-17F.S65L homodimer as well as IL-17A/IL-17F.S65L heterodimer failed to induce expression of *Il6* and *Cxcl1*, the signature genes in IL-17RA/RC signaling pathway (Chapter 3) [99]. I further determined the *in vivo* activities of the IL-17F.S65L mutation during OPC as described in chapter 3. *Il17f*$^{S65L/S65L}$ and *Il17a*$^{-/-}$ mice showed similar susceptibility to *C. albicans* oral infection, but *Il17f*$^{-/-}$ and WT mice were fully resistant. These data indicated that the IL-17F.S65L mutation can block IL-17RA/RC signaling *in vivo.* Therefore, IL-17F.S65L mice could be a useful tool to determine the biological functions of the IL-17RA/RC signaling pathway, and to help elucidate the mechanism by which IL-17A and IL-17F play differing roles in various disease contexts.

To better understand how IL-17F promotes intestinal inflammation, and why IL-17A and IL-17F behave oppositely in the DSS colitis model, *Il17f*$^{S65L/S65L}$ mice were subjected to DSS treatment. Consistent with observations in OPC, *Il17f*$^{S65L/S65L}$ mice showed a similar phenotype to *Il17a*$^{-/-}$ mice, namely increased susceptibility to DSS. However, *Il17f*$^{S65L/S65L}$ and *Il17a*$^{-/-}$ mice do not appear to share the same mechanism of protection against DSS-induced inflammation. *Il17a*$^{-/-}$ mice showed increased intestinal epithelial permeability during DSS colitis, indicating that IL-17A might function to promote the repair of intestinal epithelium [167, 169]. In contrast, gut epithelial integrity was comparable between *Il17f*$^{S65L/S65L}$ and WT mice post-DSS treatment. We do not know the basis for this, but based on the observation that the IL-17A homodimer is functional in patients with the IL-17F.S65L mutation, the remaining IL-17A homodimers in *Il17f*$^{S65L/S65L}$ mice might be sufficient to protect the intestinal epithelium during DSS colitis.

C. XIVa, part of the commensal microbiome, has long been known to regulate intestinal inflammation by promoting differentiation of Tregs [170]. I found that decreased colonization of *C.* XIVa correlated with decreased colonic Treg levels in *Il17f*$^{S65L/S65L}$ mice during DSS colitis. Cohousing *Il17f*$^{S65L/S65L}$ and *Il17f*$^{+/-}$ mice together led to decreased levels of *C.* XIVa in *Il17f*$^{+/-}$ mice, which could worsen the severity of colitis in *Il17f*$^{+/-}$ mice. Therefore, the *C.* XIVa-mediated downregulation of Tregs might explain the elevated inflammation following DSS treatment in *Il17f*$^{S65L/S65L}$ mice. Notably, if the IL-17F.S65L mutation modulates *C.* XIVa level by antimicrobial peptides, which have a directly killing effect on bacteria, then we would expect to see increased levels of *C.* XIVa in *Il17f*$^{S65L/S65L}$ mice when *Il17f*$^{S65L/S65L}$ and *Il17f*$^{+/-}$ mice are cohoused. However, I observed decreased levels of *C.* XIVa in *Il17f*$^{+/-}$ mice after cohousing, indicating that the IL-17F.S65L mutation indirectly downregulates intestinal colonization of *C.* XIVa. Further efforts will be needed to sort out how this occurs.

Recently, crystal structure analysis revealed that IL-17F can bind to an IL-17RC homodimeric receptor complex [23]. I speculate that this finding may help to explain the contrasting phenotypes of *Il17a*$^{-/-}$ mice and *Il17f*$^{-/-}$ mice in the context of DSS colitis (Figure 4.7). IL-17A may signal through the IL-17RA/RC receptor complex to protect mice from epithelial damage, while IL-17F may be signaling through the IL-17RC/RC receptor to promote inflammation during DSS colitis (Figure 4.1). The IL-17F.S65L mutation specifically impairs an interaction between IL-17F and the IL-17RA subunit. Thus, this single point mutation is likely to only block the binding of IL-17F to IL-17RA/RC receptor complex without disturbing the IL-17F/IL-17RC axis. Regarding the phenotype in the DSS colitis model, we postulate that the IL-17F.S65L mutation may lack signaling through the IL-17RA/RC complex, while keeping the IL-17F/IL-17RC axis intact. This could potentially explain why *Il17f*$^{S65L/S65L}$ mice showed a

phenotype similar to that of *Il17a*$^{-/-}$ mice, even though the IL-17F.S65L mutation is localized on IL-17F. Notably, the phenotype of the *Il17f*$^{S65L/S65L}$ mice is not as strong as that of *Il17a*$^{-/-}$ mice, since most of the *Il17a*$^{-/-}$ mice needed to be sacrificed before day 8 post-treatment, while *Il17f*$^{S65L/S65L}$ mice survived somewhat longer. Furthermore, impaired gut epithelial integrity has been reported in *Il17a*$^{-/-}$ mice, yet I did not observe this in *Il17f*$^{S65L/S65L}$ mice. Together, these data are consistent with a model in which a functional IL-17A homodimer could partially compensate for the loss of IL-17RA/RC signaling in *Il17f*$^{S65L/S65L}$ mice.

To further explore the ramifications of the *Il17f*$^{S65L/S65L}$ mutation, we used an AGN model. IL-17A and IL-17F are both reported to be pathogenic in this setting [88]. We confirmed the disease-promoting effects of both IL-17A and IL-17F in our hands, but interestingly and unexpectedly, the IL17F.S65L mutation did not ameliorate the kidney damage during AGN. This intriguing observation could also be explained by the aforementioned IL-17F/IL-17RC hypothesis: that is, the IL-17RA/RC heterodimeric receptor complex and the IL-17RC/RC homodimeric complex might mediate non-redundant signaling pathways to promote inflammation during AGN. The IL-17F.S65L mutation only blocks binding to the IL-17RA/RC receptor, thus leaving the IL-17F/IL-17RC axis intact. Although IL-17RA/RC-mediated signaling could be impaired by the IL-17F.S65L mutation, the remaining IL-17A homodimers may be sufficient to induce kidney damage via signaling through the IL-17RA/RC heterodimeric receptor. Therefore, the IL-17F.S65L mutation does not result in decreased inflammation or kidney damage during AGN.

Based on these *in vivo* results, I hypothesized that IL-17F could signal through the IL-17RC/RC homodimeric receptor complex. This hypothesis was tested in cell line-based assays by determining the gene activation profile of *Il17ra*$^{-/-}$ fibroblasts upon IL-17F treatment (Fig 4.5). RNAseq analysis revealed that IL-17F failed to induce expression of any IL-17F target genes in

an IL-17RA-deficient fibroblast cell line. Although I do see certain genes that are upregulated by IL-17F treatment in *Il17ra*$^{-/-}$ fibroblasts, these genes are not upregulated in WT fibroblasts upon IL-17F activation. Additionally, these genes appear to have a low overall expression level. Thus, although statistically significant, these differences might not be biologically significant. Taken together, these data imply that IL-17RA is required for IL-17F-mediated signaling. There results contrast with a report showing that IL-33 may be a target gene downstream of the IL-17F/IL-17RC axis in an IL-17RA independent manner [22]. However, I found no evidence of IL-17F-mediated IL-33 induction in multiple cell lines. Notably, the expression of IL-17RC varies in different cell types and is particularly high in colonic epithelial cells [85]. Thus, signaling through the IL-17RC homodimeric receptor complex may be tissue- and cell type-specific. mRNA screening in colonic epithelial cells or organoids might provide informative results regarding the IL-17F/IL-17RC axis.

In summary, *Il17f*$^{S65L/S65L}$ mice were used to delineate the different biological activities of IL-17A and IL-17F in two autoimmune disease models. In the DSS colitis model, *Il17a*$^{-/-}$ and *Il17f*$^{-/-}$ mice were reported to have opposite phenotypes. I showed that *Il17f*$^{S65L/S65L}$ mice exhibited more severe disease during DSS colitis, which is similar to findings in *Il17a*$^{-/-}$ mice. In an AGN model, both IL-17A and IL-17F promote kidney damage. Surprisingly, the kidney damage in *Il17f*$^{S65L/S65L}$ mice is comparable to that in WT mice. The results from both of the *in vivo* experiments can be explained by a hypothesized IL-17F/IL-17RC axis, but this hypothesis was not supported by my cell-line based experiments. Thus, further studies are still required to fully understand the mechanism by which IL-17A and IL-17F exert differing biological activities in various disease models.

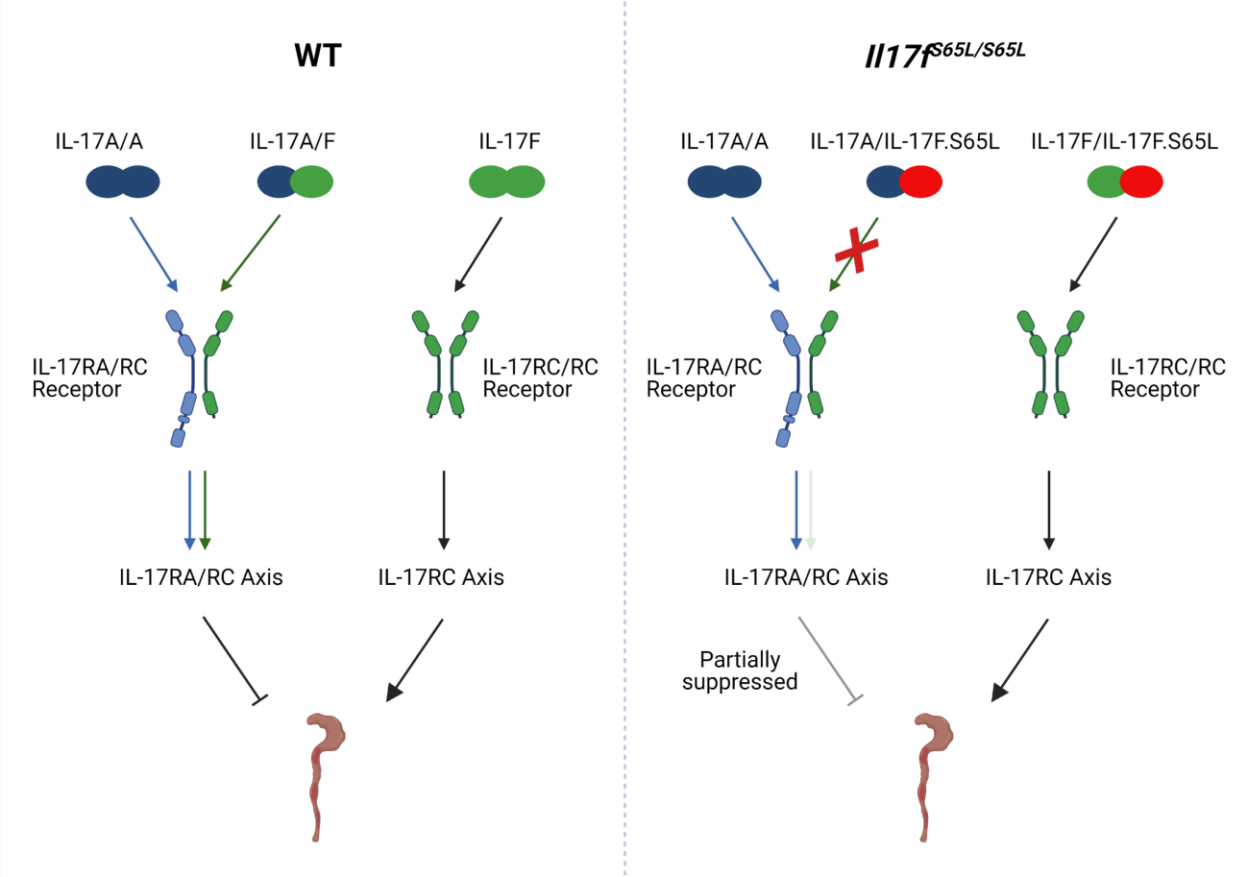

Figure 4.7 Speculative IL-17RA/RC and IL-17RC axis in DSS colitis model

IL-17RA/RC axis prevents the DSS induced colitis, whereas IL-17RC axis promotes the DSS induced colitis. Since both IL-17A and IL-17A/F are purposed to activate the IL-17RA/RC axis, IL-17F.S65L mutation could partially suppress the IL-17RA/RC axis. Therefore, *Il17f*$^{S65L/S65L}$ mice showed a pathogenic phenotype in DSS colitis model, but the gut epithelial integrity is not impaired by IL-17F.S65L mutation.

5.0 Conclusion and Future directions

5.1 Summary

In this dissertation, I took advantage of a naturally occurring mutation, IL-17F.S65L, to explore the *in vivo* biological activities of IL-17A and IL-17F during infection and autoimmune disease. In Chapter 3, I found that *Il17f*$^{S65L/S65L}$ mice were mildly susceptible to OPC, which is similar to the susceptibility of *Il17a*$^{-/-}$ mice to OPC, but strikingly different from that of *Il17f*$^{-/-}$ mice. The increased susceptibility in *Il17f*$^{S65L/S65L}$ mice might be attributed to impaired expression of CXC chemokines and reduced neutrophil recruitment to the oral mucosa. I further found that the cellular sources of IL-17F are γδ T cells, innate TCRαβ^{+} cells, and potentially ILC3s, which are canonical activators for innate type 17 immunity. The activation of innate type 17 immunity during OPC could be modulated by commensal microbiome such as SFB but does not require c-Fos expression in the oral epithelium. These data indicated a protective role of IL-17F during OPC and help to reconcile the observations that while IL-17F-deficient mice are fully resistant to OPC, a loss-of-function mutation in IL-17F leads to CMCD in humans.

In Chapter 4, the *Il17f*$^{S65L/S65L}$ mice were used in two autoimmune disease models, DSS-induced colitis and AGN. *Il17f*$^{S65L/S65L}$ mice shared a similar phenotype with *Il17a*$^{-/-}$ mice during DSS colitis, in which both were susceptible to pathology resulting from DSS treatment. However, unlike IL-17A, the IL-17F.S65L mutation does not appear to influence the gut epithelial integrity after DSS treatment. Instead, enteric *C.* XIVa colonization, as well as colonic Tregs, were both found to be decreased in *Il17f*$^{S65L/S65L}$ mice. The decreased *C.* XIVa colonization might be attributed to the increased severity of DSS colitis in *Il17f*$^{S65L/S65L}$ mice, because cohousing

Il17f$^{S65L/S65L}$ and *Il17f*$^{-/-}$ mice resulted in lower *C.* XIVa levels and worse disease outcomes in *Il17f*$^{-/-}$ mice. In the AGN model, *Il17f*$^{S65L/S65L}$ and WT mice showed comparable kidney damage, surprisingly different from both *Il17a*$^{-/-}$ and *Il17f*$^{-/-}$ mice. Therefore, *Il17f*$^{S65L/S65L}$ mice exhibit a *Il17a*$^{-/-}$-like phenotype in DSS colitis model, but the *Il17a*$^{-/-}$-like phenotype was surprisingly not observed in AGN model.

5.2 Unifying discussion, outstanding questions and future directions

Current and previous studies of the IL-17 family of cytokines reveal many similarities between IL-17A and IL-17F. Structurally, IL-17A and IL-17F share 56% homology at the amino acid sequence level [6]. These two cytokines also adopt a cysteine knot fold as a unique structural feature that distinguishes them from other families of cytokines [12]. This distinctive structure underlies the binding of IL-17A and IL-17F to the IL-17RA/IL-17RC receptor complex, and these cytokines induce quantitatively similar signaling pathways [21]. Thus, IL-17A and IL-17F have similar, yet not entirely overlapping, biological functions *in vitro.*

Consistent with the *in vitro* results, IL-17A and IL-17F exhibit similar *in vivo* biological activities in many models, for example AGN. Loss of either IL-17A and IL-17F prevents the development of AGN, as *Il17a*$^{-/-}$ and *Il17f*$^{-/-}$ mice are equally resistant to this disease [88]. Despite the similarities between IL-17A and IL-17F that are seen in structural analysis, and *in vitro* studies, IL-17A and IL-17F still exert distinct *in vivo* biological activities, which has been demonstrated in both infections and autoimmune diseases. In many settings, IL-17A plays a critical role while IL-17F is less essential. A model of murine OPC is an example of this category; whereas *Il17a*$^{-/-}$ mice exhibit increased susceptibility to OPC compared to WT mice, the antifungal activity of IL-17F

can be only detected under IL-17A and IL-17F double blockade condition, which caused an elevated susceptibility to OPC over IL-17A single blockade [87]. In a rare second category, IL-17A and IL-17F exhibit opposite biological activities, namely in the DSS colitis model. IL-17A deficiency worsens DSS-induced colitis, but loss of IL-17F leads to a protective phenotype [86, 89]. Therefore, IL-17A and IL-17F show similar *in vivo* biological activities in most cases, but still behave differently in certain animal models. The mechanism of the different *in vivo* functions of IL-17A and IL-17F is largely unknown.

To further understand the *in vivo* biological activities of IL-17F, I developed an IL-17F.S65L mutant mouse strain. The human IL-17F.S65L mutation has an apparent dominant negative effect according to Puel *et al.*, inhibiting signaling of the IL-17AF heterodimer and IL-17F homodimer when paired with a wild type counterpart *in vitro* [99]. As noted, the serine residue at position 65 of IL-17F is important for the interaction between IL-17F and IL-17RA [19]. Thus, replacement of the polar serine with a non-polar leucine impairs the binding of IL-17F to IL-17RA. Therefore, IL-17F.S65L mutation could serve as a useful tool to understand the function of IL-17F.

In my dissertation, *Il17f*$^{S65L/S65L}$ mice were evaluated in three mouse models, OPC, DSS colitis, and AGN, with some unexpected outcomes. In the OPC model, blocking IL-17A in *Il17f*$^{-/-}$ mice led to an increased fungal burden that was even higher than that of IL-17A singly deficient mice [87]. Thus, I expected that treating *Il17f*$^{S65L/S65L}$ mice with anti-IL-17A neutralizing antibodies would cause a higher susceptibility to OPC compared to IL-17A blockade in WT mice; in other words, that the *Il17f*$^{S65L/S65L}$ would be deficient in IL-17A, IL-17F, and IL-17AF signaling in this situation. However, surprisingly, IL-17A blockade in *Il17f*$^{S65L/S65L}$ mice caused only a similar fungal susceptibility to mice with an IL-17A deficiency.

In the DSS colitis model, IL-17F deficient mice, either by neutralizing antibody or genomic deletion, show ameliorated inflammation [86, 89]. In contrast, *Il17f*$^{S65L/S65L}$ mice show exacerbated colitis after DSS treatment, even though these mice contain an IL-17F loss-of-function mutation. In the AGN model, *Il17a*$^{-/-}$ and *Il17f*$^{-/-}$ mice are equally resistant to kidney damage [88]. Since IL-17F.S65L mutation is deficient in the ability to signal and leads to an *Il17a*$^{-/-}$-like phenotype in the OPC and DSS colitis models, I predicted that *Il17f*$^{S65L/S65L}$ mice would be similarly resistant to kidney damage in AGN model. However, my data revealed that the IL-17F.S65L mutation does not impact the kidney damage at all during AGN. Thus, there is clearly context-specific activity of IL-17F, which needs to be defined in greater detail.

To explain the unexpected results from *Il17f*$^{S65L/S65L}$ mice, I made two speculations. First, based on the crystallographic structural analysis showing that IL-17F can interact with IL-17RC/RC homodimeric receptor [23], I postulate a model in which that IL-17F can signal through an IL-17RC/IL-17RC homodimeric receptor, and the signals mediated by this complex are nonredundant to the signals mediated by a heterodimeric IL-17RA/IL-17RC receptor complex. Hereafter, I will refer to the IL-17F-mediated IL-17RC/IL-17RC signaling as the **IL-17RC axis** and the more canonical IL-17RA/IL-17RC signaling as the **IL-17RA/RC axis**. Second, the binding site of IL-17F S65 is located at IL-17RA [19]. Therefore, I hypothesize that the IL-17F.S65L mutation specifically blocks the IL-17RA/RC axis but does not impact the IL-17RC axis. All of the unexpected findings in *Il17f*$^{S65L/S65L}$ mice could be explained by these possibilities, as outlined in detail below.

If the above model is correct, then in murine OPC the IL-17RA/RC axis would be predicted to potently clear *C. albicans* from the oral cavity. The IL-17RC axis may also exert some fungal clearance activity but is apparently dispensable when the IL-17RA/RC axis is functional. In

support of this, our current and previous studies showed that blocking IL-17F alone does not impact the susceptibility of OPC, while inhibiting IL-17F in IL-17A deficient mice can further increase the fungal burden upon *C. albicans* oral infection [87]. In *Il17f*$^{S65L/S65L}$ mice, the IL-17RA/RC axis would be impaired by the IL-17F.S65L mutation, but the IL-17RC axis would still be intact. Consistent with this model, we found that *Il17f*$^{S65L/S65L}$ mice have a fungal burden that is similar to *Il17a*$^{-/-}$ mice during OPC. Thus, treating *Il17f*$^{S65L/S65L}$ mice with anti-IL-17A neutralizing antibodies would not be expected to further increase the susceptibility to OPC, as the IL-17RA/RC axis is fully blocked by IL-17F.S65L mutation and of course anti-IL-17A neutralizing antibodies do not affect the IL-17RC axis. (Figure 5.1) (the mechanism of how IL-17F.S65L could completely block IL-17RA/IL-17RC signaling is discussed in detail in Chapter 3.3).

If these speculations are true, then in the DSS colitis model I propose that the IL-17RA/RC axis mediates the protective role of IL-17A, whereas the IL-17RC axis signaling mediates the pathogenic activity of IL-17F. Since we posit that the IL-17F.S65L mutation only blocks the IL-17RA/IL-17RC signaling pathway, it makes sense that *Il17f*$^{S65L/S65L}$ mice exhibit a qualitatively similar phenotype to *Il17a*$^{-/-}$ mice, rather than to *Il17f*$^{-/-}$ mice. Notably, *Il17a*$^{-/-}$ mice were reported to have increased intestinal epithelial permeability during DSS colitis [167, 169]. However, I showed that the gut epithelial integrity in *Il17f*$^{S65L/S65L}$ mice was comparable to WT mice post-DSS treatment. Although I have not yet probed the mechanism of this difference between *Il17a*$^{-/-}$ mice and *Il17f*$^{S65L/S65L}$ mice, I hypothesize that the residual IL-17A homodimers in *Il17f*$^{S65L/S65L}$ mice are sufficient to protect the intestinal epithelium during DSS colitis. Therefore, this model could reconcile the conflict that *Il17f*$^{-/-}$mice are protected from DSS-induced colitis, while mice containing a loss-of-function mutation on IL-17F have a pathogenic phenotype (Figure 4.7).

The results from *Il17f*$^{S65L/S65L}$ mice in the AGN model are intriguing, since *Il17f*$^{S65L/S65L}$ mice do not share a similar phenotype with *Il17a*$^{-/-}$ mice in this model, unlike the OPC and DSS colitis models. To explain this unexpected result, I hypothesize that the pathogenic roles of the IL-17RA/RC axis and IL-17RC axis are mediated by different mechanisms. In this setting, loss of either axis would prevent the development of AGN. In other words, *Il17a*$^{-/-}$ mice are resistant to AGN due to loss of the IL-17RA/RC axis, while the phenotype of *Il17f*$^{-/-}$ mice could be attributed to a deficiency of IL-17RC axis. Since I predict that IL-17F.S65L mutation only inhibits the IL-17RA/RC axis, *Il17f*$^{S65L/S65L}$ mice are thus different from *Il17f*$^{-/-}$ mice in AGN. In terms of the IL-17RA/RC axis, although the IL-17F.S65L mutation blocks this pathway, the remaining IL-17A homodimers might be sufficient to compensate for the impact of the IL-17F.S65L mutation. By this logic, we can explain why the *Il17f*$^{S65L/S65L}$ mice do not share a same phenotype with *Il17a*$^{-/-}$ mice during AGN. Taken together, the enigmatic findings from *Il17f*$^{S65L/S65L}$ mice in the AGN model could be explained by the speculative model that I discussed above, though clearly direct experimentation is needed to prove this directly (Figure 5.2).

Notably, in explaining the unexpected phenotypes of *Il17f*$^{S65L/S65L}$ mice based on these speculations, the predicted compensatory effect of the remaining IL-17A homodimers must be different among the three animal models. One way to explain these different compensation effects could be attributed to the IL-17AF heterodimer, which has been convincingly demonstrated to exist but is hard to study due to lack of reagents that can block it while sparing IL-17A and IL-17F homodimers. As *Puel et al*. demonstrated, the IL-17F.S65L mutation blocks the signaling activities of both IL-17AF and IL-17F. If IL-17AF is indeed the major activator for the IL-17RA/IL-17RC signaling during OPC, then the IL-17F.S65L mutation should fully inhibit the signals mediated by IL-17RA/RC axis, as discussed in Chapter 3.3. In contrast, in AGN, the IL-17RA/RC axis might

be preferentially activated by the IL-17A homodimer. Therefore, any compensation from the remaining IL-17A homodimers could promote kidney damage in *Il17f*$^{S65L/S65L}$ mice during AGN, perhaps explaining what makes *Il17f*$^{S65L/S65L}$ mice different from *Il17a*$^{-/-}$ mice in this setting. In the case of DSS colitis, both IL-17A and IL-17AF are speculated to be involved in the IL-17RA/RC axis. Thus, the remaining IL-17A could only partially compensate for the loss of the IL-17RA/RC axis, and thus the *Il17f*$^{S65L/S65L}$ mice still exhibit a phenotype similar to *Il17a*$^{-/-}$ mice during DSS colitis.

Although the models discussed above could help to explain the unexpected results obtained with *Il17f*$^{S65L/S65L}$ mice, none yet have empirical support. Indeed, my RNAseq analysis on *Il17ra*$^{-/-}$ fibroblasts indicated that IL-17RA is required for all IL-17F-induced genes, at least in fibroblasts, which make the first model less likely. The second model could be confirmed by biophysical approaches, such as isothermal titration calorimetry or crystallographic analysis, which could be good experiments for future research. Therefore, the *in vivo* function of IL-17F clearly requires more in-depth focus.

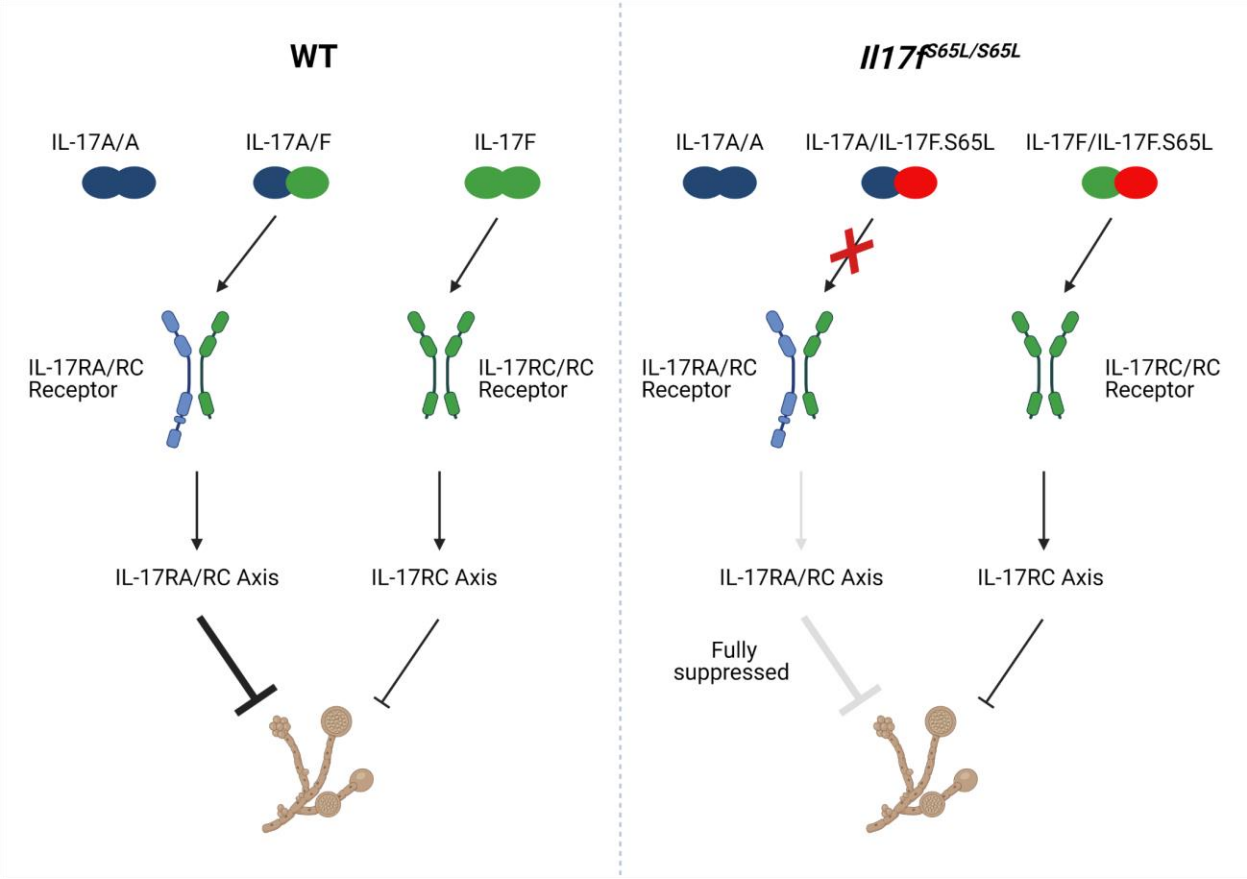

Figure 5.1 Speculative IL-17RA/RC and IL-17RC axis in OPC model

IL-17RA/RC axis promotes fungal clearance during OPC, while the anti-fungal activity of IL-17RC axis is to a lesser extent. Upon *C. albicans* oral infection, IL-17RA/RC axis is mostly activated via IL-17A/F heterodimer, which could be blocked by IL-17F.S65L mutation. Thus, we could find a fully suppressed IL-17RA/RC axis in *Il17f*$^{S65L/S65L}$ mice during OPC, which is similar to *Il17a*$^{-/-}$ mice.

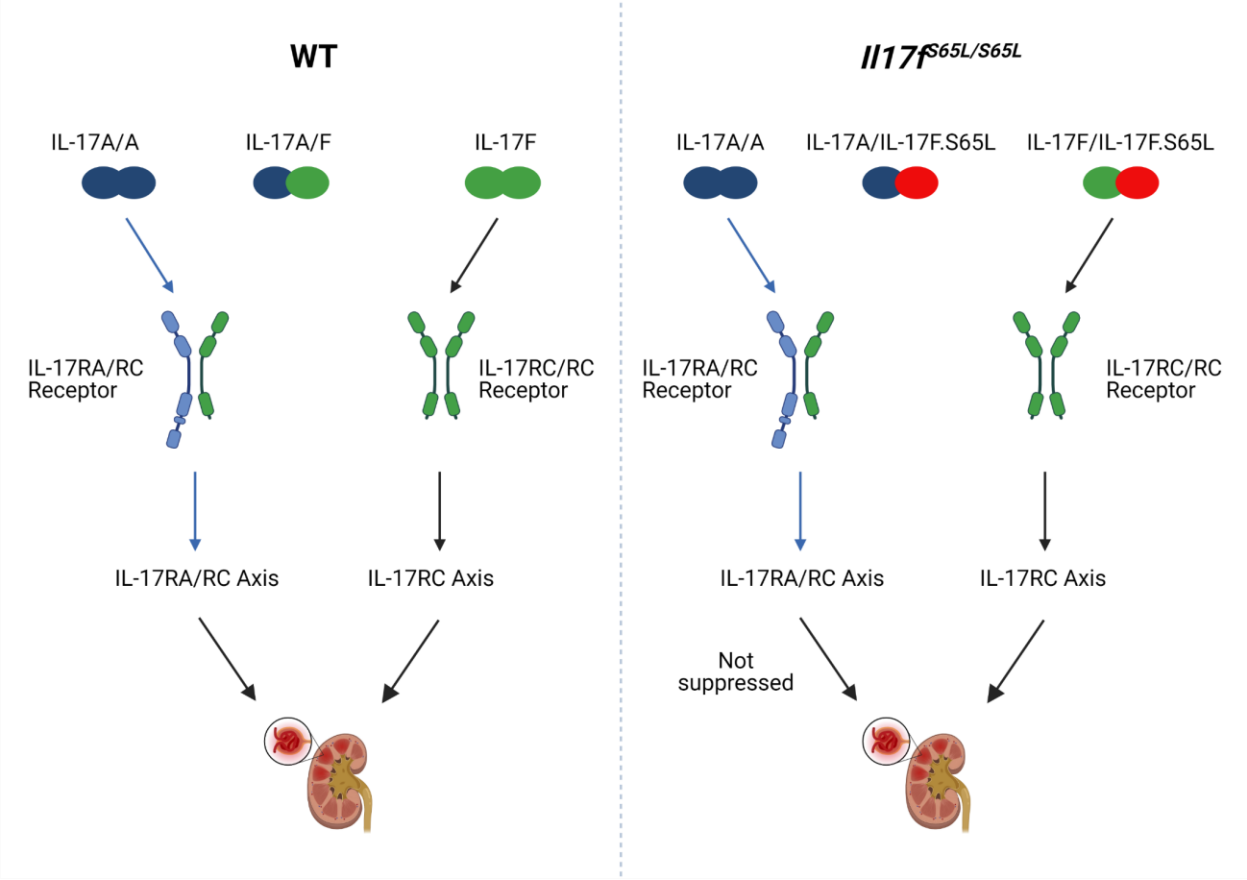

Figure 5.2 Speculative IL-17RA/RC and IL-17RC axis in AGN model

Both IL-17RA/RC axis and IL-17RC axis promote kidney damage in AGN model. The IL-17RA/RC axis is speculated to be only activated by IL-17A homodimer in this model. Therefore, IL-17F.S65L mutation does not impair the IL-17RA/RC axis, which makes *Il17f*$^{S65L/S65L}$ mice have a comparable phenotype to WT mice during AGN.

5.3 Conclusion

The work presented in this dissertation has expanded our understanding of the similarities and differences between IL-17A and IL-17F, though it has raised many questions as well. To understand the *in vivo* function of IL-17F, I took advantage of the IL-17F.S65L mutation, which is a dominant negative mutation that blocks the function of both IL-17F and IL-17AF. I developed

a mouse strain with the IL-17F.S65L mutation and used these mice in multiple infectious and autoimmune disease models, where IL-17A and IL-17F exert similar or distinct biological activities. Surprisingly, *Il17f*$^{S65L/S65L}$ mice exhibited unexpected phenotypes in all of the animal models. As outlined above, a speculative model of the IL-17RC axis can be used to explain these unexpected results from *Il17f*$^{S65L/S65L}$ mice, which could be a platform for future hypothesis testing of the functions of the enigmatic IL-17F cytokine.

Bibliography

1. Bennett, I.L., Jr. and P.B. Beeson, *Studies on the pathogenesis of fever. II. Characterization of fever-producing substances from polymorphonuclear leukocytes and from the fluid of sterile exudates.* J Exp Med, 1953. **98**(5): p. 493-508.

2. Cohen, S., P.E. Bigazzi, and T. Yoshida, *Commentary. Similarities of T cell function in cell-mediated immunity and antibody production.* Cell Immunol, 1974. **12**(1): p. 150-9.

3. Dinarello, C.A., *Historical insights into cytokines.* Eur J Immunol, 2007. **37 Suppl 1**: p. S34-45.

4. Morán, G.P.-M., R.; Cardona, AG.; Quintero-Ronderos, P.; Rodríguez, EG., *Cytokines, chemokines and growth factors*, in *Autoimmunity: From Bench to Bedside*, J.M. Anaya, et al., Editors. 2013, EI Rosario Univeristy Press;: Bogota (Colombia).

5. Fort, M.M., et al., *IL-25 induces IL-4, IL-5, and IL-13 and Th2-associated pathologies in vivo.* Immunity, 2001. **15**(6): p. 985-95.

6. Hymowitz, S.G., et al., *IL-17s adopt a cystine knot fold: structure and activity of a novel cytokine, IL-17F, and implications for receptor binding.* EMBO J, 2001. **20**(19): p. 5332-41.

7. Lee, J., et al., *IL-17E, a novel proinflammatory ligand for the IL-17 receptor homolog IL-17Rh1*. J Biol Chem, 2001. **276**(2): p. 1660-4.

8. Li, H., et al., *Cloning and characterization of IL-17B and IL-17C, two new members of the IL-17 cytokine family.* Proc Natl Acad Sci U S A, 2000. **97**(2): p. 773-8.

9. Shi, Y., et al., *A novel cytokine receptor-ligand pair. Identification, molecular characterization, and in vivo immunomodulatory activity.* J Biol Chem, 2000. **275**(25): p. 19167-76.

10. Starnes, T., et al., *Cutting edge: IL-17D, a novel member of the IL-17 family, stimulates cytokine production and inhibits hemopoiesis.* J Immunol, 2002. **169**(2): p. 642-6.

11. Starnes, T., et al., *Cutting edge: IL-17F, a novel cytokine selectively expressed in activated T cells and monocytes, regulates angiogenesis and endothelial cell cytokine production.* J Immunol, 2001. **167**(8): p. 4137-40.

12. Zhang, X., et al., *Structure and function of interleukin-17 family cytokines.* Protein Cell, 2011. **2**(1): p. 26-40.

13. Gerhardt, S., et al., *Structure of IL-17A in complex with a potent, fully human neutralizing antibody.* J Mol Biol, 2009. **394**(5): p. 905-21.

14. Moseley, T.A., et al., *Interleukin-17 family and IL-17 receptors.* Cytokine Growth Factor Rev, 2003. **14**(2): p. 155-74.

15. Gaffen, S.L., *Structure and signalling in the IL-17 receptor family.* Nat Rev Immunol, 2009. **9**(8): p. 556-67.

16. Monin, L. and S.L. Gaffen, *Interleukin 17 Family Cytokines: Signaling Mechanisms, Biological Activities, and Therapeutic Implications.* Cold Spring Harb Perspect Biol, 2018. **10**(4).

17. Novatchkova, M., et al., *The STIR-domain superfamily in signal transduction, development and immunity.* Trends Biochem Sci, 2003. **28**(5): p. 226-9.

18. Ely, L.K., S. Fischer, and K.C. Garcia, *Structural basis of receptor sharing by interleukin 17 cytokines.* Nat Immunol, 2009. **10**(12): p. 1245-51.

19. Liu, S., et al., *Crystal structures of interleukin 17A and its complex with IL-17 receptor A.* Nat Commun, 2013. **4**: p. 1888.

20. Yao, Z., et al., *Molecular characterization of the human interleukin (IL)-17 receptor.* Cytokine, 1997. **9**(11): p. 794-800.

21. Toy, D., et al., *Cutting edge: interleukin 17 signals through a heteromeric receptor complex.* J Immunol, 2006. **177**(1): p. 36-9.

22. De Luca, A., et al., *The IL-17F/IL-17RC Axis Promotes Respiratory Allergy in the Proximal Airways.* Cell Rep, 2017. **20**(7): p. 1667-1680.

23. Goepfert, A., et al., *Structural Analysis Reveals that the Cytokine IL-17F Forms a Homodimeric Complex with Receptor IL-17RC to Drive IL-17RA-Independent Signaling.* Immunity, 2020. **52**(3): p. 499-512 e5.

24. Su, Y., et al., *Interleukin-17 receptor D constitutes an alternative receptor for interleukin-17A important in psoriasis-like skin inflammation.* Sci Immunol, 2019. **4**(36).

25. Amatya, N., A.V. Garg, and S.L. Gaffen, *IL-17 Signaling: The Yin and the Yang.* Trends Immunol, 2017. **38**(5): p. 310-322.

26. Kao, C.Y., et al., *IL-17 markedly up-regulates beta-defensin-2 expression in human airway epithelium via JAK and NF-kappaB signaling pathways.* J Immunol, 2004. **173**(5): p. 3482-91.

27. Kao, C.Y., et al., *Requirements for two proximal NF-kappaB binding sites and IkappaB-zeta in IL-17A-induced human beta-defensin 2 expression by conducting airway epithelium.* J Biol Chem, 2008. **283**(22): p. 15309-18.

28. Onishi, R.M., et al., *SEF/IL-17R (SEFIR) is not enough: an extended SEFIR domain is required for il-17RA-mediated signal transduction.* J Biol Chem, 2010. **285**(43): p. 32751-9.

29. Bertelsen, T., et al., *IL-17F regulates psoriasis-associated genes through IkappaBzeta.* Exp Dermatol, 2017. **26**(3): p. 234-241.

30. Hot, A., et al., *IL-17A- versus IL-17F-induced intracellular signal transduction pathways and modulation by IL-17RA and IL-17RC RNA interference in rheumatoid synoviocytes.* Ann Rheum Dis, 2011. **70**(2): p. 341-8.

31. Kawaguchi, M., et al., *Induction of granulocyte-macrophage colony-stimulating factor by a new cytokine, ML-1 (IL-17F), via Raf I-MEK-ERK pathway.* J Allergy Clin Immunol, 2004. **114**(2): p. 444-50.

32. Zrioual, S., et al., *Genome-wide comparison between IL-17A- and IL-17F-induced effects in human rheumatoid arthritis synoviocytes.* J Immunol, 2009. **182**(5): p. 3112-20.

33. Wright, J.F., et al., *Identification of an Interleukin 17F/17A Heterodimer in Activated Human CD4+ T Cells.* J Biol Chem, 2007. **282**(18): p. 13447-55.

34. Chang, S.H. and C. Dong, *A novel heterodimeric cytokine consisting of IL-17 and IL-17F regulates inflammatory responses.* Cell Res, 2007. **17**(5): p. 435-40.

35. Wright, J.F., et al., *The human IL-17F/IL-17A heterodimeric cytokine signals through the IL-17RA/IL-17RC receptor complex.* J Immunol, 2008. **181**(4): p. 2799-805.

36. Ho, A.W., et al., *IL-17RC is required for immune signaling via an extended SEF/IL-17R signaling domain in the cytoplasmic tail.* J Immunol, 2010. **185**(2): p. 1063-70.

37. Hu, Y., et al., *IL-17RC is required for IL-17A- and IL-17F-dependent signaling and the pathogenesis of experimental autoimmune encephalomyelitis.* J Immunol, 2010. **184**(8): p. 4307-16.

38. Maitra, A., et al., *Distinct functional motifs within the IL-17 receptor regulate signal transduction and target gene expression.* Proc Natl Acad Sci U S A, 2007. **104**(18): p. 7506-11.

39. Gu, C., L. Wu, and X. Li, *IL-17 family: cytokines, receptors and signaling.* Cytokine, 2013. **64**(2): p. 477-85.

40. Chang, S.H., H. Park, and C. Dong, *Act1 adaptor protein is an immediate and essential signaling component of interleukin-17 receptor.* J Biol Chem, 2006. **281**(47): p. 35603-7.

41. Qian, Y., et al., *The adaptor Act1 is required for interleukin 17-dependent signaling associated with autoimmune and inflammatory disease.* Nat Immunol, 2007. **8**(3): p. 247-56.

42. Ho, A.W. and S.L. Gaffen, *IL-17RC: a partner in IL-17 signaling and beyond.* Semin Immunopathol, 2010. **32**(1): p. 33-42.

43. Liu, C., et al., *Act1, a U-box E3 ubiquitin ligase for IL-17 signaling.* Sci Signal, 2009. **2**(92): p. ra63.

44. Song, X. and Y. Qian, *The activation and regulation of IL-17 receptor mediated signaling.* Cytokine, 2013. **62**(2): p. 175-82.

45. Leonardi, A., et al., *CIKS, a connection to Ikappa B kinase and stress-activated protein kinase.* Proc Natl Acad Sci U S A, 2000. **97**(19): p. 10494-9.

46. Lv, F., et al., *The role of Act1, a NF-kappaB-activating protein, in IL-6 and IL-8 levels induced by IL-17 stimulation in SW982 cells.* Pharm Biol, 2013. **51**(11): p. 1444-50.

47. Schwandner, R., K. Yamaguchi, and Z. Cao, *Requirement of tumor necrosis factor receptor-associated factor (TRAF)6 in interleukin 17 signal transduction.* J Exp Med, 2000. **191**(7): p. 1233-40.

48. Andoh, A., et al., *Interleukin (IL)-4 and IL-17 synergistically stimulate IL-6 secretion in human colonic myofibroblasts.* Int J Mol Med, 2002. **10**(5): p. 631-4.

49. Andoh, A., et al., *Extracellular signal-regulated kinases 1 and 2 participate in interleukin-17 plus tumor necrosis factor-alpha-induced stabilization of interleukin-6 mRNA in human pancreatic myofibroblasts.* Biochim Biophys Acta, 2002. **1591**(1-3): p. 69-74.

50. Hata, K., et al., *IL-17 stimulates inflammatory responses via NF-kappaB and MAP kinase pathways in human colonic myofibroblasts.* Am J Physiol Gastrointest Liver Physiol, 2002. **282**(6): p. G1035-44.

51. Shen, F. and S.L. Gaffen, *Structure-function relationships in the IL-17 receptor: implications for signal transduction and therapy.* Cytokine, 2008. **41**(2): p. 92-104.

52. Ruddy, M.J., et al., *Functional cooperation between interleukin-17 and tumor necrosis factor-alpha is mediated by CCAAT/enhancer-binding protein family members.* J Biol Chem, 2004. **279**(4): p. 2559-67.

53. Miossec, P., *Interleukin-17 in rheumatoid arthritis: if T cells were to contribute to inflammation and destruction through synergy.* Arthritis Rheum, 2003. **48**(3): p. 594-601.

54. Hartupee, J., et al., *IL-17 enhances chemokine gene expression through mRNA stabilization.* J Immunol, 2007. **179**(6): p. 4135-41.

55. Karlsen, J.R., N. Borregaard, and J.B. Cowland, *Induction of neutrophil gelatinase-associated lipocalin expression by co-stimulation with interleukin-17 and tumor necrosis factor-alpha is controlled by IkappaB-zeta but neither by C/EBP-beta nor C/EBP-delta.* J Biol Chem, 2010. **285**(19): p. 14088-100.

56. Sun, D., et al., *Treatment with IL-17 prolongs the half-life of chemokine CXCL1 mRNA via the adaptor TRAF5 and the splicing-regulatory factor SF2 (ASF).* Nat Immunol, 2011. **12**(9): p. 853-60.

57. Herjan, T., et al., *HuR is required for IL-17-induced Act1-mediated CXCL1 and CXCL5 mRNA stabilization.* J Immunol, 2013. **191**(2): p. 640-9.

58. Shen, F., et al., *IL-17 Receptor Signaling Inhibits C/EBPbeta by Sequential Phosphorylation of the Regulatory 2 Domain.* Sci Signal, 2009. **2**(59): p. ra8.

59. Zhu, S., et al., *Modulation of experimental autoimmune encephalomyelitis through TRAF3-mediated suppression of interleukin 17 receptor signaling.* J Exp Med, 2010. **207**(12): p. 2647-62.

60. Garg, A.V., et al., *The deubiquitinase A20 mediates feedback inhibition of interleukin-17 receptor signaling.* Sci Signal, 2013. **6**(278): p. ra44.

61. Ma, A. and B.A. Malynn, *A20: linking a complex regulator of ubiquitylation to immunity and human disease.* Nat Rev Immunol, 2012. **12**(11): p. 774-85.

62. Garg, A.V., et al., *MCPIP1 Endoribonuclease Activity Negatively Regulates Interleukin-17-Mediated Signaling and Inflammation.* Immunity, 2015. **43**(3): p. 475-87.

63. Somma, D., et al., *CIKS/DDX3X Interaction Controls the Stability of the Zc3h12a mRNA Induced by IL-17.* J Immunol, 2015. **194**(7): p. 3286-94.

64. Liang, J., et al., *MCP-induced protein 1 deubiquitinates TRAF proteins and negatively regulates JNK and NF-kappaB signaling.* J Exp Med, 2010. **207**(13): p. 2959-73.

65. Harrington, L.E., et al., *Interleukin 17-producing CD4+ effector T cells develop via a lineage distinct from the T helper type 1 and 2 lineages.* Nat Immunol, 2005. **6**(11): p. 1123-32.

66. Park, H., et al., *A distinct lineage of CD4 T cells regulates tissue inflammation by producing interleukin 17.* Nat Immunol, 2005. **6**(11): p. 1133-41.

67. Cua, D.J. and C.M. Tato, *Innate IL-17-producing cells: the sentinels of the immune system.* Nat Rev Immunol, 2010. **10**(7): p. 479-89.

68. Annunziato, F., et al., *Type 17 T helper cells-origins, features and possible roles in rheumatic disease.* Nat Rev Rheumatol, 2009. **5**(6): p. 325-31.

69. Zuniga, L.A., et al., *Th17 cell development: from the cradle to the grave.* Immunol Rev, 2013. **252**(1): p. 78-88.

70. Curtis, M.M. and S.S. Way, *Interleukin-17 in host defence against bacterial, mycobacterial and fungal pathogens.* Immunology, 2009. **126**(2): p. 177-85.

71. Langrish, C.L., et al., *IL-23 drives a pathogenic T cell population that induces autoimmune inflammation.* J Exp Med, 2005. **201**(2): p. 233-40.

72. Murphy, C.A., et al., *Divergent pro- and antiinflammatory roles for IL-23 and IL-12 in joint autoimmune inflammation.* J Exp Med, 2003. **198**(12): p. 1951-7.

73. Chabaud, M., et al., *Human interleukin-17: A T cell-derived proinflammatory cytokine produced by the rheumatoid synovium.* Arthritis Rheum, 1999. **42**(5): p. 963-70.

74. Lock, C., et al., *Gene-microarray analysis of multiple sclerosis lesions yields new targets validated in autoimmune encephalomyelitis.* Nat Med, 2002. **8**(5): p. 500-8.

75. Matusevicius, D., et al., *Interleukin-17 mRNA expression in blood and CSF mononuclear cells is augmented in multiple sclerosis.* Mult Scler, 1999. **5**(2): p. 101-4.

76. Teunissen, M.B., et al., *Interleukin-17 and interferon-gamma synergize in the enhancement of proinflammatory cytokine production by human keratinocytes.* J Invest Dermatol, 1998. **111**(4): p. 645-9.

77. Chiricozzi, A. and J.G. Krueger, *IL-17 targeted therapies for psoriasis.* Expert Opin Investig Drugs, 2013. **22**(8): p. 993-1005.

78. Gordon, K.B., et al., *Phase 3 Trials of Ixekizumab in Moderate-to-Severe Plaque Psoriasis.* N Engl J Med, 2016. **375**(4): p. 345-56.

79. Langley, R.G., et al., *Secukinumab in plaque psoriasis--results of two phase 3 trials.* N Engl J Med, 2014. **371**(4): p. 326-38.

80. Blair, H.A., *Brodalumab: A Review in Moderate to Severe Plaque Psoriasis.* Drugs, 2018. **78**(4): p. 495-504.

81. Reich, K., et al., *Bimekizumab versus ustekinumab for the treatment of moderate to severe plaque psoriasis (BE VIVID): efficacy and safety from a 52-week, multicentre, double-blind, active comparator and placebo controlled phase 3 trial.* Lancet, 2021. **397**(10273): p. 487-498.

82. Fitzpatrick, L.R., *Inhibition of IL-17 as a pharmacological approach for IBD.* Int Rev Immunol, 2013. **32**(5-6): p. 544-55.

83. Blauvelt, A., *Safety of secukinumab in the treatment of psoriasis.* Expert Opin Drug Saf, 2016. **15**(10): p. 1413-20.

84. Mease, P., et al., *Safety of Ixekizumab in Patients With Psoriatic Arthritis: Results From a Pooled Analysis of Three Clinical Trials.* Arthritis Care Res (Hoboken), 2019. **71**(3): p. 367-378.

85. Ishigame, H., et al., *Differential roles of interleukin-17A and -17F in host defense against mucoepithelial bacterial infection and allergic responses.* Immunity, 2009. **30**(1): p. 108-19.

86. Yang, X.O., et al., *Regulation of inflammatory responses by IL-17F.* J Exp Med, 2008. **205**(5): p. 1063-75.

87. Whibley, N., et al., *Antibody blockade of IL-17 family cytokines in immunity to acute murine oral mucosal candidiasis.* J Leukoc Biol, 2016. **99**(6): p. 1153-64.

88. Riedel, J.H., et al., *IL-17F Promotes Tissue Injury in Autoimmune Kidney Diseases.* J Am Soc Nephrol, 2016. **27**(12): p. 3666-3677.

89. Tang, C., et al., *Suppression of IL-17F, but not of IL-17A, provides protection against colitis by inducing Treg cells through modification of the intestinal microbiota.* Nat Immunol, 2018. **19**(7): p. 755-765.

90. Brown, G.D., et al., *Hidden killers: human fungal infections.* Sci Transl Med, 2012. **4**(165): p. 165rv13.

91. Havlickova, B., V.A. Czaika, and M. Friedrich, *Epidemiological trends in skin mycoses worldwide.* Mycoses, 2008. **51 Suppl 4**: p. 2-15.

92. Acosta-Rodriguez, E.V., et al., *Surface phenotype and antigenic specificity of human interleukin 17-producing T helper memory cells.* Nat Immunol, 2007. **8**(6): p. 639-46.

93. Bacher, P., et al., *Human Anti-fungal Th17 Immunity and Pathology Rely on Cross-Reactivity against Candida albicans.* Cell, 2019. **176**(6): p. 1340-1355 e15.

94. van de Veerdonk, F.L., et al., *Milder clinical hyperimmunoglobulin E syndrome phenotype is associated with partial interleukin-17 deficiency.* Clin Exp Immunol, 2010. **159**(1): p. 57-64.

95. Zielinski, C.E., et al., *Pathogen-induced human TH17 cells produce IFN-gamma or IL-10 and are regulated by IL-1beta.* Nature, 2012. **484**(7395): p. 514-8.

96. Boisson, B., et al., *An ACT1 mutation selectively abolishes interleukin-17 responses in humans with chronic mucocutaneous candidiasis.* Immunity, 2013. **39**(4): p. 676-86.

97. Levy, R., et al., *Genetic, immunological, and clinical features of patients with bacterial and fungal infections due to inherited IL-17RA deficiency.* Proc Natl Acad Sci U S A, 2016. **113**(51): p. E8277-E8285.

98. Ling, Y., et al., *Inherited IL-17RC deficiency in patients with chronic mucocutaneous candidiasis.* J Exp Med, 2015. **212**(5): p. 619-31.

99. Puel, A., et al., *Chronic mucocutaneous candidiasis in humans with inborn errors of interleukin-17 immunity.* Science, 2011. **332**(6025): p. 65-8.

100. Li, J., et al., *Inborn errors of immunity underlying fungal diseases in otherwise healthy individuals.* Curr Opin Microbiol, 2017. **40**: p. 46-57.

101. Milner, J.D. and S.M. Holland, *The cup runneth over: lessons from the ever-expanding pool of primary immunodeficiency diseases.* Nat Rev Immunol, 2013. **13**(9): p. 635-48.

102. Okada, S., et al., *IMMUNODEFICIENCIES. Impairment of immunity to Candida and Mycobacterium in humans with bi-allelic RORC mutations.* Science, 2015. **349**(6248): p. 606-613.

103. Saunte, D.M., et al., *Candida infections in patients with psoriasis and psoriatic arthritis treated with interleukin-17 inhibitors and their practical management.* Br J Dermatol, 2017. **177**(1): p. 47-62.

104. Kamai, Y., et al., *New model of oropharyngeal candidiasis in mice.* Antimicrob Agents Chemother, 2001. **45**(11): p. 3195-7.

105. Conti, H.R., et al., *Th17 cells and IL-17 receptor signaling are essential for mucosal host defense against oral candidiasis.* J Exp Med, 2009. **206**(2): p. 299-311.

106. Ferreira, M.C., et al., *Interleukin-17-induced protein lipocalin 2 is dispensable for immunity to oral candidiasis.* Infect Immun, 2014. **82**(3): p. 1030-5.

107. Huang, W., et al., *Requirement of interleukin-17A for systemic anti-Candida albicans host defense in mice.* J Infect Dis, 2004. **190**(3): p. 624-31.

108. Kagami, S., et al., *IL-23 and IL-17A, but not IL-12 and IL-22, are required for optimal skin host defense against Candida albicans.* J Immunol, 2010. **185**(9): p. 5453-62.

109. Gladiator, A., et al., *Cutting edge: IL-17-secreting innate lymphoid cells are essential for host defense against fungal infection.* J Immunol, 2013. **190**(2): p. 521-5.

110. Lo, H.J., et al., *Nonfilamentous C. albicans mutants are avirulent.* Cell, 1997. **90**(5): p. 939-49.

111. Park, H., et al., *Role of the fungal Ras-protein kinase A pathway in governing epithelial cell interactions during oropharyngeal candidiasis.* Cell Microbiol, 2005. **7**(4): p. 499-510.

112. Gow, N.A. and B. Hube, *Importance of the Candida albicans cell wall during commensalism and infection.* Curr Opin Microbiol, 2012. **15**(4): p. 406-12.

113. Wheeler, R.T., et al., *Dynamic, morphotype-specific Candida albicans beta-glucan exposure during infection and drug treatment.* PLoS Pathog, 2008. **4**(12): p. e1000227.

114. Dennehy, K.M., et al., *Reciprocal regulation of IL-23 and IL-12 following co-activation of Dectin-1 and TLR signaling pathways.* Eur J Immunol, 2009. **39**(5): p. 1379-86.

115. Gringhuis, S.I., et al., *Dectin-1 directs T helper cell differentiation by controlling noncanonical NF-kappaB activation through Raf-1 and Syk.* Nat Immunol, 2009. **10**(2): p. 203-13.

116. Tassi, I., et al., *Requirement of phospholipase C-gamma2 (PLCgamma2) for Dectin-1-induced antigen presentation and induction of TH1/TH17 polarization.* Eur J Immunol, 2009. **39**(5): p. 1369-78.

117. Gross, O., et al., *Syk kinase signalling couples to the Nlrp3 inflammasome for anti-fungal host defence.* Nature, 2009. **459**(7245): p. 433-6.

118. Hise, A.G., et al., *An essential role for the NLRP3 inflammasome in host defense against the human fungal pathogen Candida albicans.* Cell Host Microbe, 2009. **5**(5): p. 487-97.

119. Netea, M.G., et al., *Immune sensing of Candida albicans requires cooperative recognition of mannans and glucans by lectin and Toll-like receptors.* J Clin Invest, 2006. **116**(6): p. 1642-50.

120. Tomalka, J., et al., *A novel role for the NLRC4 inflammasome in mucosal defenses against the fungal pathogen Candida albicans.* PLoS Pathog, 2011. **7**(12): p. e1002379.

121. Villamon, E., et al., *Myeloid differentiation factor 88 (MyD88) is required for murine resistance to Candida albicans and is critically involved in Candida -induced production of cytokines.* Eur Cytokine Netw, 2004. **15**(3): p. 263-71.

122. Yuan, X. and K.R. Wilhelmus, *Toll-like receptors involved in the pathogenesis of experimental Candida albicans keratitis.* Invest Ophthalmol Vis Sci, 2010. **51**(4): p. 2094-100.

123. Moyes, D.L., et al., *Candidalysin is a fungal peptide toxin critical for mucosal infection.* Nature, 2016. **532**(7597): p. 64-8.

124. Verma, A.H., et al., *Oral epithelial cells orchestrate innate type 17 responses to Candida albicans through the virulence factor candidalysin.* Sci Immunol, 2017. **2**(17).

125. Verma, A.H., et al., *IL-36 and IL-1/IL-17 Drive Immunity to Oral Candidiasis via Parallel Mechanisms.* J Immunol, 2018. **201**(2): p. 627-634.

126. Ho, J., et al., *Candidalysin activates innate epithelial immune responses via epidermal growth factor receptor.* Nat Commun, 2019. **10**(1): p. 2297.

127. Moyes, D.L., et al., *Activation of MAPK/c-Fos induced responses in oral epithelial cells is specific to Candida albicans and Candida dubliniensis hyphae.* Med Microbiol Immunol, 2012. **201**(1): p. 93-101.

128. Moyes, D.L., et al., *A biphasic innate immune MAPK response discriminates between the yeast and hyphal forms of Candida albicans in epithelial cells.* Cell Host Microbe, 2010. **8**(3): p. 225-35.

129. Conti, H.R., et al., *Oral-resident natural Th17 cells and gammadelta T cells control opportunistic Candida albicans infections.* J Exp Med, 2014. **211**(10): p. 2075-84.

130. Fan, D., et al., *Activation of HIF-1alpha and LL-37 by commensal bacteria inhibits Candida albicans colonization.* Nat Med, 2015. **21**(7): p. 808-14.

131. St Leger, A.J., et al., *An Ocular Commensal Protects against Corneal Infection by Driving an Interleukin-17 Response from Mucosal gammadelta T Cells.* Immunity, 2017. **47**(1): p. 148-158 e5.

132. Break, T.J., et al., *Aberrant type 1 immunity drives susceptibility to mucosal fungal infections.* Science, 2021. **371**(6526).

133. Presland, R.B. and R.J. Jurevic, *Making sense of the epithelial barrier: what molecular biology and genetics tell us about the functions of oral mucosal and epidermal tissues.* J Dent Educ, 2002. **66**(4): p. 564-74.

134. Byrd, K.M., et al., *Heterogeneity within Stratified Epithelial Stem Cell Populations Maintains the Oral Mucosa in Response to Physiological Stress.* Cell Stem Cell, 2019. **25**(6): p. 814-829 e6.

135. Tanaka, T., et al., *Identification of stem cells that maintain and regenerate lingual keratinized epithelial cells.* Nat Cell Biol, 2013. **15**(5): p. 511-8.

136. Alcolea, M.P. and P.H. Jones, *Lineage analysis of epidermal stem cells.* Cold Spring Harb Perspect Med, 2014. **4**(1): p. a015206.

137. Blanpain, C. and E. Fuchs, *Stem cell plasticity. Plasticity of epithelial stem cells in tissue regeneration.* Science, 2014. **344**(6189): p. 1242281.

138. Presland, R.B. and B.A. Dale, *Epithelial structural proteins of the skin and oral cavity: function in health and disease.* Crit Rev Oral Biol Med, 2000. **11**(4): p. 383-408.

139. Conti, H.R., et al., *IL-17 Receptor Signaling in Oral Epithelial Cells Is Critical for Protection against Oropharyngeal Candidiasis.* Cell Host Microbe, 2016. **20**(5): p. 606-617.

140. Desai, J.V. and M.S. Lionakis, *The role of neutrophils in host defense against invasive fungal infections.* Curr Clin Microbiol Rep, 2018. **5**(3): p. 181-189.

141. Huppler, A.R., et al., *Role of neutrophils in IL-17-dependent immunity to mucosal candidiasis.* J Immunol, 2014. **192**(4): p. 1745-52.

142. Aggor, F.E.Y., et al., *Oral epithelial IL-22/STAT3 signaling licenses IL-17-mediated immunity to oral mucosal candidiasis.* Sci Immunol, 2020. **5**(48).

143. Tomalka, J., et al., *beta-Defensin 1 plays a role in acute mucosal defense against Candida albicans.* J Immunol, 2015. **194**(4): p. 1788-95.

144. Gill, S.R., et al., *Metagenomic analysis of the human distal gut microbiome.* Science, 2006. **312**(5778): p. 1355-9.

145. Ng, S.C., et al., *Worldwide incidence and prevalence of inflammatory bowel disease in the 21st century: a systematic review of population-based studies.* Lancet, 2017. **390**(10114): p. 2769-2778.

146. Geremia, A., et al., *Innate and adaptive immunity in inflammatory bowel disease.* Autoimmun Rev, 2014. **13**(1): p. 3-10.

147. Salim, S.Y. and J.D. Soderholm, *Importance of disrupted intestinal barrier in inflammatory bowel diseases.* Inflamm Bowel Dis, 2011. **17**(1): p. 362-81.

148. Anderson, C.A., et al., *Meta-analysis identifies 29 additional ulcerative colitis risk loci, increasing the number of confirmed associations to 47.* Nat Genet, 2011. **43**(3): p. 246-52.

149. Consortium, U.I.G., et al., *Genome-wide association study of ulcerative colitis identifies three new susceptibility loci, including the HNF4A region.* Nat Genet, 2009. **41**(12): p. 1330-4.

150. Duerr, R.H., et al., *A genome-wide association study identifies IL23R as an inflammatory bowel disease gene.* Science, 2006. **314**(5804): p. 1461-3.

151. Rafa, H., et al., *IL-23/IL-17A axis correlates with the nitric oxide pathway in inflammatory bowel disease: immunomodulatory effect of retinoic acid.* J Interferon Cytokine Res, 2013. **33**(7): p. 355-68.

152. Youssef, T., et al., *Evaluation of interleukin 23 (IL-23) as a non-invasive test of disease severity in patients with ulcerative colitis.* Arab J Gastroenterol, 2018. **19**(3): p. 116-120.

153. Zheng, Z.D., X.Q. Wan, and L.Y. Liu, *Serum contents of IL-23 and IL-17 in the patients with ulcerative colitis and the clinical significance.* Xi Bao Yu Fen Zi Mian Yi Xue Za Zhi, 2011. **27**(2): p. 203-6.

154. Zhu, X.M., et al., *Serum IL-6, IL-23 profile and Treg/Th17 peripheral cell populations in pediatric patients with inflammatory bowel disease.* Pharmazie, 2017. **72**(5): p. 283-287.

155. Cox, J.H., et al., *Opposing consequences of IL-23 signaling mediated by innate and adaptive cells in chemically induced colitis in mice.* Mucosal Immunol, 2012. **5**(1): p. 99-109.

156. Hue, S., et al., *Interleukin-23 drives innate and T cell-mediated intestinal inflammation.* J Exp Med, 2006. **203**(11): p. 2473-83.

157. Kullberg, M.C., et al., *IL-23 plays a key role in Helicobacter hepaticus-induced T cell-dependent colitis.* J Exp Med, 2006. **203**(11): p. 2485-94.

158. Uhlig, H.H., et al., *Differential activity of IL-12 and IL-23 in mucosal and systemic innate immune pathology.* Immunity, 2006. **25**(2): p. 309-18.

159. Yen, D., et al., *IL-23 is essential for T cell-mediated colitis and promotes inflammation via IL-17 and IL-6.* J Clin Invest, 2006. **116**(5): p. 1310-6.

160. Niederreiter, L., T.E. Adolph, and A. Kaser, *Anti-IL-12/23 in Crohn's disease: bench and bedside.* Curr Drug Targets, 2013. **14**(12): p. 1379-84.

161. Takatori, H., et al., *Lymphoid tissue inducer-like cells are an innate source of IL-17 and IL-22.* J Exp Med, 2009. **206**(1): p. 35-41.

162. Eken, A., et al., *IL-23R+ innate lymphoid cells induce colitis via interleukin-22-dependent mechanism.* Mucosal Immunol, 2014. **7**(1): p. 143-54.

163. Fujino, S., et al., *Increased expression of interleukin 17 in inflammatory bowel disease.* Gut, 2003. **52**(1): p. 65-70.

164. Hueber, W., et al., *Secukinumab, a human anti-IL-17A monoclonal antibody, for moderate to severe Crohn's disease: unexpected results of a randomised, double-blind placebo-controlled trial.* Gut, 2012. **61**(12): p. 1693-700.

165. Targan, S.R., et al., *A Randomized, Double-Blind, Placebo-Controlled Phase 2 Study of Brodalumab in Patients With Moderate-to-Severe Crohn's Disease.* Am J Gastroenterol, 2016. **111**(11): p. 1599-1607.

166. Cao, A.T., et al., *Th17 cells upregulate polymeric Ig receptor and intestinal IgA and contribute to intestinal homeostasis.* J Immunol, 2012. **189**(9): p. 4666-73.

167. Lee, J.S., et al., *Interleukin-23-Independent IL-17 Production Regulates Intestinal Epithelial Permeability.* Immunity, 2015. **43**(4): p. 727-38.

168. Ogawa, A., et al., *Neutralization of interleukin-17 aggravates dextran sulfate sodium-induced colitis in mice.* Clin Immunol, 2004. **110**(1): p. 55-62.

169. Song, X., et al., *Growth Factor FGF2 Cooperates with Interleukin-17 to Repair Intestinal Epithelial Damage.* Immunity, 2015. **43**(3): p. 488-501.

170. Atarashi, K., et al., *Induction of colonic regulatory T cells by indigenous Clostridium species.* Science, 2011. **331**(6015): p. 337-41.

171. Mayne, C.G. and C.B. Williams, *Induced and natural regulatory T cells in the development of inflammatory bowel disease.* Inflamm Bowel Dis, 2013. **19**(8): p. 1772-88.

172. Chamouard, P., et al., *Diminution of Circulating CD4+CD25 high T cells in naive Crohn's disease.* Dig Dis Sci, 2009. **54**(10): p. 2084-93.

173. Maul, J., et al., *Peripheral and intestinal regulatory CD4+ CD25(high) T cells in inflammatory bowel disease.* Gastroenterology, 2005. **128**(7): p. 1868-78.

174. Saruta, M., et al., *Characterization of FOXP3+CD4+ regulatory T cells in Crohn's disease.* Clin Immunol, 2007. **125**(3): p. 281-90.

175. Singh, B., et al., *Control of intestinal inflammation by regulatory T cells.* Immunol Rev, 2001. **182**: p. 190-200.

176. Martin, B., et al., *Suppression of CD4+ T lymphocyte effector functions by CD4+CD25+ cells in vivo.* J Immunol, 2004. **172**(6): p. 3391-8.

177. Fantini, M.C., et al., *Transforming growth factor beta induced FoxP3+ regulatory T cells suppress Th1 mediated experimental colitis.* Gut, 2006. **55**(5): p. 671-80.

178. O'Connor, W., Jr., et al., *A protective function for interleukin 17A in T cell-mediated intestinal inflammation.* Nat Immunol, 2009. **10**(6): p. 603-9.

179. Strzepa, A. and M. Szczepanik, *IL-17-expressing cells as a potential therapeutic target for treatment of immunological disorders.* Pharmacol Rep, 2011. **63**(1): p. 30-44.

180. Leppkes, M., et al., *RORgamma-expressing Th17 cells induce murine chronic intestinal inflammation via redundant effects of IL-17A and IL-17F.* Gastroenterology, 2009. **136**(1): p. 257-67.

181. Wedebye Schmidt, E.G., et al., *TH17 cell induction and effects of IL-17A and IL-17F blockade in experimental colitis.* Inflamm Bowel Dis, 2013. **19**(8): p. 1567-76.

182. Zhang, Z., et al., *Critical role of IL-17 receptor signaling in acute TNBS-induced colitis.* Inflamm Bowel Dis, 2006. **12**(5): p. 382-8.

183. Buonocore, S., et al., *Innate lymphoid cells drive interleukin-23-dependent innate intestinal pathology.* Nature, 2010. **464**(7293): p. 1371-5.

184. Coresh, J., et al., *Prevalence of chronic kidney disease in the United States.* JAMA, 2007. **298**(17): p. 2038-47.

185. Kurts, C., et al., *The immune system and kidney disease: basic concepts and clinical implications.* Nat Rev Immunol, 2013. **13**(10): p. 738-53.

186. Jennette, J.C., et al., *2012 revised International Chapel Hill Consensus Conference Nomenclature of Vasculitides.* Arthritis Rheum, 2013. **65**(1): p. 1-11.

187. McAdoo, S.P. and C.D. Pusey, *Anti-Glomerular Basement Membrane Disease.* Clin J Am Soc Nephrol, 2017. **12**(7): p. 1162-1172.

188. Anguiano, L., R. Kain, and H.J. Anders, *The glomerular crescent: triggers, evolution, resolution, and implications for therapy.* Curr Opin Nephrol Hypertens, 2020. **29**(3): p. 302-309.

189. Jennette, J.C., *Rapidly progressive crescentic glomerulonephritis.* Kidney Int, 2003. **63**(3): p. 1164-77.

190. Kambham, N., *Crescentic Glomerulonephritis: an update on Pauci-immune and Anti-GBM diseases.* Adv Anat Pathol, 2012. **19**(2): p. 111-24.

191. Bar, E., et al., *IL-17 regulates systemic fungal immunity by controlling the functional competence of NK cells.* Immunity, 2014. **40**(1): p. 117-27.

192. Chan, L.C., et al., *Nonredundant Roles of Interleukin-17A (IL-17A) and IL-22 in Murine Host Defense against Cutaneous and Hematogenous Infection Due to Methicillin-Resistant Staphylococcus aureus.* Infect Immun, 2015. **83**(11): p. 4427-37.

193. Sivick, K.E., et al., *The innate immune response to uropathogenic Escherichia coli involves IL-17A in a murine model of urinary tract infection.* J Immunol, 2010. **184**(4): p. 2065-75.

194. Crispin, J.C., et al., *Expanded double negative T cells in patients with systemic lupus erythematosus produce IL-17 and infiltrate the kidneys.* J Immunol, 2008. **181**(12): p. 8761-6.

195. Wong, C.K., et al., *Hyperproduction of IL-23 and IL-17 in patients with systemic lupus erythematosus: implications for Th17-mediated inflammation in auto-immunity.* Clin Immunol, 2008. **127**(3): p. 385-93.

196. Lin, J.R., et al., *Interleukin-17 promotes the production of underglycosylated IgA1 in DAKIKI cells.* Ren Fail, 2018. **40**(1): p. 60-67.

197. Stangou, M., et al., *Up-regulation of urinary markers predict outcome in IgA nephropathy but their predictive value is influenced by treatment with steroids and azathioprine.* Clin Nephrol, 2013. **80**(3): p. 203-10.

198. Krebs, C.F., et al., *Pathogen-induced tissue-resident memory TH17 (TRM17) cells amplify autoimmune kidney disease.* Sci Immunol, 2020. **5**(50).

199. Ooi, J.D., et al., *IL-23, not IL-12, directs autoimmunity to the Goodpasture antigen.* J Am Soc Nephrol, 2009. **20**(5): p. 980-9.

200. Paust, H.J., et al., *The IL-23/Th17 axis contributes to renal injury in experimental glomerulonephritis.* J Am Soc Nephrol, 2009. **20**(5): p. 969-79.

201. Ramani, K., et al., *An essential role of interleukin-17 receptor signaling in the development of autoimmune glomerulonephritis.* J Leukoc Biol, 2014. **96**(3): p. 463-72.

202. Turner, J.E., et al., *IL-17A production by renal gammadelta T cells promotes kidney injury in crescentic GN.* J Am Soc Nephrol, 2012. **23**(9): p. 1486-95.

203. Su, H., C.T. Lei, and C. Zhang, *Interleukin-6 Signaling Pathway and Its Role in Kidney Disease: An Update.* Front Immunol, 2017. **8**: p. 405.

204. Yang, H.C., Y. Zuo, and A.B. Fogo, *Models of chronic kidney disease.* Drug Discov Today Dis Models, 2010. **7**(1-2): p. 13-19.

205. Morel, L. and E.K. Wakeland, *Susceptibility to lupus nephritis in the NZB/W model system.* Curr Opin Immunol, 1998. **10**(6): p. 718-25.

206. Reddy, P.S., et al., *Mapping similarities in mTOR pathway perturbations in mouse lupus nephritis models and human lupus nephritis.* Arthritis Res Ther, 2008. **10**(6): p. R127.

207. Santiago-Raber, M.L., et al., *Genetic basis of murine lupus.* Autoimmun Rev, 2004. **3**(1): p. 33-9.

208. Hellmark, T., C. Johansson, and J. Wieslander, *Characterization of anti-GBM antibodies involved in Goodpasture's syndrome.* Kidney Int, 1994. **46**(3): p. 823-9.

209. Reynolds, J., et al., *Strain susceptibility to active induction and passive transfer of experimental autoimmune glomerulonephritis in the rat.* Nephrol Dial Transplant, 2006. **21**(12): p. 3398-408.

210. Reynolds, J., et al., *Experimental autoimmune glomerulonephritis (EAG) induced by homologous and heterologous glomerular basement membrane in two substrains of Wistar-Kyoto rat.* Nephrol Dial Transplant, 1998. **13**(1): p. 44-52.

211. Xie, C., et al., *Strain distribution pattern of susceptibility to immune-mediated nephritis.* J Immunol, 2004. **172**(8): p. 5047-55.

212. Ishizaki, M., et al., *Experimental mesangioproliferative glomerulonephritis in rats induced by intravenous administration of anti-thymocyte serum.* Acta Pathol Jpn, 1986. **36**(8): p. 1191-203.

213. Liu, N., et al., *Coagulation in the mesangial area promotes ECM accumulation through factor V expression in MsPGN in rats.* Am J Physiol Renal Physiol, 2004. **287**(4): p. F612-20.

214. Wada, Y., et al., *Impairment of vascular regeneration precedes progressive glomerulosclerosis in anti-Thy 1 glomerulonephritis.* Kidney Int, 2002. **61**(2): p. 432-43.

215. Cosgrove, D., et al., *Collagen COL4A3 knockout: a mouse model for autosomal Alport syndrome.* Genes Dev, 1996. **10**(23): p. 2981-92.

216. LeBleu, V., et al., *Stem cell therapies benefit Alport syndrome.* J Am Soc Nephrol, 2009. **20**(11): p. 2359-70.

217. Miner, J.H. and J.R. Sanes, *Molecular and functional defects in kidneys of mice lacking collagen alpha 3(IV): implications for Alport syndrome.* J Cell Biol, 1996. **135**(5): p. 1403-13.

218. Sugimoto, H., et al., *Bone-marrow-derived stem cells repair basement membrane collagen defects and reverse genetic kidney disease.* Proc Natl Acad Sci U S A, 2006. **103**(19): p. 7321-6.

219. Lee, Y.K., et al., *Late developmental plasticity in the T helper 17 lineage.* Immunity, 2009. **30**(1): p. 92-107.

220. Concordet, J.P. and M. Haeussler, *CRISPOR: intuitive guide selection for CRISPR/Cas9 genome editing experiments and screens.* Nucleic Acids Res, 2018. **46**(W1): p. W242-W245.

221. Pelletier, S., S. Gingras, and D.R. Green, *Mouse genome engineering via CRISPR-Cas9 for study of immune function.* Immunity, 2015. **42**(1): p. 18-27.

222. Conti, H.R., et al., *Animal models for candidiasis.* Curr Protoc Immunol, 2014. **105**: p. 19 6 1-19 6 17.

223. Solis, N.V. and S.G. Filler, *Mouse model of oropharyngeal candidiasis.* Nat Protoc, 2012. **7**(4): p. 637-42.

224. Altmeier, S., et al., *IL-1 Coordinates the Neutrophil Response to C. albicans in the Oral Mucosa.* PLoS Pathog, 2016. **12**(9): p. e1005882.

225. Oda, N., et al., *Interleukin-17F induces pulmonary neutrophilia and amplifies antigen-induced allergic response.* Am J Respir Crit Care Med, 2005. **171**(1): p. 12-8.

226. Pandiyan, P., et al., *Isolation of T cells from mouse oral tissues.* Biol Proced Online, 2014. **16**(1): p. 4.

227. Sroussi, H.Y., et al., *Substitution of methionine 63 or 83 in S100A9 and cysteine 42 in S100A8 abrogate the antifungal activities of S100A8/A9: potential role for oxidative regulation.* FEMS Immunol Med Microbiol, 2009. **55**(1): p. 55-61.

228. Yano, J., M.C. Noverr, and P.L. Fidel, Jr., *Cytokines in the host response to Candida vaginitis: Identifying a role for non-classical immune mediators, S100 alarmins.* Cytokine, 2012. **58**(1): p. 118-28.

229. Conti, H.R., et al., *New mechanism of oral immunity to mucosal candidiasis in hyper-IgE syndrome.* Mucosal Immunol, 2011. **4**(4): p. 448-55.

230. Yang, D., et al., *Beta-defensins: linking innate and adaptive immunity through dendritic and T cell CCR6.* Science, 1999. **286**(5439): p. 525-8.

231. Shen, F., et al., *Combined Blockade of TNF-alpha and IL-17A Alleviates Progression of Collagen-Induced Arthritis without Causing Serious Infections in Mice.* J Immunol, 2019. **202**(7): p. 2017-2026.

232. Bar, E., et al., *A novel Th cell epitope of Candida albicans mediates protection from fungal infection.* J Immunol, 2012. **188**(11): p. 5636-43.

233. Hernandez-Santos, N., et al., *Th17 cells confer long-term adaptive immunity to oral mucosal Candida albicans infections.* Mucosal Immunol, 2013. **6**(5): p. 900-10.

234. Sparber, F., et al., *Langerin+ DCs regulate innate IL-17 production in the oral mucosa during Candida albicans-mediated infection.* PLoS Pathog, 2018. **14**(5): p. e1007069.

235. Ivanov, II, et al., *Induction of intestinal Th17 cells by segmented filamentous bacteria.* Cell, 2009. **139**(3): p. 485-98.

236. Richardson, J.P., et al., *Candidalysin Drives Epithelial Signaling, Neutrophil Recruitment, and Immunopathology at the Vaginal Mucosa.* Infect Immun, 2018. **86**(2).

237. Fidel, P.L., Jr., *Candida-host interactions in HIV disease: implications for oropharyngeal candidiasis.* Adv Dent Res, 2011. **23**(1): p. 45-9.

238. Moyes, D.L. and J.R. Naglik, *Mucosal immunity and Candida albicans infection.* Clin Dev Immunol, 2011. **2011**: p. 346307.

239. Lionakis, M.S. and S.M. Levitz, *Host Control of Fungal Infections: Lessons from Basic Studies and Human Cohorts.* Annu Rev Immunol, 2018. **36**: p. 157-191.

240. Deodhar, A., et al., *Long-term safety of secukinumab in patients with moderate-to-severe plaque psoriasis, psoriatic arthritis, and ankylosing spondylitis: integrated pooled clinical trial and post-marketing surveillance data.* Arthritis Res Ther, 2019. **21**(1): p. 111.

241. Farah, C.S., et al., *Distinct roles for interleukin-12p40 and tumour necrosis factor in resistance to oral candidiasis defined by gene-targeting.* Oral Microbiol Immunol, 2006. **21**(4): p. 252-5.

242. Goupil, M., et al., *Defective IL-17- and IL-22-dependent mucosal host response to Candida albicans determines susceptibility to oral candidiasis in mice expressing the HIV-1 transgene.* BMC Immunol, 2014. **15**: p. 49.

243. Naglik, J.R., J.P. Richardson, and D.L. Moyes, *Candida albicans pathogenicity and epithelial immunity.* PLoS Pathog, 2014. **10**(8): p. e1004257.

244. Shao, T.Y., et al., *Commensal Candida albicans Positively Calibrates Systemic Th17 Immunological Responses.* Cell Host Microbe, 2019. **25**(3): p. 404-417 e6.

245. Salvatori, O., et al., *Innate Immunity and Saliva in Candida albicans-mediated Oral Diseases.* J Dent Res, 2016. **95**(4): p. 365-71.

246. Vylkova, S., et al., *Distinct antifungal mechanisms: beta-defensins require Candida albicans Ssa1 protein, while Trk1p mediates activity of cysteine-free cationic peptides.* Antimicrob Agents Chemother, 2006. **50**(1): p. 324-31.

247. Ganz, T., *Defensins: antimicrobial peptides of innate immunity.* Nat Rev Immunol, 2003. **3**(9): p. 710-20.

248. Joly, S., et al., *Correlation between beta-defensin expression and induction profiles in gingival keratinocytes.* Mol Immunol, 2005. **42**(9): p. 1073-84.

249. Graham, C.E., et al., *Enterococcus faecalis bacteriocin EntV inhibits hyphal morphogenesis, biofilm formation, and virulence of Candida albicans.* Proc Natl Acad Sci U S A, 2017. **114**(17): p. 4507-4512.

250. Bader, O., et al., *Photo quiz. A 32-year-old man with ulcerative mucositis, skin lesions, and nail dystrophy. Chronic mucocutaneous candidiasis by multidrug-resistant Candida albicans.* Clin Infect Dis, 2012. **54**(7): p. 972, 1035-6.

251. Trautwein-Weidner, K., et al., *IL-17-mediated antifungal defense in the oral mucosa is independent of neutrophils.* Mucosal Immunol, 2015. **8**(2): p. 221-31.

252. Bhaskaran, N., et al., *Role of Short Chain Fatty Acids in Controlling Tregs and Immunopathology During Mucosal Infection.* Front Microbiol, 2018. **9**: p. 1995.

253. Pandiyan, P., et al., *Microbiome Dependent Regulation of Tregs and Th17 Cells in Mucosa.* Front Immunol, 2019. **10**: p. 426.

254. Kilian, M., *The oral microbiome - friend or foe?* Eur J Oral Sci, 2018. **126 Suppl 1**: p. 5-12.

255. Lee, Y.K., et al., *Proinflammatory T-cell responses to gut microbiota promote experimental autoimmune encephalomyelitis.* Proc Natl Acad Sci U S A, 2011. **108 Suppl 1**: p. 4615-22.

256. Gauguet, S., et al., *Intestinal Microbiota of Mice Influences Resistance to Staphylococcus aureus Pneumonia.* Infect Immun, 2015. **83**(10): p. 4003-14.

257. Conti, H.R., et al., *Signaling through IL-17C/IL-17RE is dispensable for immunity to systemic, oral and cutaneous candidiasis.* PLoS One, 2015. **10**(4): p. e0122807.

258. Goepfert, A., et al., *The human IL-17A/F heterodimer: a two-faced cytokine with unique receptor recognition properties.* Sci Rep, 2017. **7**(1): p. 8906.

259. Guarner, F. and J.R. Malagelada, *Role of bacteria in experimental colitis.* Best Pract Res Clin Gastroenterol, 2003. **17**(5): p. 793-804.

260. Smith, P.M., et al., *The microbial metabolites, short-chain fatty acids, regulate colonic Treg cell homeostasis.* Science, 2013. **341**(6145): p. 569-73.

261. Jin, L., et al., *Salivary factor LTRIN from Aedes aegypti facilitates the transmission of Zika virus by interfering with the lymphotoxin-beta receptor.* Nat Immunol, 2018. **19**(4): p. 342-353.

262. Sands, B.E., et al., *Ustekinumab as Induction and Maintenance Therapy for Ulcerative Colitis.* N Engl J Med, 2019. **381**(13): p. 1201-1214.

263. Sandborn, W.J., et al., *Efficacy and Safety of Mirikizumab in a Randomized Phase 2 Study of Patients With Ulcerative Colitis.* Gastroenterology, 2020. **158**(3): p. 537-549 e10.